8-2017

Complete Denitrification by the Non-Denitrifier *Anaeromyxobacter dehalogenans*: The Role of Coupled Biotic-Abiotic Reactions

Jenny Rae Onley
University of Tennessee, Knoxville, jmerryfi@vols.utk.edu

To the Graduate Council:

I am submitting herewith a dissertation written by Jenny Rae Onley entitled "Complete Denitrification by the Non-Denitrifier *Anaeromyxobacter dehalogenans*: The Role of Coupled Biotic-Abiotic Reactions." I have examined the final electronic copy of this dissertation for form and content and recommend that it be accepted in partial fulfillment of the requirements for the degree of Doctor of Philosophy, with a major in Microbiology.

Frank E. Löffler, Major Professor

We have read this dissertation and recommend its acceptance:

Alison Buchan, Qiang He, Karen Lloyd

Accepted for the Council:
Dixie L. Thompson

Vice Provost and Dean of the Graduate School

(Original signatures are on file with official student records.)

Complete Denitrification by the Non-Denitrifier *Anaeromyxobacter dehalogenans*: The Role of Coupled Biotic-Abiotic Reactions

A Dissertation Presented for the

Doctor of Philosophy

Degree

The University of Tennessee, Knoxville

Jenny Rae Onley

August 2017

To Jared

for your endless love and support

Acknowledgements

I would like to thank my PhD advisor, Dr. Frank Löffler, for his continued support. I appreciate his excitement for new ideas and discoveries; science can be a weary pursuit at times, and it is only through a real passion for science that we can persevere. I am grateful for the resources he provided, which stem from countless hours of hard work reading papers and writing grants. The work in this dissertation would have been impossible without him. Thank you also to Dr. Rob Sanford at the University of Illinois, who contributed ideas and patiently answered my many questions. I appreciate his thoughtful discussions and knowledgeable perspectives.

There is not enough room to thank everyone who has positively impacted my time at UT. My success comes from working within a community of excellent scientists, both within and outside of my lab. Thank you to my committee members: Dr. Alison Buchan, Dr. Karen Lloyd, and Dr. Qiang He. Their thoughtful questions and suggestions greatly improved my dissertation research. Thank you to Cindy Swift, who keeps the Löffler lab running and brings a fresh perspective to our research projects. Thank you to the research assistant professors and post-doctorate fellows who have worked in the Löffler lab, including Kirsti Ritalahti, Jarrod Pollock, Silke Nissen, Gillian Walshe-Langford, Jeongdae Im, Jun Yan, Sukhwan Yoon and Devrim Kaya. Their training was indispensible and they modeled what it means to be a scientist. Thank you especially to Silke, who taught me many techniques, and who showed great patience and self-sacrifice. Her passion for training and teaching kept our lab going for a number of years, and I am grateful I had her as a mentor. Thank you to the graduate students who provided training, assistance, and excellent conversation along the way: Elizabeth Padilla-Crespo, Burcu Şimşir, Yi Yang, Meng Bi, and Nannan Jiang. And especially to Steven Higgins, my lab bench buddy, who provided valuable scientific discussions and has been an excellent sounding board for my ideas. Thank you to Samiha Ahsan, my undergraduate mentee, whose contributed her time and ideas to my project and provided a cheerful and encouraging presence in the lab. Thank you to the rest of the Löffler lab, both past and present members; you all contributed to the team and I am grateful I was a part of it.

Thank you to Dr. Jeffrey Becker and the rest of the faculty who provided thoughtful comments on my projects over the years. A unique quality of our department

is our close connection with the Oak Ridge National Laboratory, and I am grateful for our collaborators and colleagues at ORNL as well (especially Dr. Chris Schadt, who allowed me to do a rotation in his lab). Thank you as well to my fellow graduate students in the Microbiology department who have provided stimulating scientific conversation and support. They are too many to name but I truly appreciate the community of scientists at UT. A special thanks to Samantha Coy and Pooja Saraf Dogra, who really took care of me the last two years of graduate school and are beautiful ladies, inside and out.

I am grateful to Steven Higgins, Samiha Ahsan, and Ashley Frank for their suggestions and revisions of my dissertation. A special thanks to Steven and also Luis Orellana at the Georgia Institute of Technology, who patiently helped me sharpen my bioinformatic skills.

I am also grateful for the funding agencies that supported my research, especially the US Department of Energy Genomic Science Program (Award DE-SC0006662).

Thank you to my family as well: Mom, Dad, Holly, Mandy, and Devon. You kept me grounded and encouraged me. Special thanks to Mom and Dad, for cultivating my love of science and helping me to pursue my dreams. They saw the spark when I was young, and fanned it into a flame.

Finally, I would like to thank my husband, Jared Onley. He has shown me faithful love and support through the ups and downs of graduate school. He believed in me though the entire process. During his own arduous trek through medical school and residency, he continued to sacrifice his time and energy and support me. It has been rewarding to have a scientifically minded husband with whom to share my exciting discoveries (as well as an abundance of boring details). I am eternally grateful to my supporter and cheerleader.

Abstract

Nitrous oxide (N_2O) is a potent greenhouse gas and ozone-depleting substance produced by many different pathways in the nitrogen cycle, including nitrification, denitrification, and chemodenitrification. Abiotic sources of N_2O such as the chemical reaction between nitrite (NO_2^-) and ferrous ion (Fe[II]) are generally neglected in studies of N turnover in soils. Abiotic controls containing nitrate (NO_3^-) and ferric iron (Fe[III]) fail to capture potential reactions between intermediates of N cycle pathways (e.g., NO_2^- as an intermediate in NO_3^- reduction to ammonium [NH_4^+] or nitrogen gas) or replenishment of reactants by iron cycling. Recent studies suggest that Fe(II) plays an important role in N turnover through combined biotic and abiotic reactions. *Anaeromyxobacter dehalogenans* strain 2CP-C is a common soil bacterium with a versatile metabolism, including microaerobic and anaerobic respiration. *A. dehalogenans* reduces Fe(III) to Fe(II) and reduces NO_3^- to NH_4^+ via respiratory ammonification. The present work investigates the mechanisms by which *A. dehalogenans* utilizes O_2 and the synergistic effects of Fe(III) and NO_3^- reduction. Evidence for respiration of 21% O_2 via a low-affinity cytochrome *c* oxidase is presented, further expanding the respiratory versatility of *A. dehalogenans.* A previously unrecognized ecophysiological role is revealed in which *A. dehalogenans* reduces NO_3^- to approximately 50% N_2 and 50% NH_4^+ via coupled biotic-abiotic reactions, revealing a mechanism for denitrification in the absence of nitric oxide (NO)-forming NO_2^- reductases. Further analysis of publicly available sequenced genomes reveal other microorganisms with the potential to couple biotic-abiotic reactions for reduction of NO_3^- to N_2 in the absence of NO-forming NO_2^- reductases. Finally, the effects of sulfide and molybdenum are tested, demonstrating that *A. dehalogenans* reduces NO_3^- to NH_4^+ and NO_2^- to N_2O in the presence of Fe(II) and sulfide, due to the inhibition of NO_3^- and N_2O reductases by sulfide sequestration of trace metals. Collectively, this work demonstrates an underestimated mechanism for denitrification and expands our knowledge of the role of *A. dehalogenans* in O_2 respiration and Fe and N cycling. Future efforts assessing the fate of N in agricultural soils should take into account the iron, molybdenum, and sulfide content of soils in addition to molecular information.

Table of Contents

List of Tables

List of Figures

List of Abbreviations

4-[2-hydroxyethyl]-1-piperazineethanesulfonic acid	HEPES
Ammonium	NH_4^+
Anaeromyxobacter dehalogenans	*A. dehalogenans*
Basic local alignment tool	BLAST
Deoxyribonucleic acid	DNA
Dissimilatory iron-reducing bacteria	DIRB
Expectation value	E value
Ferric Iron	Fe(III)
Ferrous Iron	Fe(II)
Gas chromatograph	GC
Liquid chromatography coupled mass spectrometry	LC-MS/MS
Membrane-bound NO_3^- reductase gene	*narG*
Molybdenum	Mo
Nitrate	NO_3^-
NO_3^--Dependent Iron Oxidation	NDFO
Nitric Oxide	NO
Nitrite	NO_2^-
NO_2^- reductase gene ($NO_2^- \rightarrow NH_4^+$)	*nrfA*
NO_2^- reductase genes ($NO_2^- \rightarrow NO$)	*nirK*/*nirS*
Nitrogen gas	N_2
Nitrous oxide	N_2O
N_2O reductase gene	*nosZ*
Oxygen gas	O_2
Partial pressure of oxygen	pO_2
Periplasmic NO_3^- reductase genes	*napA*
Polymerase chain reaction	PCR
Quantitative PCR	qPCR
Reactive oxygen species	ROS
Species (plural)	spp.
Thermal conductivity detector	TCD

Chapter 1: Introduction

Background

The nitrogen (N) cycle exerts an incredible influence on humans and the planet, and in return, humans have dramatically altered the N cycle over the last 100 years. After the discovery of the Haber-Bosch process, which fixes N_2 into ammonia, humans increased their production of reactive N to approximately 100 Tg per year (Fields, 2004). The combustion of fossil fuels and overuse of N fertilizer contributes to smog, low-lying ozone, the greenhouse gas effect, eutrophication, and drinking water contamination (Fields, 2004). The production of nitrous oxide (N_2O) is of special interest, since N_2O is a potent greenhouse gas and ozone-depleting substance. The N cycle is well studied and microbial sources of N_2O include denitrification and nitrification. Currently the presence of key denitrification genes *nirK*/*nirS* ($NO_2^- \rightarrow NO$) and *nosZ* ($N_2O \rightarrow N_2$) and environmental conditions (e.g., O_2 concentration and pH) are used to assess the potential for N_2O production and consumption. However, these tools do not always predict N_2O flux and do not take into account the interactions between the N cycle and the iron (Fe) cycle or the effects of sulfide.

The work in this dissertation focuses on the synergy between the Fe, N, and sulfur cycles. *Anaeromyxobacter dehalogenans* strain 2CP-C was studied because this organism reduces ferric iron (Fe[III]) to Fe(II), NO_3^- to NH_4^+, and N_2O to N_2 (with a recently-discovered clade II NosZ), is widely distributed in agricultural soils where N_2O emissions are of special concern, and possesses mechanisms to thrive in both oxic and anoxic conditions. The sections below provide a brief description of the Fe and N cycle and *Anaeromyxobacter*. Further background details are contained within the appropriate chapters.

The nitrogen cycle

As stated above, N impacts humans and the health of planet Earth more extensively than almost every other element on Earth. Fertilizer use has increased to meet the needs of a growing human population, and common N fertilizers in the United States include ammonia (NH_3), ammonium (NH_4^+), nitrate (NO_3^-), and urea (Nehring, 2013). Fertilizer runoff into bodies of water cause harmful algal blooms that introduce toxins

into drinking water and create hypoxic zones that kill local fauna (Fields, 2004; Diaz and Rosenberg, 2008). Excess fertilization can also cause nutrient leaching from agricultural soils (Fields, 2004). Gaseous products of the N cycle, such as N_2O, contribute to global warming. N_2O is a potent greenhouse gas with a global warming potential 310 times greater than that of carbon dioxide (Finlayson-Pitts and Pitts Jr., 2000; Lashof and Ahuja, 1990), and contributes to ozone destruction (Ravishankara *et al.*, 2009). The greatest fraction (75%) of N_2O from U.S. anthropogenic sources is from agricultural soil management (EPA 2015). Atmospheric N_2O concentrations are rising mainly due to increased applications of nitrogenous fertilizers (Reay *et al.*, 2012). Thus it is crucial to understand factors that control the fate of N in agricultural soils.

The majority of Earth's N is in the form of N_2 gas in the atmosphere, and for use by organisms must be fixed into organic forms. N_2 is fixed to ammonia naturally via lightning and microbial N fixation (via nitrogenase [Nif]) and is chemically fixed by the Haber-Bosch process (Fields, 2004; Canfield *et al.*, 2010). Ammonia can also be produced by urea hydrolysis. NH_4^+ is transformed to nitrite (NO_2^-) via a two-step process: NH_4^+ oxidation to hydroxylamine (by NH_4^+ monooxygenase [Amo]) and hydroxylamine oxidation to NO_2^- (by hydroxylamine monooxygenase [Hao]). NO_2^- is oxidized by NO_2^- oxidoreductase (*nxr*). NH_4^+ can also be oxidized via anaerobic NH_4^+ oxidation (Anammox), in which NH_4^+ oxidation and NO_2^- reduction are coupled, and N_2 is the end product. NO_3^- either undergoes reduction to NO_2^- via dissimilatory NO_3^- reductases (NapA or NarG) or assimilatory NO_3^- reductases (Nas) (Figure 1.1). NO_2^- can be reduced via denitrification or respiratory ammonification. In denitrification, NO_2^- is reduced to nitric oxide (NO) via either a copper-containing NO_2^- reductase (NirK) or iron-containing NO_2^- reductase (NirS) (Figure 1.1). NO can be further reduced to N_2O via the nitric oxide reductase (Nor), can be reduced to N_2O via the N_2O reductase (NosZ). Denitrifiers may be capable of reducing NO_3^- completely to N_2, or may incompletely reduce NO_3^-/NO_2^- to N_2O. In respiratory ammonification (also referred to as dissimilatory NO_3^- reduction to NH_4^+ [DNRA]), NO_2^- is reduced to NH_4^+ via the NO_2^- reductase (NrfA) (Figure 1.1). While NH_4^+ is retained in soils leading to N retention, the formation of gaseous products in denitrification contributes to N loss from soils and N_2O emissions. Chemodenitrification, a non-biological process, describes the chemical decomposition of

NO_3^- and NO_2^- (Nelson and Bremner, 1970; Buresh and Moraghan, 1976; Moraghan and Buresh, 1977; Ottley *et al.*, 1997). Although NO_3^- is not reduced by ferrous iron (Fe[II]) in a short time scale (i.e., hours), abiotic NO_2^- reduction to N_2O by Fe(II) can quickly occur at circumneutral pH (Buresh and Moraghan, 1976; Moraghan and Buresh, 1977). The product of chemodenitrification depends on the iron mineral, and NH_4^+ can be produced when wüstite or green rust is present (Hansen *et al.*, 1996; Rakshit *et al.*, 2005; Picardal, 2012; Etique *et al.*, 2014). Although chemodenitrification was considered for several decades to be an insignificant contributor to N flux, renewed interest in chemodenitrification has produced several studies that suggest chemodenitrification may play an important role in the N cycle (Zhu *et al.*, 2013; Jones *et al.*, 2015; Buchwald *et al.*, 2016). If that is the case, current assessments of the fate of N and N_2O flux in agricultural soils (often via molecular techniques) may underestimate the N_2O production potential of soils.

As described above, both dissimilatory biological pathways (nitrification and denitrification) and abiotic decomposition contribute to N_2O production. Additionally, non-denitrifying bacteria can have nitric oxide reductases, which may serve to detoxify NO and produce N_2O. Combined biotic-abiotic reactions can contribute to N_2O flux as well; these are further reviewed in Chapter 2.

The iron cycle

Dissimilatory iron-reducing bacteria (DIRB) couple the reduction of ferric (Fe[III]) to ferrous (Fe[II]) iron to microbial growth, and the first isolate was described in the late 1980's (Lovley and Phillips, 1988), although there was abundant evidence for microbial Fe(III) prior to isolation (Lovley and Phillips, 1986; Lovley, 1987). Fe(III) can also be reduced abiotically by sulfide (Kappler and Straub, 2005). Fe(III) exists predominantly in insoluble forms of iron oxyhydroxides (Cornell and Schwertmann, 2003; Kappler and Straub, 2005), creating a unique challenge for microbial reduction. Microorganisms have developed three strategies for overcoming this obstacle, which have been reviewed in the literature (Lovley *et al.*, 2004; DiChristina, 2005; Kappler and Straub, 2005; Weber *et al.*, 2006a). First, some microorganisms attach directly to the iron mineral via outer membrane *c*-type cytochromes. Secondly, microorganisms reduce

electron shuttles such as humic acids, extracellular cytochromes, inorganic sulfuric species, and cysteine (Doong and Schink, 2002; Flynn *et al.*, 2014; Lohmayer *et al.*, 2014; Smith *et al.*, 2014). Finally, microorganisms can produce compounds that chelate and solubilize Fe(III) (Kappler and Straub, 2005). It is apparent that multiheme *c*-type cytochromes play an important role in all three Fe(III)-reduction strategies, but the complete suite of proteins required for Fe(III) reduction remains to be identified.

Dissimilatory iron reduction plays an important role in the environment. DIRB contribute anywhere from 10% to nearly 100% of the organic matter oxidation in sediments (Lovley, 2013). The production of reactive Fe(II) minerals, such as magnetite, contribute to degradation or reduction of contaminants, either indirectly through the Fenton reaction (McKinzi and DiChristina, 1999) or through a direct reaction between Fe(II) minerals and carbon tetrachloride (Matheson and Tratnyek, 1994), technetium (Marshall *et al.*, 2009), or uranium (Scott *et al.*, 2005). Additionally, Fe(III) minerals sorb contaminants, and the reduction of Fe(III) can solubilize contaminants such as uranium and arsenic (Cummings *et al.*, 1999; Weber *et al.*, 2006a).

Fe(II) oxidation can also be coupled to microbial growth. Fe(II) can be oxidized abiotically at neutral pH by oxygen (O_2), NO_2^-, and manganese oxide, but in microoxic and anoxic habitats, iron-oxidizing bacteria can compete energetically with abiotic oxidation (Kappler and Straub, 2005; Weber *et al.*, 2006a). Fe(II) oxidation can be accomplished by anaerobic phototrophic Fe(II) oxidation, which is limited by light availability, or NO_3^--dependent Fe(II) oxidation (NDFO). Whether or not NDFO is truly an enzymatic process has been questioned, since the intermediate of NO_3^- reduction, NO_2^-, can react with Fe(II) (Klueglein and Kappler, 2013); however, this is currently debated and there is evidence for enzymatic involvement in NDFO (Carlson *et al.*, 2013). Whether NDFO is accomplished by abiotic processes or a combination of enzymatic and abiotic processes, it demonstrates one way in which the Fe cycle and the N cycle are linked. Denitrification, respiratory ammonification, and nitrification produce NO_2^- as an intermediate, and since NO_2^- reacts with Fe(II), these processes create the possibility for an abiotic link between the Fe cycle and the N cycle. *Klebsiella mobilis*, a bacterium incapable of Fe(II) oxidation, reduces NO_3^- to NH_4^+ and oxidizes Fe(II) stepwise to green rust and goethite via combined abiotic and biotic reactions (Etique *et al.*, 2014). Another

example of abiotic and biotic combined reactions is that of denitrification and iron reduction. *Shewanella putrefaciens* strain 200, an organism that typically reduces NO_3^- to NH_4^+, was shown to reduce NO_3^- to N_2O when cultures were growing on both Fe(III) and NO_3^- (Cooper *et al.*, 2003). Isotope experiments demonstrated that the N_2O was formed by an abiotic reaction between NO_2^- and Fe(II). Other potential interactions between N and Fe cycling remain to be explored.

Anaeromyxobacter: A unique member of *Myxococcales*

The myxobacteria are members of the *Myxococcales* and have amazingly complex behavioral patterns. *Myxococcales* is a class of Gram-negative, rod-shaped Deltaproteobacteria. Myxobacteria are complex organisms that display gliding motility and produce secondary metabolites (Reichenbach, 1999). They have a sophisticated social life in which they form fruiting bodies, which are multicellular structures containing myxospores (Reichenbach, 1999; Madigan *et al.*, 2015). Myxobacteria produce secondary metabolites and are found in a wide variety of habitats, including Antarctica and tropical environments (Reichenbach, 1999). However, most myxobacteria grow best around 30°C and are isolated from soil (Reichenbach, 1999). Myxobacteria were classified as obligate aerobes until 2002, when the *Anaeromyxobacter* genus was first described.

Anaeromyxobacter belong to the *Anaeromyxobacteraceae* the family of *Myxococcoales*, and were the first myxobacteria discovered with the ability to grow anaerobically. The first strain, 2CP-1, was isolated with 2-chlorophenol (2-CPh) from Michigan stream sediment (Cole *et al.*, 1994). In 2002, four more strains were isolated and the genus *Anaeromyxobacter* was created to describe the new myxobacteria members capable of anaerobic growth (Sanford *et al.*, 2002). Strain 2CP-2 was isolated from Michigan pond sediment, strains 2CP-3 and 2CP-5 were isolated from Michigan yard compost, and strain 2CP-C was isolated from Cameroon rain forest soil (Sanford *et al.*, 2002). The *Anaeromyxobacter dehalogenans* species was also described, and shown to utilize acetate, succinate, pyruvate, formate, and H_2 as electron donors and O_2, NO_3^-, fumarate, 2-CPh, 2-bromophenol, and 2,6-dichlorophenol as electron acceptors (Sanford *et al.*, 2002). These strains were only capable of aerobic growth with low levels of O_2,

and displayed a red pigment when growing anaerobically (Sanford *et al.*, 2002). Later strain FAc12 was isolated from rice paddy soil and was shown to utilize citrate and glucose as electron donors (Treude *et al.*, 2003). Rice paddies are routinely flooded and drained, and thus cycle between anoxic and oxic conditions, conditions to which the microaerophilic *A. dehalogenans* is well-adapted. Dehalogenation of dichlorophenol was shown to be constitutive in *A. dehalogenans* strain 2CP-C cultures, but dehalogenation proceeded more quickly after induction by chlorinated and brominated phenols (He and Sanford, 2002). The early isolated strains of *Anaeromyxobacter* are able to dechlorinate chlorinated phenols and two putative reductive dehalogenase genes are present on the genome of *A. dehalogenans* strain 2CP-C (Thomas *et al.*, 2008). However, the genome of *Anaeromyxobacter* sp. Fw109-5 does not contain genes for reductive dehalogenation (Hwang *et al.*, 2015). *A. dehalogenans* strain 2CP-C can reduce ferric citrate, ferric pyrophosphate, and amorphous ferric oxyhydroxide, and reduction of ferric pyrophosphate is constitutive (He and Sanford, 2003). The mechanism by which *Anaeromyxobacter* reduces insoluble forms of Fe(III) is unknown, but reduction rates increased with the addition of anthraquinone 2,6-disulfonate (AQDS), a humic acid analog, suggesting that *A. dehalogenans* may utilize electron shuttles. Additionally, proteomic analysis during growth with ferric citrate (which can be reduced outside of the cell by some organisms) and insoluble manganese oxide showed expression of cytochromes with similarity to outer membrane cytochromes that are used by *Shewanella* to reduce insoluble metal oxides (Nissen et al. 2012). As with several other dissimilatory iron-reducing bacteria (DIRB), *A. dehalogenans* strain 2CP-C was later demonstrated to reduce uranium(VI) to U(IV), coupling reduction to growth (Wu *et al.*, 2006; Sanford *et al.*, 2007; Marshall *et al.*, 2009). U(IV) was produced as extracellular precipitates, suggesting that outer membrane cytochromes are responsible for U(VI) reduction (Marshall *et al.*, 2009). Strain 2CP-C was also shown to both directly reduce technetium and to reduce technetium via coupled biotic-abiotic reactions (Marshall *et al.*, 2009). In this study, strain 2CP-C reduced ferrihydrite (an Fe[III] mineral) to magnetite (a mixed Fe[III]/Fe[II] mineral), and the magnetite subsequently reduced technetium (Marshall *et al.*, 2009). *Anaeromyxobacter* sp. strain PSR-1 was isolated from arsenic-contaminated soil and was shown to couple arsenate reduction to growth (Kudo *et al.*, 2013), although

respiratory arsenate reductase genes were not identified on the draft genome of strain PSR-1 (Tonomura *et al.*, 2015). Strains 2CP-C and 2CP-1 were shown to reduce selenium(VI) (He and Yao, 2010), and concentrated cells of *A. dehalogenans* strain K reduced hexahydro-1,3,5-trinitro-1,3,5-triazine, an explosive that contaminates military sites (Kwon and Finneran, 2008).

A. dehalogenans strains were shown to reduce NO_3^- to NH_4^+ via NO_2^- as the intermediate (Sanford *et al.*, 2002). Despite its classification as a non-denitrifier, the sequenced genome of *A. dehalogenans* strain 2CP-C contains a *nos* operon, and strain 2CP-C reduces N_2O as a terminal electron acceptor with NosZ (a N_2O reductase). Interestingly, the *nosZ* gene encoded by strain 2CP-C was shown to be a part of a phylogenetically distinct clade of *nosZ*, coined atypical or clade II *nosZ* (Sanford *et al.*, 2012; Jones *et al.*, 2013). Clade II *nosZ* are not amplified by primers designed to amplify clade I *nosZ*, and many of the organisms with clade II *nosZ* do not have complete NO_3^- reduction to N_2 pathways (e.g., lack *nirS*/*nirK*), suggesting that clade II *nosZ* provide a previously unknown N_2O sink (Sanford *et al.*, 2012; Jones *et al.*, 2013). Additionally, clade II NosZ has a higher affinity for N_2O than clade I NosZ, suggesting that they are more competitive under environmental levels (i.e., ppm) of N_2O (Yoon *et al.*, 2016), and clade II *nosZ* genes are more abundant than clade I *nosZ* genes in many environments (Orellana *et al.*, 2014). *Anaeromyxobacter* type *nosZ* sequences were found to be the most abundant *nosZ* genes in Illinois agricultural soils (Orellana *et al.*, 2014), suggesting an important role of *Anaeromyxobacter* in N cycling.

Habitats of *Anaeromyxobacter*

In accordance with the respiratory versatility of *Anaeromyxobacter*, *Anaeromyxobacter* species are found in many different types of environments, including contaminated environments. *Anaeromyxobacter* are found in tropical soils, rice paddy soils, agricultural soils, anoxic lake sediments, and soils and sediments contaminated with uranium, nitric acid, arsenic, and polychlorinated biphenyls. *Anaeromyxobacter* is abundant in sediments contaminated with uranium and nitric acid, at numbers comparable to the common DIRB *Geobacter* (Petrie *et al.*, 2003; Thomas *et al.*, 2009; Xu *et al.*, 2010). *Anaeromyxobacter* sequences were detected in Ohio River sediments

contaminated with polychlorinated biphenyls (D'Angelo and Nunez, 2010), in anoxic Lake Coeur d'Alene sediments contaminated with metals (Cummings *et al.*, 2003), and in Alabama freshwater wetland sediment microcosms enriched with goethite and NO_3^- (Weber *et al.*, 2006b). *Anaeromyxobacter* species are widely distributed in Illinois soils (Sanford *et al.*, 2012) and appear to compose a significant portion of the N_2O-reducing community (Orellana *et al.*, 2014). *Anaeromyxobacter* are frequently detected in rice paddy soils (e.g., Treude et al. 2003) and *Anaeromyxobacter* sequences were detected on rice nodal roots (Ikenaga *et al.*, 2003). *Anaeromyxobacter* and other DIRB play an important role in carbon turnover in rice paddies and oxidize and assimilate acetate (Hori *et al.*, 2007).

Rationale and Hypotheses

Molecular techniques (i.e., measurements of genes, transcripts, and proteins) are currently employed to assess the contributions of biotic pathways to N_2O production and consumption in soils. Abiotic reactions are frequently not considered, and the intersection between biotic and abiotic processes requires further exploration. Recent studies indicate that combined biotic-abiotic reactions yield N cycle products that cannot be predicted by the N cycle genes of an organism. It is unknown if combined biotic-abiotic reactions can substantially contribute to complete reduction of NO_3^- to N_2. Additionally, the role of biotic-abiotic N cycle reactions in the metabolism and ecology of *A. dehalogenans* is unknown. A relationship between sulfide and NO_3^- reduction was demonstrated in several environmental studies, but the full mechanisms behind that relationship and the consequences for chemodenitrification remain to be uncovered. Finally, previous studies speculated that the low affinity cytochrome *c* oxidase (cytochrome aa_3) encoded by *A. dehalogenans* is utilized for O_2 detoxification, but further research is required to confirm the role of cytochrome aa_3. It is hypothesized here that *A. dehalogenans* has adaptations for survival under oxic conditions, and that through synergistic effects between NO_2^-, iron, sulfide, and molybdenum, *A. dehalogenans* facilitates NO_3^- reduction to NH_4^+, N_2O, and N_2. The research presented in this dissertation addresses the knowledge gaps listed above with the following specific hypotheses:

1. *A. dehalogenans* facilitates chemodenitrification through ferric iron and nitrate reduction and produces nitrogen gas through coupled biotic-abiotic reactions.

2. Other bacteria demonstrate a chemodenitrifier potential similar to *A. dehalogenans* (i.e., have nitrate reductases, nitrous oxide reductases, and the ability to reduce ferric iron).

3. Sulfide changes the final products of nitrate reduction in the presence of ferrous iron due to reduced bioavailability of molybdopterin and copper (key trace metals for nitrate reductase and nitrous oxide reductase, respectively).

4.a. *A. dehalogenans* utilizes cytochrome aa_3 as a non-respiratory enzyme to decrease O_2 concentrations to levels at which *A. dehalogenans* can respire O_2 with cytochrome cbb_3.

4.b. Alternative hypothesis: *A. dehalogenans* utilizes cytochrome aa_3 to couple growth to O_2 respiration under oxic conditions.

References

Buchwald C, Grabb K, Hansel CM, Wankel SD. (2016). Constraining the role of iron in environmental nitrogen transformations: Dual stable isotope systematics of abiotic NO_2^- reduction by Fe(II) and its production of N_2O. *Geochim Cosmochim Acta* **186**: 1–12.

Buresh RJ, Moraghan JT. (1976). Chemical reduction of nitrate by ferrous iron. *J Environ Qual* **5**: 320–325.

Canfield DE, Glazer AN, Falkowski PG. (2010). The evolution and future of Earth's nitrogen cycle. *Science* **330**: 192–196.

Carlson HK, Clark IC, Blazewicz SJ, Iavarone AT, Coates JD. (2013). Fe(II) oxidation is an innate capability of nitrate-reducing bacteria that involves abiotic and biotic reactions. *J Bacteriol* **195**: 3260–8.

Cole JR, Cascarelli AL, Mohn WW, Tiedje JM. (1994). Isolation and characterization of a novel bacterium growing via reductive dehalogenation of 2-chlorophenol. *Appl Environ Microbiol* **60**: 3536–42.

Cooper DC, Picardal FW, Schimmelmann A, Coby AJ. (2003). Chemical and biological interactions during nitrate and goethite reduction by *Shewanella putrefaciens* 200. *Appl Environ Microbiol* **69**: 3517–3525.

Cornell RM, Schwertmann U. (2003). The Iron Oxides: Structure, Properties, Reactions, Occurences and Uses. 2nd ed. Wiley-VCH: Weinheim.

Cummings D., Snoeyenbos-West O., Newby DT, Niggemyer AM, Lovley DR, Achenbach LA, *et al.* (2003). Diversity of Geobacteraceae species inhabiting metal-polluted freshwater lake sediments ascertained by 16S rDNA analyses. *Microb Ecol* **46**: 257–269.

Cummings DE, Caccavo Jr. F, Fendorf S, Rosenzweig RF. (1999). Arsenic mobilization by the dissimilatory Fe(III)-reducing bacterium *Shewanella alga* BrY. *Environ Sci Technol* **33**: 723–729.

D'Angelo E, Nunez A. (2010). Effect of environmental conditions on polychlorinated biphenyl transformations and bacterial communities in a river sediment. *J Soils Sediments* **10**: 1186–1199.

Diaz RJ, Rosenberg R. (2008). Spreading dead zones and consequences for marine

ecosystems. *Science* **321**: 926–929.

DiChristina TJ. (2005). Enzymology of electron transport: energy generation with geochemical consequences. *Rev Mineral Geochemistry* **59**: 27–52.

Doong RA, Schink B. (2002). Cysteine-mediated reductive dissolution of poorly crystalline iron(III) oxides by *Geobacter sulfurreducens*. *Environ Sci Technol* **36**: 2939–2945.

Etique M, Jorand FP a, Zegeye A, Grégoire B, Despas C, Ruby C. (2014). Abiotic process for Fe(II) oxidation and green rust mineralization driven by a heterotrophic nitrate reducing bacteria (*Klebsiella mobilis*). *Environ Sci Technol* **48**: 3742–51.

Fields S. (2004). Global nitrogen; Cycling out of control. *Environ Health Perspect* **112**: A556–A563.

Finlayson-Pitts BJ, Pitts Jr. JN. (2000). Chemistry of the upper and lower atmosphere: theory, experiments and applications. Academic Press: San Diego, CA.

Flynn TM, O'Loughlin EJ, Mishra B, Dichristina TJ, Kemner KM. (2014). Sulfur-mediated electron shuttling during bacterial iron reduction. *Science* **344**: 1039–1042.

Hansen HCB, Koch CB, Nancke-Krogh H, Borggaard OK, Sørensen J. (1996). Abiotic nitrate reduction to ammonium: Key role of green rust. *Environ Sci Technol* **30**: 2053–2056.

He Q, Sanford RA. (2003). Characterization of Fe(III) reduction by chlororespiring *Anaeromxyobacter dehalogenans*. *Appl Environ Microbiol* **69**: 2712–2718.

He Q, Sanford R a. (2002). Induction characteristics of reductive dehalogenation in the *ortho*-halophenol-respiring bacterium, *Anaeromyxobacter dehalogenans*. *Biodegradation* **13**: 307–316.

He Q, Yao K. (2010). Microbial reduction of selenium oxyanions by *Anaeromyxobacter dehalogenans*. *Bioresour Technol* **101**: 3760–3764.

Hori T, Noll M, Igarashi Y, Friedrich MW, Conrad R. (2007). Identification of acetate-assimilating microorganisms under methanogenic conditions in anoxic rice field soil by comparative stable isotope probing of RNA. *Appl Environ Microbiol* **73**: 101–109.

Hwang C, Copeland A, Lucas S, Lapidus A, Barry K, del Rio GT, *et al.* (2015).

Complete genome sequence of *Anaeromyxobacter* sp. Fw109-5, an anaerobic, metal-reducing bacterium isolated from a contaminated subsurface environment. *Genome Announc* **3**: 1–2.

Ikenaga M, Asakawa S, Muraoka Y, Kimura M. (2003). Bacterial communities associated with nodal roots of rice plants along with the growth stages: Estimation by PCR-DGGE and sequence analyses. *Soil Sci Plant Nut* **49**: 591–602.

Jones CM, Graf DRH, Bru D, Philippot L, Hallin S. (2013). The unaccounted yet abundant nitrous oxide-reducing microbial community: a potential nitrous oxide sink. *ISME J* **7**: 417–26.

Jones LC, Peters B, Lezama Pacheco JS, Casciotti KL, Fendorf S. (2015). Stable isotopes and iron oxide mineral products as markers of chemodenitrification. *Environ Sci Technol* **49**: 3444–3452.

Kappler A, Straub KL. (2005). Geomicrobiological cycling of iron. *Rev Mineral Geochemistry* **59**: 85–108.

Klueglein N, Kappler A. (2013). Abiotic oxidation of Fe(II) by reactive nitrogen species in cultures of the nitrate-reducing Fe(II) oxidizer *Acidovorax* sp. BoFeN1 – questioning the existence of enzymatic Fe(II) oxidation. *Geobiology* **11**: 180–190.

Kudo K, Yamaguchi N, Makino T, Ohtsuka T, Kimura K, Dong DT, *et al.* (2013). Release of arsenic from soil by a novel dissimilatory arsenate-reducing bacterium, *Anaeromyxobacter* sp. Strain PSR-1. *Appl Environ Microbiol* **79**: 4635–42.

Kwon MJ, Finneran KT. (2008). Hexahydro-1,3,5-trinitro-1,3,5-triazine (RDX) and octahydro-1,3,5,7-tetranitro-1,3,5,7-tetrazocine (HMX) biodegradation kinetics amongst several Fe(III)-reducing genera. *Soil Sediment Contam* **17**: 189–203.

Lashof DA, Ahuja DR. (1990). Relative contributions of greenhouse gas emissions to global warming. *Nature* **344**: 529–531.

Lohmayer R, Kappler A, Lösekann-Behrens T, Planer-Friedrich B. (2014). Sulfur species as redox partners and electron shuttles for ferrihydrite reduction by *Sulfurospirillum deleyianum*. *Appl Environ Microbiol* **80**: 3141–9.

Lovley D. (2013). Dissimilatory Fe(III)- and Mn(IV)-reducing prokaryotes. In: Rosenberg E, DeLong EF, Lory S, Stackebrandt E, Thompson F (eds). *The Prokaryotes*. Springer Berlin Heidelberg: Berlin Heidelberg, pp 287–308.

Lovley DR. (1987). Organic matter mineralization with the reduction of ferric iron: A review. *Geomicrobiology* **5**: 375–399.

Lovley DR, Holmes DE, Nevin KP. (2004). Dissimilatory Fe(III) and Mn(IV) reduction. In: Poole RK (ed) Vol. Volume 49. *Advances in Microbial Physiology*. Academic Press: London, pp 219–286.

Lovley DR, Phillips EJP. (1988). Novel mode of microbial energy metabolism: Organic carbon oxidation coupled to dissimilatory reduction of iron or manganese. *Appl Environ Microbiol* **54**: 1472–1480.

Lovley DR, Phillips EJP. (1986). Organic matter mineralization with reduction of ferric iron in anaerobic sediments. *Appl Environ Microbiol* **51**: 683–689.

Madigan M, Martinko JM, Bender KS, Buckley DH, Stahl DA. (2015). Brock Biology of Microorganisms. 14th ed. Pearson.

Marshall MJ, Dohnalkova AC, Kennedy DW, Plymale AE, Thomas SH, Löffler FE, *et al.* (2009). Electron donor-dependent radionuclide reduction and nanoparticle formation by *Anaeromyxobacter dehalogenans* strain 2CP-C. *Environ Microbiol* **11**: 534–43.

Matheson LJ, Tratnyek PG. (1994). Reductive dehalogenation of chlorinated methanes by iron metal. *Environ Sci Technol* **28**: 2045–2053.

McKinzi AM, DiChristina TJ. (1999). Microbially driven fenton reaction for transformation of pentachlorophenol. *Environ Sci Technol* **33**: 1886–1891.

Moraghan JT, Buresh RJ. (1977). Chemical reduction of nitrite and nitrous oxide by ferrous iron. *Soil Sci Soc Am J* **41**: 47–50.

Nehring R. (2013). Fertilizer use and price. *USDA Econ Res Serv*. http://www.ers.usda.gov/data-products/fertilizer-use-and-price.aspx (Accessed February 3, 2015).

Nelson DW, Bremner JM. (1970). Role of soil minerals and metallic cations in nitrite decomposition and chemodenitrification in soils. *Soil Biol Biochem* **2**: 1–8.

Orellana LH, Rodriguez-R LM, Higgins S, Chee-Sanford JC, Sanford RA, Ritalahti KM, *et al.* (2014). Detecting nitrous oxide reductase (*nosZ*) genes in soil metagenomes: method development and implications for the nitrogen cycle. *MBio* **5**: 1–8.

Ottley CJ, Davison W, Edmunds WM. (1997). Chemical catalysis of nitrate reduction by

iron(II). *Geochim Cosmochim Acta* **61**: 1819–1828.

Petrie L, North NN, Dollhopf SL, Balkwill DL, Kostka JE. (2003). Enumeration and characterization of iron(III)-reducing microbial communities from acidic subsurface sediments contaminated with uranium(VI). *Appl Environ Microbiol* **69**: 7467–7479.

Picardal F. (2012). Abiotic and microbial interactions during anaerobic transformations of Fe(II) and NO_x^-. *Front Microbiol* **3**: 112.

Rakshit S, Matocha CJ, Haszler GR. (2005). Nitrate reduction in the presence of wüstite. *J Environ Qual* **34**: 1286–1292.

Ravishankara AR, Daniel JS, Portmann RW. (2009). Nitrous oxide (N_2O): The dominant ozone-depleting substance emitted in the 21st century. *Science* **326**: 123–125.

Reay DS, Davidson EA, Smith KA, Smith P, Melillo JM, Dentener F, *et al.* (2012). Global agriculture and nitrous oxide emissions. *Nat Clim Chang* **2**: 410–416.

Reichenbach H. (1999). The ecology of the myxobacteria. *Environ Microbiol* **1**: 15–21.

Sanford RA, Cole JR, Tiedje JM. (2002). Characterization and description of *Anaeromyxobacter dehalogenans* gen. nov., sp. nov., an aryl-halorespiring facultative anaerobic myxobacterium. *Appl Environ Microbiol* **68**: 893–900.

Sanford RA, Wagner DD, Wu Q, Chee-Sanford JC, Thomas SH, Cruz-García C, *et al.* (2012). Unexpected nondenitrifier nitrous oxide reductase gene diversity and abundance in soils. *Proc Natl Acad Sci U S A* **109**: 19709–14.

Sanford RA, Wu Q, Sung Y, Thomas SH, Amos BK, Prince EK, *et al.* (2007). Hexavalent uranium supports growth of *Anaeromyxobacter dehalogenans* and *Geobacter* spp. with lower than predicted biomass yields. *Environ Microbiol* **9**: 2885–93.

Scott TB, Allen GC, Heard PJ, Randell MG. (2005). Reduction of U(VI) to U(IV) on the surface of magnetite. *Geochim Cosmochim Acta* **69**: 5639–5646.

Smith J a, Tremblay P-L, Shrestha PM, Snoeyenbos-West OL, Franks AE, Nevin KP, *et al.* (2014). Going wireless: Fe(III) oxide reduction without pili by *Geobacter sulfurreducens* strain JS-1. *Appl Environ Microbiol*. e-pub ahead of print, doi: 10.1128/AEM.01122-14.

Thomas SH, Padilla-Crespo E, Jardine PM, Sanford RA, Löffler FE. (2009). Diversity and distribution of *Anaeromyxobacter* strains in a uranium-contaminated subsurface

environment with a nonuniform groundwater flow. *Appl Environ Microbiol* **75**: 3679–87.

Thomas SH, Wagner RD, Arakaki AK, Skolnick J, Kirby JR, Shimkets LJ, *et al.* (2008). The mosaic genome of *Anaeromyxobacter dehalogenans* strain 2CP-C suggests an aerobic common ancestor to the delta-proteobacteria. *PLoS One* **3**: 1–12.

Tonomura M, Ehara A, Suzuki H, Amachi S. (2015). Draft genome sequence of *Anaeromyxobacter* sp. Strain PSR-1, an arsenate-respiring bacterium isolated from arsenic-contaminated soil. *Genome Announc* **3**: 1–2.

Treude N, Rosencrantz D, Liesack W, Schnell S. (2003). Strain FAc12, a dissimilatory iron-reducing member of the *Anaeromyxobacter* subgroup of *Myxococcales*. *FEMS Microbiol Ecol* **44**: 261–269.

Weber KA, Achenbach LA, Coates JD. (2006a). Microorganisms pumping iron: anaerobic microbial iron oxidation and reduction. *Nat Rev Microbiol* **4**: 752–64.

Weber K a, Urrutia MM, Churchill PF, Kukkadapu RK, Roden EE. (2006b). Anaerobic redox cycling of iron by freshwater sediment microorganisms. *Environ Microbiol* **8**: 100–13.

Wu Q, Sanford RA, Löffler FE. (2006). Uranium(VI) Reduction by *Anaeromyxobacter dehalogenans* Strain 2CP-C. *Appl Environ Microbiol* **72**: 3608–3614.

Xu M, Wu W-M, Wu L, He Z, Van Nostrand JD, Deng Y, *et al.* (2010). Responses of microbial community functional structures to pilot-scale uranium in situ bioremediation. *ISME J* **4**: 1060–70.

Yoon S, Nissen S, Park D, Sanford RA, Löffler FE. (2016). Nitrous oxide reduction kinetics distinguish bacteria harboring clade I NosZ from those harboring clade II NosZ. *Appl Environ Microbiol* **82**: 3793–3800.

Zhu X, Silva LCR, Doane TA, Horwath WR. (2013). Iron: The forgotten driver of nitrous oxide production in agricultural soil. *PLoS One* **8**: e60146.

(2015). Draft inventory of U.S. greenhouse gas emissions and sinks: 1990-2013. EPA. Washington D.C.

Appendix: Figures

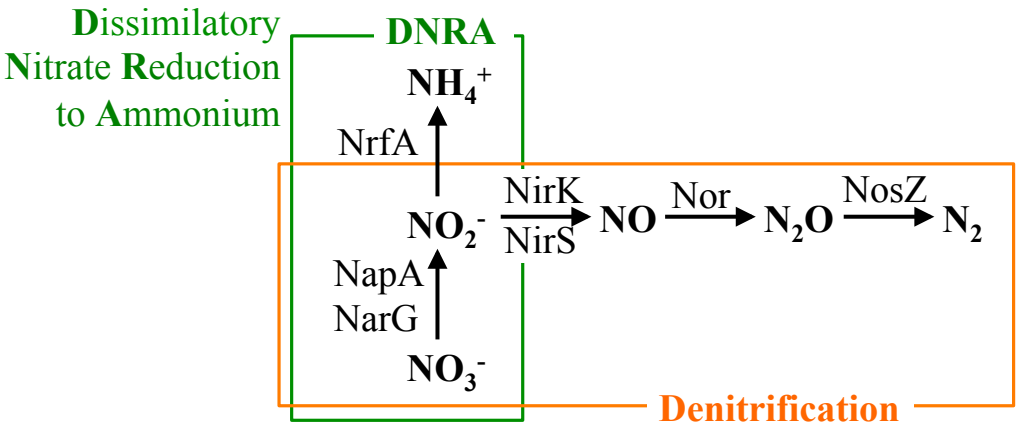

Figure 1.1. Biological NO_3^- reduction pathways with their respective enzymes.

Chapter 2: Chemodenitrification by *Anaeromyxobacter dehalogenans* and Implications for the Nitrogen Cycle

This chapter is based on a manuscript draft by Onley et al.:

Onley JR, Ahsan S, Sanford RA, and Löffler FE. Complete Denitrification by the Non-Denitrifier *Anaeromyxobacter dehalogenans* and Implications for the Nitrogen Cycle.

My primary contributions to the work include (i) designing and implementing experiments, (ii) assay troubleshooting and refinement, (iii) reviewing and summarizing relevant literature, (iv) gathering, analyzing, and summarizing data, (v) initial writing of the manuscript, and (vi) revising manuscript and coordinating revisions of the manuscript.

Abstract

The metabolically versatile soil bacterium *Anaeromyxobacter dehalogenans* couples growth to the reduction of NO_3^- via NO_2^- as intermediate to NH_4^+ and to N_2O reduction to N_2. Consistent with the observed physiology, genomic studies identified *nrfA* ($NO_2^- \rightarrow NH_4^+$) and *nosZ* ($N_2O \rightarrow N_2$) genes, but *nirS* and *nirK* ($NO_2^- \rightarrow NO$) genes were absent, confirming its characterization as a non-denitrifier. *A. dehalogenans* also reduces soluble and insoluble forms of Fe(III) to Fe(II), known to chemically react with NO_2^-. Following the addition of 1 mM NO_3^- or NO_2^- (i.e., 100 μmoles) to *A. dehalogenans* strain 2CP-C cultures grown with Fe(III) citrate, cultures yielded 54 ± 7 μmoles and 113 ± 2 μmoles N_2O-N, respectively. The N_2O formed was subsequently consumed by *A. dehalogenans*, indicating that the organism converts NO_3^- to N_2 in the presence of Fe(II) through linked biotic-abiotic reactions. During NO_3^- reduction in the absence of Fe(II), only small amounts (≤ 1 μmole) of N_2O-N were observed. A chemical reaction of NO_2^- with Fe(II) (i.e., chemodenitrification) was evidenced by N_2O formation in abiotic controls containing Fe(II) and 100 μmoles of NO_2^-. Subsequent N_2O consumption required the presence of live *A. dehalogenans* cells. Despite the absence of *nirS* and *nirK*, *A. dehalogenans* cultures produced gaseous products from NO_3^- and NO_2^-, indicating that gene content alone is insufficient to predict microbial denitrification potential. A survey of 4,739 complete bacterial genomes revealed 51 genomes with genes encoding NO_3^- and N_2O reductases but lacking *nirS* and *nirK*. Seven of these organisms are confirmed iron reducers and 27 genomes have at least six putative *c*-type cytochrome genes with four or

more predicted heme-binding domains, a characteristic of metal-reducing bacteria. Considering the ubiquity of iron in diverse biomes and the broad distribution of dissimilatory Fe(III) and NO_3^--to-NO_2^- reducers, denitrification independent of NO-forming NO_2^- reductases (through combined biotic-abiotic reactions) may have substantial contributions to N loss and N_2O flux.

Introduction

Reactive N availability limits primary production in most natural and managed ecosystems, and to meet the demands of a growing human population for food, feed and biofuel crops, global fertilizer usage continues to increase. The Haber-Bosch process introduces about 100 Tg of reactive N (e.g., ammonium) each year into the environment worldwide as fertilizer (Fields, 2004). As a consequence, no other basic element cycle has been more perturbed than the N cycle. A substantial amount of the fixed N is lost from the soil due to microbial nitrification (ammonium oxidation to nitrate; $NH_4^+ \rightarrow NO_3^-$) and subsequent microbial denitrification (nitrate reduction to nitrous oxide/nitrogen gas; $NO_3^- \rightarrow N_2O/N_2$). Both nitrification and denitrification generate N_2O (Stein, 2011), a potent greenhouse gas with ozone depletion potential (Lashof and Ahuja, 1990; Finlayson-Pitts and Pitts Jr., 2000; Ravishankara *et al.*, 2009). Even more troubling is that according to the "progressive N limitation" hypothesis (Luo *et al.*, 2004), extended N limitation will occur under a warming scenario, requiring even more fertilizer for crop production. To estimate N losses from soils to the atmosphere (i.e., emissions of the gaseous denitrification products N_2O and N_2), the measurement of the keystone denitrification genes *nirS* and *nirK*, which both encode nitric oxide (NO)-forming nitrite (NO_2^-) reductases, has been applied. Some studies demonstrated a positive correlation between the abundance of denitrification genes (i.e., *nirK*, *nirS*, and/or *nosZ*) and NO_3^- /NO_2^- conversion to gaseous products (Morales *et al.*, 2010; Lee and Kang, 2015); however, other studies failed to establish this relationship (Wallenstein *et al.*, 2006; Dandie *et al.*, 2008; Ma *et al.*, 2008; Henderson *et al.*, 2010). Recent studies showed that commonly used *nirK*/*nirS* qPCR primers yield poor coverage of *nirK*/*nirS* sequences in metagenomes and underestimate the true *nirK*/*nirS* gene abundance in environmental samples (Wei *et al.*, 2015; Bonilla-Rosso *et al.*, 2016). Recently, novel clade II *nosZ* genes were identified, which are not amplified by all previously designed primers targeting the typical clade I *nosZ* sequences (Sanford *et al.*, 2012; Jones *et al.*, 2013). Metagenomic datasets revealed that clade II *nosZ* genes are more prevalent in many soil ecosystems and potential relevant contributors to N_2O consumption (Sanford *et al.*, 2012; Jones *et al.*, 2013; Orellana *et al.*, 2014; Yoon *et al.*, 2016). Separate molecular tools are needed to account for fungal denitrification, a process that generates N_2O (not N_2) as a

final product (Higgins *et al.*, 2016). Further, chemical denitrification (chemodenitrification), a process in which NO_2^- is converted to N_2O in a chemical reaction with ferrous iron (Moraghan and Buresh, 1977), has not been attributed a major role in soil N loss. However, recent studies have reaffirmed that Fe(II) reacts quickly with NO_2^- to form N_2O under a range of NO_2^- and Fe(II) concentrations (Jones *et al.*, 2015; Buchwald *et al.*, 2016). In addition to information generated with molecular approaches, abiotic factors should also be considered for improving N cycling studies, as a multitude of environmental parameters, such as water-filled pore space, soil type, total N, reduction-oxidation potential (Eh), and reactive iron content influence N_2O emissions (Dandie *et al.*, 2008; Zhu *et al.*, 2013; Fan *et al.*, 2016).

Anaeromyxobacter are members of the order Myxococcales, commonly referred to as myxobacteria. *Anaeromyxobacter* strains are found in subsurface environments, sediments, and a variety of soil types, particularly agricultural soils (Sanford *et al.*, 2002, 2012; Petrie *et al.*, 2003). *Anaeromyxobacter dehalogenans* reduces NO_3^- to NH_4^+ with NO_2^- as the intermediate via the respiratory ammonification pathway (Sanford *et al.*, 2002, 2012). Although *Anaeromyxobacter* strains possess the gene for the clade II N_2O reductase (*nosZ*) to reduce N_2O to N_2, they are not classified as denitrifying organisms due to the absence of *nirK* and *nirS*. The ability to utilize other growth-supporting electron acceptors including oxygen and oxidized metal species such as Mn(IV) and Fe(III) suggest that *Anaeromyxobacter* strains are well adapted to fluctuating redox conditions (Sanford *et al.*, 2002). Remarkably, experiments with *A. dehalogenans* demonstrated that the ability of using Fe(III) as an electron acceptor is constitutive (He and Sanford, 2003). Thus, *A. dehalogenans* produces ferrous iron (Fe[II]) as product of Fe(III) reduction and NO_2^- as an intermediate in respiratory ammonification. It is well-established that Fe(II) and NO_2^- react to form N_2O (Moraghan and Buresh, 1977; Jones *et al.*, 2015; Buchwald *et al.*, 2016). In addition to producing N_2O through chemodenitrification, NO_3^- and NO_2^- can react with certain Fe(II) minerals such as green rust and wüstite to produce NH_4^+ (Rakshit *et al.*, 2005; Etique *et al.*, 2014). Several studies have shown that microorganisms couple abiotic and biotic reactions to turn over Fe(III)/Fe(II) and N compounds (Cooper *et al.*, 2003; Klueglein and Kappler, 2013; Etique *et al.*, 2014). These observations highlight that detailed knowledge about coupled

biotic-abiotic reactions is relevant for developing a predictive understanding of N cycling. Since little is known how organisms with incomplete NO_3^- reduction to N_2 pathways (e.g., with genes encoding NO_3^- and N_2O reductases but lacking *nirK*/*nirS*) might bridge the iron and N cycles, the effect of iron on NO_3^- and NO_2^- reduction in pure cultures of *A. dehalogenans* was tested. These experiments demonstrated that *A. dehalogenans* facilitates chemodenitrification through Fe(III) and NO_3^- reduction and ultimately produces N_2 through coupled biotic-abiotic reactions.

Materials and Methods

Chemicals

HEPES (4-[2-hydroxyethyl]-1-piperazineethanesulfonic acid) (≥99%), L-cysteine hydrochloride monohydrate (98.5-101.0%), anhydrous sodium acetate (≥99.2%), sodium hydroxide pellets (≥99.0%), sodium nitrite (≥99.6%), ammonium chloride, ferric chloride hexahydrate (≥99.7%), and ferrous ammonium sulfate hexahydrate (101.2%) were purchased from Fisher Scientific (Fair Lawn, NJ). N_2O (99%), Fe(III) citrate, and ferrous chloride tetrahydrate (≥99.0%) were purchased from Sigma-Aldrich (St. Louis, MO). Sodium phosphate dibasic (≥99.6%) and sodium nitrate (100.8%) were purchased from J.T. Baker (Phillipsburg, NJ). Ferrozine iron reagent (≥98%) and sodium sulfide nonahydrate were purchased from Acros Organics (New Jersey). Hydrochloric acid (36.5-38% w/w) was purchased from Aqua Solutions, Inc. Dissolved acetylene and compressed nitrogen (ultra high purity) were purchased AirGas (Radnor, PA).

Culture Conditions

Anaeromyxobacter dehalogenans strain 2CP-C was grown in a defined mineral salts medium (Löffler *et al.*, 1996) with the following modifications: bicarbonate was replaced with 50 mM HEPES, sodium sulfide was omitted (except where indicated), phosphate was reduced from 1.47 mM to 0.29 mM, L-cysteine was decreased from 0.2 mM to 0.1 mM, and the headspace was 100% N_2. Acetate (1 or 10 mM) served as the electron donor and was added during medium preparation. The medium was adjusted to a pH of 7.2 by the drop-wise addition of a 10 M sodium hydroxide solution. Using the

Hungate technique to avoid oxygen contamination, the medium was dispensed in 100 mL aliquots into 160 mL serum bottles with N_2 in the headspace and sealed with butyl rubber stoppers and an aluminum crimp. Filter-sterilized vitamin stock solutions were added to autoclaved serum bottles containing medium. Fe(III) citrate, NO_3^-, or N_2O served as electron acceptors and were added from anoxic, sterilized stocks (except N_2O gas, which was filter-sterilized from a gas canister). Nalgene PES syringe filters (0.2 μm) were purchased from Thermo Scientific (Rochester, NY) and used for all filter-sterilized solutions. For growth with NO_3^- as the electron acceptor, the NH_4^+ concentrations in the medium were decreased to 3 mM to allow accurate quantification of NH_4^+ generated from NO_3^-, and moles of NH_4^+ are reported as total NH_4^+ minus the 300 μmoles NH_4^+ present in the medium. In acetylene controls, 10% of the culture headspace was replaced with acetylene to inhibit N_2O conversion to N_2. All cultures were incubated without shaking at 30°C in the dark. Cultures grown in the same medium with the same electron donors and acceptors as the experimental cultures were used for the seed cultures, with the exception of Fe(III) oxyhydroxide cultures, which were inoculated from cultures grown with fumarate. All experiments used triplicate culture vessels unless indicated otherwise, and experiments were repeated in at least two independent experiments.

The Fe(III) citrate stock solution was prepared with some modifications to published procedures (Kostka and Nealson, 1998). A 1 M, rather than 5 M, Fe(III) citrate solution was prepared in 100 mL ultrapure water. Ferric citrate (24.5 g) was added to 100 mL of a 1.7 M NaOH solution, the solution boiled until it turned dark, translucent brown, and the solution was cooled. Then the solution was neutralized (pH 7.0) by the addition of a 10 M NaOH solution as described (Kostka and Nealson, 1998). The solution was dispensed into two 160 mL serum bottles and purged with N_2 gas before sealing with a rubber stopper and autoclaving. The final stock solution contained Fe(II) (approximately 0.1-0.2 M as determined by the ferrozine assay [Stookey, 1970]). Poorly crystalline Fe(III) oxide was prepared from ferric chloride hexahydrate as described (Lovley, 2013) with the exception that the Fe(III) oxide was centrifuged at 2,050 *g* and washed at least three times to remove dissolved chloride. Fe(III) oxide stocks were sterilized by daily heating in a 90°C water bath and overnight cooling at room temperature over a 5-day period. A ferrous chloride stock solution was prepared by adding 9.9 g of ferrous chloride

tetrahydrate to 100 mL of ultrapure water degassed with N_2. The stock solution was prepared in an anoxic chamber (Coy Laboratory Products, Grass Lake, MI) to avoid oxidation of the Fe(II), and was stored in N_2-gassed, sealed serum bottles after filter sterilization.

Microcosm Setup

Illinois agriculture soil was collected from an agricultural field in Havana, Illinois at 0-10 cm in September 2014. Total extractable iron in the soil samples is approximately 145 ppm. Puerto Rico soil was collected in February 2016 from the Luquillo Long-Term Ecological Research site in El Yunque National Forest. Microcosms were set up by adding soil to open medium bottles in an anoxic chamber (Coy Laboratory Products, Grass Lake, MI) with 2% hydrogen and 98% N_2, then sealing with a rubber stopper. Azide controls were prepared by adding 3 mM sodium azide from an anoxic stock solution. Heat-killed controls were by autoclaving for 40 minutes at 121°C. For microcosms with O_2, bottles were covered with a sterile aluminum foil cap instead of sealing with a rubber stopper. All microcosms were incubated at room temperature in the dark, and included acetylene to inhibit N_2O reduction.

Analytical Methods

N_2O in the headspace of cultures was quantified by injecting 1 mL headspace samples into an Agilent 3000A Micro GC with a polystyrene-divinylbenzene Plot Q column, a thermal conductivity detector, and helium as the carrier gas (Agilent Technologies, Santa Clara, CA). The column pressure and temperature were 25 psi and 50°C, respectively. Culture bottles were incubated at 30°C but were removed from the incubator during sampling. To account for cooling during sample extraction, the temperature of an uninoculated medium bottle was measured with a glass thermometer and the temperature was used to select the appropriate Ostwald coefficient. N_2O concentrations in the liquid phase were calculated using an Ostwald coefficient of 0.6788, 0.5937, or 0.5241 for temperatures of 20°C, 25°C, or 30°C, respectively (Wilhelm *et al.*, 1977). Total N_2O-N (i.e., total N_2O amounts divided by 2) in culture vessels (designated as "per vessel") is reported as the sum of the aqueous phase N_2O-N mass, the headspace

N_2O-N mass, and any N_2O-N that was removed during liquid and headspace sampling. N_2O production rates were calculated by finding the slope in the linear range of N_2O mass increases over time. Acetate was quantified by high-performance liquid chromatography (Agilent Technologies 1200 series, Santa Clara, CA) using an organic acid analysis column (Bio-Rad Aminex HPX-87H Ion Exclusion column, Hercules, CA) heated to 30°C. The eluent was 4 mM sulfuric acid prepared in ultrapure (Milli-Q, EMD-Millipore, Darmstadt, Germany) water and the flow rate was 0.6 mL per minute.

NH_4^+ was quantified with an ion chromatograph (Dionex ICS-1100) and a Dionex IonPac Cation Exchange CS16 column heated to 30°C. The eluent was 20 mM sulfuric acid and the flow rate was 1 mL per minute. NO_3^- and NO_2^- were quantified with a reagent-free ion chromatograph with eluent generation (RFIC-EG) (Dionex ICS-2100, Sunnyvale, CA) and a Dionex IonPac® AS18 4x250mm analytical column heated to 30°C. The eluent was 10 mM potassium hydroxide and the flow rate was 1 mL per minute. Acid-extractable Fe(III)/Fe(II) were measured using an alteration of the ferrozine assay (Stookey, 1970). Ferrozine buffer was made with 1 g/L Acros Organics FerroZine™ iron reagent in 50 mM HEPES buffer. Cultures were shaken vigorously by hand, suspensions withdrawn by syringe, and 100 or 500 µL was incubated overnight in 5 mL of 0.04 M sulfamic acid. Sulfamic acid was used to avoid inaccuracies of quantifying Fe(II) in the presence of NO_2^- (Klueglein and Kappler, 2013). After shaking the vial, 20 µL were withdrawn and mixed with 1 mL of ferrozine buffer. The absorbance of the resulting purple color was measured using the Thermo Scientific Spectronic 20D+ spectrophotometer at a wavelength of 562 nm. Samples were measured quickly after mixing with the ferrozine buffer to avoid possible interference of Fe(III) (Im *et al.*, 2013). For total iron measurements, 200 µL of 10% (w/v) hydroxylamine-HCl in water was added to the 5 mL sulfamic acid extractions and incubated at room temperature overnight before mixing 20 µL with 1 mL ferrozine buffer. Absorbance measurements were compared with standards made with ferrous ammonium sulfate hexahydrate. For experiments in which NO_2^- was added to Fe(III) citrate grown cultures, samples were dissolved in 0.5 M HCl, and Fe(II) concentrations are not reported when NO_2^- was present in the culture.

Cell Enumeration

Genomic DNA was extracted using the provided protocol in the MoBio PowerSoil® DNA Isolation kit (Carlsbad, CA). Cells were enumerated with qPCR using the Applied Biosystems ViiA™ 7 Real-Time PCR System. Results were analyzed with the ViiA™ 7 software (version 1.2.3). To target and enumerate the *A. dehalogenans* 16S rRNA gene, an established TaqMan assay was applied (Thomas *et al.*, 2010). The TaqMan Universal PCR Master Mix without AmpErase® uracil N-glycosylase (UNG) was used. Calibration curves were established using ten-fold serial dilutions of a plasmid carrying the *A. dehalogenans* 2CP-C 16S gene. The plasmid was extracted with the QIAprep Spin Miniprep kit. DNA concentrations were measured via the Life Technologies Qubit dsDNA BR Assay (Eugene, OR).

Genomic and Phylogenetic Analyses

Genomes from the National Center for Biotechnology Information (NCBI) (4,739 genomes) were searched for N cycle genes (i.e., *narG*, *napA*, *nirK*, *nirS*, and *nosZ*) by performing a Hidden Markov Model search with HMMER 3.1b2 (hmmer.org). Hidden Markov Models (HMMs) for NarG, NapA, NirK, NirS, and NosZ were downloaded from FunGene (Fish *et al.*, 2013). The annotated proteins of available complete bacterial genomes (i.e., labeled as "Latest" and "Complete Genome") from the NCBI Reference Sequence (RefSeq) database were downloaded in April, 2016 and used as the target files when running HMMer. HMMer was run locally using a BASH script and the hmmsearch function with a target E-value cutoff of $\leq 1x10^{-10}$. Results were parsed and analyzed using Python (https://www.python.org/). False positives were removed by searching for the absence of conserved domains visually in Geneious software suite version 8.1.9 (Kearse *et al.*, 2012) and with the Reverse Position-Specific Basic Local Alignment Tool (RPS-BLAST) (Marchler-Bauer *et al.*, 2002). The NCBI Conserved Domains Database (CDD) was downloaded in September 2016 from the NCBI FTP website (ftp://ftp.ncbi.nih.gov/pub/mmdb/cdd/little_endian/Cdd_LE.tar.gz) and used for RPS-BLAST. Proteins that did not match conserved domains (e.g., type 1 copper site and type 2 copper site for NirK) with an E-value $< 1x10^{-30}$ were excluded from further analysis.

Available bacterial 16S rRNA gene sequences containing *narG*/*napA* and *nosZ* genes, but lacking *nirK* and *nirS* genes, and 4 outgroup archaeal 16S rRNA genes were downloaded from NCBI and used to construct a phylogenetic tree. Full length 16S rRNA gene sequences were aligned with the SILVA Incremental Aligner version 1.2.11 (Yilmaz *et al.*, 2014) using default settings with unaligned bases removed from the alignment ends. Aligned positions containing only gaps were manually removed in Geneious. JModelTest 2 (Darriba *et al.*, 2012) was used to predict the optimal evolutionary model for tree reconstruction. A maximum likelihood tree was constructed with 100 bootstrap replicates with PhyML 3.0 (Guindon *et al.*, 2010) using a Generalized Time Reversible (GTR) (Tavaré, 1986) model with gamma distributed rate heterogeneity and a proportion of invariable sites.

The organisms represented in the phylogenetic tree were searched in the literature for the ability to utilize Fe(III) as a terminal electron acceptor. The numbers of *c*-type cytochrome genes per genome were approximated via bioinformatic analysis of genome sequences and were not confirmed experimentally. *c*-type cytochromes were determined by using a Python script modeled after a published script (Wagner *et al.*, 2012), which searched for the heme *c* binding motifs CxxCH, CxxxCH, and CxxxxCH in the annotated proteins of RefSeq genomes. Candidate *c*-type cytochromes were further screened by running PSI-BLAST against the nr NCBI database (downloaded in December 2016) and eliminating any sequences that did not match to annotated *c*-type cytochromes with an E-value $\leq 1x10^{-11}$.

Results

A. dehalogenans reduces NO_3^- to N_2 in the presence of Fe(II)

The addition of 100 µmoles NO_3^- to *A. dehalogenans* strain 2CP-C cultures that had reduced 480 (±20) µmoles of Fe(III) (as Fe[III] citrate) resulted in the rapid formation of 54 (±7) µmoles N_2O-N and 63 (±5) µmoles NH_4^+ (Figure 2.1A). N_2O was subsequently consumed, but was stable in replicate cultures containing acetylene, which inhibits N_2O reduction (Figure 2.1B). Stoichiometric reduction of NO_3^- to NH_4^+ was previously observed in pure cultures of *A. dehalogenans*, and the organism was

consequently classified as a non-denitrifier (Sanford *et al.*, 2002). In the presence of Fe(III) and NO_3^-, *A. dehalogenans* reduced Fe(III) to Fe(II) and NO_3^- to N_2 (Figure 2.1) and a cell increase was observed during the Fe(III) and NO_3^- reduction phases (Table 2.1; Figure 2.2). *A. dehalogenans* couples N_2O reduction with energy conservation and growth (Sanford *et al.*, 2012; Yoon *et al.*, 2016), and N_2O consumption occurred. qPCR enumeration of 16S rRNA genes could not reveal the additional increase in biomass (2.6 x 10^7 cells/mL expected from N_2O reduction after day 12) due to prior growth with Fe(III) and NO_3^- as electron acceptors (resulting in 6.0 x 10^7 cells/mL). A complicating factor for precisely enumerating gene copies was the interference of iron precipitates with DNA extraction. After Fe(III) reduction, a bright orange precipitate (Fe[III] formed from reoxidation of Fe[II]) was observed in the DNA extraction tubes. Fe(III) oxides adsorb nucleic acids thereby reducing DNA extraction efficiency (Hurt *et al.*, 2014). In the cultures lacking Fe(II) (i.e., only containing 750 nmoles Fe[II] introduced with the trace metal solution), cultures of *A. dehalogenans* reduced 200 (±10) µmoles NO_3^- to 190 (±12) µmoles NH_4^+ (Figure 2.3), which is consistent with the *A. dehalogenans* gene content and prior reports (Sanford *et al.*, 2002, 2012). The amount of N_2O-N did not exceed 1 µmole in any of the incubation vessels not amended with Fe(III) as electron acceptor (Figure 2.3). Thus, the major product of NO_3^- reduction was NH_4^+ in the absence of Fe(II) and N_2 in the presence of Fe(II).

A. dehalogenans reduces NO_2^- to N_2 in the presence of Fe(II)

Similar to NO_3^- amendment, the addition of 100 µmoles of NO_2^- to *A. dehalogenans* strain 2CP-C cultures that had consumed 100 µmoles of acetate and reduced 590 (±60) µmoles of Fe(III) resulted in rapid N_2O formation (Figure 2.4A). N_2O formation also occurred in bottles that were heat-treated prior to NO_2^- addition, indicating that the reduction of NO_2^- to N_2O was an abiotic process (Figure 2.4B). In live and killed control incubations, 113 (±2) and 109 (±9) µmoles N_2O-N were produced, respectively, indicating stoichiometric conversion of NO_2^- to N_2O.

The N_2O formed was not consumed because acetate (100 µmoles) had been depleted during the initial Fe(III) reduction phase. Following the addition of 200 µmoles of acetate on Day 18, Fe(III) reduction resumed and N_2O consumption started (Figure 2.4A).

During the initial Fe(III) and NO_2^- reduction phase, 2.1 x 10^6 cells/mL were produced, but only modest growth with N_2O as electron acceptor (i.e., 1.2 x 10^7 cells/mL) was measured due to the relative low amount of additional biomass produced (i.e., expected increase of 4.8 x 10^7 cells/mL), and interferences of iron precipitates that formed after sampling with quantitative DNA extraction (see above) (Table 2.1; Figure 2.5). In controls that were heat-killed following the initial Fe(III) reduction phase, the microbially produced Fe(II) reacted with NO_2^- leading to the formation of stoichiometric amounts of N_2O, but N_2O was stable even after acetate addition, indicating that live cells were required for N_2O reduction to occur (Figure 2.4B). Live and heat-killed cultures produced N_2O at similar rates of 1.9 (±0.03) and 1.9 (±0.13) μmoles h^{-1}, respectively (Figure 2.4A and 2.4B), whereas lower N_2O formation rates of 1.3 (±0.04) μmoles h^{-1} were measured in abiotic control incubations (800 μmoles of ferrous chloride, 100 μmoles of NO_2^-, and no cells) (Figure 2.6). These findings suggest that equimolar concentrations of microbially produced Fe(II) are more reactive than Fe(II) added as ferrous chloride. NO_2^- reduction was also monitored in *A. dehalogenans* cultures that had reduced 250 (±7) μmoles poorly crystalline Fe(III) oxyhydroxide (Figure 2.7) or 960 (±50) μmoles soluble Fe(III) (as ferric citrate; data not shown) in medium containing 0.2 mM sulfide. With insoluble and soluble forms of Fe(III), 35 (±4) and 47 (±8) μmoles N_2O-N was produced, respectively, during the reduction of 100 μmoles NO_2^-, but N_2O was not subsequently consumed by *A. dehalogenans* (Figure 2.7). Cultures of *A. dehalogenans* consistently used N_2O as a respiratory electron acceptor in defined, anoxic medium without sulfide (Figure 2.8). When 0.2 mM sulfide was included in the medium as a reductant, cultures did not reduce N_2O (Figure 2.8), despite the ability of *A. dehalogenans* to grow with other electron acceptors (e.g., NO_3^- and Fe[III]) in the presence of 0.2 mM sulfide.

Twenty-seven RefSeq genomes lacking NO-forming NO_2^- reductases show potential for denitrification

The term "chemodenitrifier" is proposed here to describe organisms that combine chemodenitrification and enzymatic reactions to reduce NO_3^- to N_2O or N_2 (i.e., denitrification that is independent of NO-forming NO_3^- reductases). Although the chemodenitrifier phenotype does not exclude organisms with a full ($NO_3^- \rightarrow N_2$) or partial

($NO_3^- \rightarrow NO/N_2O$) denitrification pathway, a search was conducted for potential chemodenitrifiers that encode *nosZ* genes and lack *nirK*/*nirS*. Chemodenitrifiers lacking *nirK*/*nirS* and encoding *nosZ* would occupy the novel ecological niche of complete NO_3^- reduction to N_2 in the absence of NO-forming NO_2^--reductases. Translated RefSeq genomes were searched for genomes that contain NO_3^- reductase amino acid sequences (i.e., NarG or NapA) and N_2O reductase amino acid sequences (i.e., NosZ) but lack NirK and NirS. Fifty-one genomes fit these criteria, and represent organisms from diverse bacterial groups (Figure 2.9). The potential chemodenitrifiers were isolated from a wide variety of habitats, including freshwater, saltwater, soil, contaminated material, and hot springs (Figure 2.9; Table 2.2). Sixteen genomes contained clade I NosZ sequences, while 35 genomes contained clade II NosZ sequences. At least seven organisms including *Aeromonas media*, four *Anaeromyxobacter* strains, *Desulfitobacterium hafniense*, and *Rhodoferax ferrireducens* were all shown to reduce Fe(III) (Figure 2.9; Table 2.2). Since many organisms are not tested for the ability to reduce Fe(III), the genomes were searched for *c*-type cytochromes with multiple heme-binding domains, a shared trait of iron-reducing bacteria (Shi *et al.*, 2007). All genomes contain 15 or more putative *c*-type cytochromes, and in 27 genomes at least six of the *c*-type cytochromes have four or more heme-binding domains (Figure 2.9).

Agricultural and tropical soils demonstrate chemodenitrification

Approximately 30 μmoles NO_2^- was quickly reduced to N_2O in microcosms containing Illinois agricultural soil with and without O_2 (Figure 2.10). NO_2^- added to anoxic microcosms that were simultaneously killed via autoclaving or azide addition showed slower and non-stoichiometric N_2O production (Figure 2.10). Soil-free controls containing medium, azide, and NO_2^- did not show NO_2^- consumption or N_2O production. (Figure 2.10). NO_2^- was completely consumed and some NH_4^+ was produced in all microcosms containing soil, except in the heat-killed and soil-free controls (Figure 2.10b).

Abiotic N_2O production was greater in microcosms with added Fe(III) and in microcosms with Puerto Rico soil. Stoichiometric NO_2^- reduction to N_2O was observed in microcosms containing 5 g Illinois soil (Figure 2.11). Only 6 μmoles N_2O was produced

in controls treated with azide before NO_2^- addition. To test the effect of added iron on N_2O production, separate microcosms were provided with 5 mM poorly crystalline iron oxides. After visible iron reduction (1.5 months), azide was added to control cultures, and 2 days later 100 μmoles NO_2^- was added. Similar concentrations of N_2O were produced in microcosms with added iron as compared with soil alone (Figure 2.11a). Approximately 50% of NO_2^- was reduced to N_2O in the azide controls with added iron (Figure 2.11). NO_2^- was completely consumed in microcosms without added Fe(III) and azide (Figure 2.11b), and no NH_4^+ was produced in the presence or absence of azide (Figure 2.11c). NO_2^- and NH_4^+ were not measured in microcosms with added ferric oxyhydroxide. Microcosms with 1 g Puerto Rico soil reduced approximately 50% of NO_2^- to N_2O (54 μmoles N_2O-N) in azide-free treatments (Figure 2.11c). N_2O production was slower in microcosms treated with azide, and only 25 μmoles N_2O was produced.

Discussion

This study reveals a novel ecological niche for *A. dehalogenans* strain 2CP-C. Previous growth studies characterized *A. dehalogenans* as a NO_3^--reducing ammonifier not able to reduce NO_2^- to NO but with the ability to reduce N_2O to N_2 (Sanford *et al.*, 2002, 2012). Genome analyses corroborated these observations and no genetic potential for NO_2^- reduction to NO (i.e., *nirS* or *nirK*) was found on the genome (Thomas *et al.*, 2008). Prior pure culture studies were performed with single electron acceptors and potential synergistic effects were not considered. The results presented here demonstrate that Fe(III) reduction profoundly affects NO_3^- and NO_2^- metabolism in *A. dehalogenans*. *A. dehalogenans* reduced NO_3^- to NO_2^- and N_2O to N_2, while Fe(II) abiotically reduced NO_2^- to N_2O. Complete NO_3^- reduction to N_2 was observed as the result of a combination of abiotic and biotic reactions in *A. dehalogenans* cultures, indicating that cultivation on single electron acceptors and genome analysis failed to capture the full metabolic potential of *A. dehalogenans*. Additionally, the present experiments were performed in closed systems. In the natural environment, N_2O may diffuse away from *A. dehalogenans* before complete reduction to N_2, suggesting that *A. dehalogenans* may contribute to N_2O emissions.

Due to a versatile metabolism, *A. dehalogenans* is an ecologically competitive bacterium. Previous studies uncovered a novel clade of *nosZ* genes (clade II) with sequences distinct from clade I *nosZ* gene, and demonstrated growth of *A. dehalogenans* coupled to N_2O reduction via the clade II NosZ (Sanford *et al.*, 2012; Yoon *et al.*, 2016). Additionally, it was shown that the clade II NosZ lends greater growth yield than clade I NosZ enzymes and that clade II NosZ has a greater affinity for N_2O than clade I NosZ, suggesting that organisms with clade II NosZ (such as *A. dehalogenans*) may outcompete organisms with clade I NosZ (Yoon *et al.*, 2016). The present study reveals further ecological advantages for *A. dehalogenans*. Chemodenitrification prevents *A. dehalogenans* from coupling growth to NO_2^- reduction in the presence of Fe(II), but per electron, *A. dehalogenans* captures more energy with N_2O reduction than NO_2^- reduction (Table 2.3). Additionally, the reaction between NO_2^- and Fe(II) yields Fe(III), and the generated Fe(III) provides an additional electron acceptor for *A. dehalogenans*. It is interesting to note that sulfide prevents N_2O reduction (Figure 2.7; Figure 2.8), likely due to the sequestration of copper by sulfide (Manconi *et al.*, 2006). Thus N_2O, rather than N_2, may be the end product in biomes with free sulfide. Interestingly, *A. dehalogenans* did not reduce Fe(III) oxyhydroxide very well in the absence of sulfide (data not shown). This may be due to a high redox potential of the medium, or *A. dehalogenans* may require sulfide for the reduction of insoluble Fe(III). Sulfide was shown to reduce Fe(III) and possibly serve as an electron shuttle (Flynn *et al.*, 2014; Hansel *et al.*, 2015). Further experimentation is required to explore the possibility that *A. dehalogenans* uses sulfide as an electron shuttle. Collectively, the experiments demonstrate that the non-denitrifier *A. dehalogenans* can reduce NO_3^- to N_2 in the presence of Fe(II), and gain more energy than from respiratory ammonification.

The coupled biotic-abiotic reactions in NO_3^-- and Fe(III)-reducing *A. dehalogenans* cultures reveal an important ecological role for organisms that have *nosZ*. Fe(II) and NO_3^- co-occur in natural environments, allowing interactions between N and iron cycling (Melton *et al.*, 2014) and suggesting that the observation of microbially mediated chemodenitrification is not limited to pure cultures of *A. dehalogenans*. The amount of iron in soil ranges from 100 to 100,000 parts per million (ppm), and in addition to Fe(III) serving as an abundant electron acceptor in anoxic soils, Fe(III) and

Fe(II) cycling commonly occurs near oxic-anoxic transition zones, thus replenishing Fe(III) for further dissimilatory Fe(III) reduction (Shacklette and Boerngen, 1984; Thamdrup, 2000; Cornell and Schwertmann, 2003; Roden *et al.*, 2012). Dissimilatory Fe(III)-reducing bacteria such as *A. dehalogenans* and *Geobacter* spp. are abundant in soils and subsurface environments (Petrie *et al.*, 2003; Lovley, 2013). NO_2^- is released only temporarily during NO_3^- reduction and ammonia oxidation (Betlach and Tiedje, 1981; Matocha *et al.*, 2012), but NO_2^- can accumulate for weeks to months in both alkaline and neutral soils (Cleemput and Samater, 1996; Gelfand and Yakir, 2008). Additionally, the enzyme kinetics of NO_3^- and NO_2^- reductases vary by organism, and for organisms in which the NO_3^- reduction rate is greater than the NO_2^- reduction rate, intermediate NO_2^- is formed before further reduction (Betlach and Tiedje, 1981). Even in conditions where NO_2^- does not accumulate, Fe(II) and NO_2^- are likely to interact. Since Fe(III) is insoluble at neutral pH, Fe(III) reduction occurs via chelated iron, electron shuttles, or direct contact with Fe(III), and Fe(II) is produced either outside of the cell or in the periplasm (Lovley *et al.*, 2004). Since Fe(II) is not produced inside the cytoplasm, it is reasonable to assume that NO_2^- must be in the periplasm or outside of the cell in order for chemodenitrification to occur. The genome of *A. dehalogenans* encodes two NO_3^- reductases: NarG (an inner-membrane bound NO_3^- reductase) and NapA (a periplasmic NO_3^- reductase). Additionally, the genome of *A. dehalogenans* encodes NarK, a NO_3^-/NO_2^- transporter, so NO_2^- produced by either NO_3^- reductase can be located in the periplasm. Since NO_2^- reductases (NrfA, NirS, and NirK) are also located in the periplasm, chemodenitrification competes with enzymatic NO_2^- reduction. The competition between abiotic and biotic reduction of NO_2^- is evidenced by the mixed end products (i.e., N_2O and NH_4^+) produced during NO_3^- reduction by *A. dehalogenans* (Figure 2.1). A microbial community with Fe(III)- and NO_3^--reducing microorganisms could facilitate chemodenitrification, especially in conditions where NO_2^- is not consumed immediately after NO_3^- reduction. As NO_3^--reducing microorganisms generate NO_2^-, NO_2^- can react with Fe(II) produced by iron reducing microorganisms. Chemodenitrification may result in the loss of NO_2^- as an electron acceptor; however, organisms with N_2O-reductases would be able to utilize the resulting N_2O as an electron

acceptor. The possession of the *nosZ* gene in Fe-rich environments would confer an ecological advantage.

Organisms that combine chemodenitrification and NO_x reduction in a similar manner to *A. dehalogenans* fill a previously unrecognized ecological niche. The term "chemodenitrifiers" is proposed to describe microorganisms that utilize chemodenitrification to reduce NO_3^- to N_2O or N_2. Chemodenitrification simply describes an abiotic decomposition of NO_2^-, whereas "chemodenitrifier" describes a microorganism that reduces NO_3^- to N_2O or N_2 via multiple enzymatic steps and at least one abiotic step. These organisms may be true denitrifiers (i.e., having NO-producing NO_2^- reductases) that reduce NO_2^- to N_2O in the absence of Fe(II) and utilize chemodenitrification in the presence of Fe(II), or non-denitrifiers that can only denitrify in the presence of Fe(II). Past studies have examined the co-occurrence of *nirK*, *nirS*, and *nosZ* in sequenced genomes, confirming that denitrification is modular and many genomes contain *nosZ* but lack *nirK* and *nirS* (Sanford *et al.*, 2012; Graf *et al.*, 2014). The observations of chemodenitrification in *A. dehalogenans* cultures reveal a possible ecophysiological explanation for microorganisms that possess *nosZ* but not *nirS* and *nirK.* To search for non-denitrifying microorganisms that share the chemodenitrifying trait of *A. dehalogenans*, the genome analysis performed in this study searched for non-denitrifiers (i.e., lack *nirS* or *nirK*) that have both a N_2O reductase and a NO_3^- reductase, then further probed for Fe(III)-reducing potential (Figure 2.9; Table 2.2). Since many organisms have not been tested for Fe(III) reduction, the number of *c*-type cytochromes with multiple heme-binding domains was used to indicate potential for Fe(III) reduction. In addition to seven known Fe(III)-reducing bacteria (including *A. dehalogenans* strain 2CP-C), 20 genomes contained six or more *c*-type cytochromes with at least four heme-binding domains. Although the complete set of proteins for Fe(III) reduction has not yet been characterized, it is known that a suite of *c*-type cytochromes (typically with four or more hemes) play a role in Fe(III) reduction (Lovley *et al.*, 2004; Shi *et al.*, 2007). Organisms with an abundance of multiheme *c*-type cytochromes are promising candidates for Fe(III) reduction and should be tested for the ability to reduce Fe(III). Overall, at least 27 organisms from diverse branches of the phylogenetic tree have potential for the chemodenitrifier trait. The chemodenitrifier potential is only a prediction based on

genome sequence analysis, and further tests are needed to confirm the physiology of the analyzed organisms. Utilizing protein prediction by sequence analysis is limited, since some proteins with very different functions can have remarkably similar protein sequences. For example, the active sites of NapA and formate dehydrogenase (FDH) are very similar, but a cysteine and a methionine residue in NapA are replaced by a selenocysteine residue and a methionine residue in FDHs, respectively (Cerqueira *et al.*, 2015). Due to the similarity between Nap, Nar, and FDH, Hidden Markov Model searches for NapA and NarG yield many hits to annotated formate dehydrogenases. To eliminate FDH matches, proteins were analyzed with RPS-BLAST and any proteins with better (i.e., lower E-value) matches to FDH domains than Nap/Nar domains were removed from the analysis. However, the confirmation of the chemodenitrifier trait is best confirmed by pure culture study.

The chemodenitrifier lifestyle was also demonstrated in NO_3^--reducing cultures of *Escherichia coli*, *Shewanella putrefaciens* strain 200, and *Wolinella succinogenes*. NO_3^--reducing cultures of *E. coli* were shown to abiotically produce N_2O through chemodenitrification when Fe(II) was present in the medium (Brons *et al.*, 1991). Cultures of *S. putrefaciens* were also shown to produce N_2O during NO_3^- and Fe(III) reduction though combined abiotic and biotic reactions (Cooper *et al.*, 2003). In contrast to the work with *A. dehalogenans*, N_2O was the end product in experiments with *E. coli* and *S. putrefaciens* strain 200. N_2O production and subsequent consumption was also demonstrated with NO_3^--replete cultures of *W. succinogenes*, a respiratory ammonifier, although NO_2^- was the main end product and only 0.15% of the NO_3^- was reduced to N_2O (Luckmann *et al.*, 2014). Like *Anaeromyxobacter*, *W. succinogenes* lacks *nirK/nirS*, and it was speculated that N_2O was produced through NO detoxification and reactions of NO_2^- with medium components (Luckmann *et al.*, 2014). When *A. dehalogenans* was grown with 200 µmoles NO_3^-, approximately 1 µmole N_2O-N was produced (less than 1% of NO_3^-) (Figure 2.3), which may be due to a reaction with the 750 nmoles iron included in the medium (from the trace metal solution). In the presence of Fe(II), *A. dehalogenans* produces substantial amounts of N_2O (i.e., greater than 50%) from available NO_3^- or NO_2^-, and has the enzymatic capability of subsequently reducing the N_2O to N_2 gas. In contrast to studies with *E. coli*, *S putrefaciens*, and *W. succinogenes*,

the present study demonstrates that a microorganism lacking NO-forming NO_2^- reductases can completely denitrify a substantial percentage of NO_3^-.

NO_2^- added to soil microcosms demonstrated chemodenitrification (i.e., N_2O production from killed soil). However, N_2O production was consistently slower in heat-killed and azide-treated controls as compared to untreated soil (Figures 2.10 and 2.11). This would suggest that biological NO_2^- reduction outcompetes chemodenitrification. Past studies have suggested that chemodenitrification does not play a significant role in NO_2^- turnover in soil due to the low concentration of reactive Fe(II) (Bremner, 1997); however, many of the studies supporting that hypothesis are performed by sterilizing soil (Zhu-Barker *et al.*, 2015). In addition to potentially altering soil chemistry, sterilizing the soil by autoclaving or adding toxic substrates inhibits dissimilatory iron-reducing bacteria (DIRB). It is well-known that Fe(III) and Fe(II) are cycled many times over by DIRB and iron-oxidizing bacteria (Thamdrup, 2000; Roden *et al.*, 2012). In the environment, Fe(III) produced by chemodenitrification can be reduced to Fe(II) by DIRB, thus replenishing the Fe(II) for further chemodenitrification (Figure 2.12a). In past experiments and the experiments presented here, DIRB were inhibited by autoclaving or azide addition; thus, any Fe(III) produced by chemodenitrification cannot be recycled to Fe(II) for further chemodenitrification (Figure 2.12b). This is supported by the fact that increased iron content yielded greater chemodenitrification (Figure 2.11). Future experiments assessing the role of chemodenitrification in soils should seek to use techniques that account for Fe(III) recycling. One potential approach is to assess the isotopic fractionation of N_2O or isotopic site preference of N_2O. If these values are influenced by the source of N_2O (i.e., biotic or abiotic), they may be used as markers of N_2O sources. However, the literature contains inconsistent values between different laboratories, and further troubleshooting is required to refine this technique (Cooper *et al.*, 2003; Heil *et al.*, 2014; Jones *et al.*, 2015; Zhu-Barker *et al.*, 2015).

The microcosm experiments shown here have some important limitations. Microcosms containing O_2 were sealed before NO_2^- addition and were not shaken, and the bottles contained a thick layer of soil (i.e., 20 g in a 30 mL bottle), so full oxygenation throughout the bottle was not ensured. It is likely that an O_2 gradient was established in these cultures, and although O_2 was present in the headspace throughout the experiment

(data not shown), microorganisms in the bottom of the serum bottles may have experienced anoxia. Another shortcoming is that NH_4^+ was produced in the azide-added soil microcosms, suggesting that respiratory ammonification still occurred (Figure 2.10c). It is possible that the concentration of azide (3 mM) was not sufficient to fully inhibit microbial activity, especially in the microcosms containing O_2, which likely had a high cell number. However, N_2O production was observed in heat-killed microcosms that were autoclaved in an autoclave certified for soil sterilization, lending support for N_2O production by abiotic mechanisms. Overall, these experiments demonstrate the potential for chemodenitrification in soil, but more sophisticated techniques, such as isotopic fractionation (Jones *et al.* 2015; Buchwald *et al.* 2016) are required to determine the relative contribution of biotic and abiotic processes to N_2O production in soils.

Collectively, the findings show complete NO_3^- reduction to N_2 mediated by a single organism via combined abiotic and biotic mechanisms in the absence of *nirS* and *nirK*. Gene content is not sufficient to predict the final products of NO_3^- reduction, putting into question attempts to link denitrification activity with the abundance and expression of *nirS* and *nirK*. Chemodenitrifiers represent understudied contributors to the formation of gaseous products from NO_3^- and NO_2^- and careful study of chemodenitrifiers may impact the current understanding of N cycling. Studies of N cycling in soils should take into account the concentration of iron and the presence of iron-reduction to determine the potential for chemodenitrification. Non-denitrifiers lacking *nirS* or *nirK* but possessing *nosZ* and *napA*/*narG* contribute to N_2O flux via coupled biotic-abiotic processes, suggesting that iron-reducing potential should be taken into consideration when prediction the fate of NO_3^- in soils.

Acknowledgments

This work was supported by the US Department of Energy, Office of Biological and Environmental Research, Genomic Science Program, Award DE-SC0006662.

We would like to thank Steven Higgins and Luis Orellana for helpful discussions.

References

Betlach MR, Tiedje JM. (1981). Kinetic explanation for accumulation of nitrite, nitric oxide, and nitrous oxide during bacterial denitrification. *Appl Environ Microbiol* **42**: 1074–1084.

Bonilla-Rosso G, Wittorf L, Jones CM, Hallin S. (2016). Design and evaluation of primers targeting genes encoding NO-forming nitrite reductases: implications for ecological inference of denitrifying communities. *Sci Rep* **6**: 1–8.

Bremner JM. (1997). Sources of nitrous oxide in soils. *Nutr Cycl Agroecosystems* **49**: 7–16.

Brons HJ, Hagen WR, Zehnder AJB. (1991). Ferrous iron dependent nitric oxide production in nitrate reducing cultures of *Escherichia coli*. *Arch Microbiol* **155**: 341–347.

Buchwald C, Grabb K, Hansel CM, Wankel SD. (2016). Constraining the role of iron in environmental nitrogen transformations: Dual stable isotope systematics of abiotic NO_2^- reduction by Fe(II) and its production of N_2O. *Geochim Cosmochim Acta* **186**: 1–12.

Cerqueira NMFSA, Gonzalez PJ, Fernandes PA, Moura JJG, Ramos MJ. (2015). Periplasmic nitrate reductase and formate dehydrogenase: Similar molecular architectures with very different enzymatic activities. *Acc Chem Res* **48**: 2875–2884.

Cleemput O Van, Samater AH. (1996). Nitrite in soils: accumulation and role in the formation of gaseous N compounds. *Fertil Res* **45**: 81–89.

Cooper DC, Picardal FW, Schimmelmann A, Coby AJ. (2003). Chemical and biological interactions during nitrate and goethite reduction by *Shewanella putrefaciens* 200. *Appl Environ Microbiol* **69**: 3517–3525.

Cornell RM, Schwertmann U. (2003). The Iron Oxides: Structure, Properties, Reactions, Occurences and Uses. 2nd ed. Wiley-VCH: Weinheim.

Dandie CE, Burton DL, Zebarth BJ, Henderson SL, Trevors JT, Goyer C. (2008).

Changes in bacterial denitrifier community abundance over time in an agricultural field and their relationship with denitrification activity. *Appl Environ Microbiol* **74**: 5997–6005.

Darriba D, Taboada GL, Doallo R, Posada D. (2012). jModelTest 2: more models, new heuristics and parallel computing. *Nat Meth* **9**: 772.

Etique M, Jorand FP a, Zegeye A, Grégoire B, Despas C, Ruby C. (2014). Abiotic process for Fe(II) oxidation and green rust mineralization driven by a heterotrophic nitrate reducing bacteria (*Klebsiella mobilis*). *Environ Sci Technol* **48**: 3742–51.

Fan X, Yu H, Wu Q, Ma J, Xu H, Yang J, *et al.* (2016). Effects of fertilization on microbial abundance and emissions of greenhouse gases (CH_4 and N_2O) in rice paddy fields. *Ecol Evol* **6**: 1–10.

Fields S. (2004). Global nitrogen; Cycling out of control. *Environ Health Perspect* **112**: A556–A563.

Finlayson-Pitts BJ, Pitts Jr. JN. (2000). Chemistry of the upper and lower atmosphere: theory, experiments and applications. Academic Press: San Diego, CA.

Fish JA, Chai B, Wang Q, Sun Y, Brown CT, Tiedje JM, *et al.* (2013). FunGene: The functional gene pipeline and repository. *Front Microbiol* **4**: 1–14.

Flynn TM, O'Loughlin EJ, Mishra B, Dichristina TJ, Kemner KM. (2014). Sulfur-mediated electron shuttling during bacterial iron reduction. *Science* **344**: 1039–1042.

Gelfand I, Yakir D. (2008). Influence of nitrite accumulation in association with seasonal patterns and mineralization of soil nitrogen in a semi-arid pine forest. *Soil Biol Biochem* **40**: 415–424.

Graf DRH, Jones CM, Hallin S. (2014). Intergenomic comparisons highlight modularity of the denitrification pathway and underpin the importance of community structure for N_2O emissions. *PLoS Biol* **9**: 1–20.

Guindon S, Dufayard J-F, Lefort V, Anisimova M, Hordijk W, Gascuel O. (2010). New algorithms and methods to estimate maximum-likelihood phylogenies: Assessing

the performance of PhyML 3.0. *Syst Biol* **59**: 307–321.

Hansel CM, Lentini CJ, Tang Y, Johnston DT, Wankel SD, Jardine PM. (2015). Dominance of sulfur-fueled iron oxide reduction in low-sulfate freshwater sediments. *ISME J* 1–13.

He Q, Sanford RA. (2003). Characterization of Fe(III) reduction by chlororespiring *Anaeromxyobacter dehalogenans*. *Appl Environ Microbiol* **69**: 2712–2718.

Heil J, Wolf B, Brüggemann N, Emmenegger L, Tuzson B, Vereecken H, *et al.* (2014). Site-specific ^{15}N isotopic signatures of abiotically produced N_2O. *Geochim Cosmochim Acta* **139**: 72–82.

Henderson SL, Dandie CE, Patten CL, Zebarth BJ, Burton DL, Trevors JT, *et al.* (2010). Changes in denitrifier abundance, denitrification gene mRNA levels, nitrous oxide emissions, and denitrification in anoxic soil microcosms amended with glucose and plant residues. *Appl Environ Microbiol* **76**: 2155–2164.

Higgins SA, Welsh A, Orellana LH, Konstantinidis KT, Chee-Sanford JC, Sanford RA, *et al.* (2016). Detection and diversity of fungal nitric oxide reductase genes (p450nor) in agricultural soils. *Appl Environ Microbiol* **82**: 2919–2928.

Hurt RA, Robeson MS, Shakya M, Moberly JG, Vishnivetskaya TA, Gu B, *et al.* (2014). Improved yield of high molecular weight DNA coincides with increased microbial diversity access from iron oxide cemented sub-surface clay environments. *PLoS One* **9**: 1–13.

Im J, Lee J, Löffler FE. (2013). Interference of ferric ions with ferrous iron quantification using the ferrozine assay. *J Microbiol Methods* **95**: 366–367.

Jones CM, Graf DRH, Bru D, Philippot L, Hallin S. (2013). The unaccounted yet abundant nitrous oxide-reducing microbial community: a potential nitrous oxide sink. *ISME J* **7**: 417–26.

Jones LC, Peters B, Lezama Pacheco JS, Casciotti KL, Fendorf S. (2015). Stable isotopes and iron oxide mineral products as markers of chemodenitrification. *Environ Sci Technol* **49**: 3444–3452.

Kearse M, Moir R, Wilson A, Stones-Havas S, Cheung M, Sturrock S, *et al.* (2012). Geneious Basic: An integrated and extendable desktop software platform for the organization and analysis of sequence data. *Bioinformatics* **28**: 1647–1649.

Klueglein N, Kappler A. (2013). Abiotic oxidation of Fe(II) by reactive nitrogen species in cultures of the nitrate-reducing Fe(II) oxidizer *Acidovorax* sp. BoFeN1 – questioning the existence of enzymatic Fe(II) oxidation. *Geobiology* **11**: 180–190.

Kostka J, Nealson KH. (1998). Iron- and manganese-reducing bacteria. In: Burlage RS, Atlas R, Stahl D, Geesey G, Sayler G (eds). *Techniques in Microbial Ecology*. Oxford University Press, Inc.: New York, p 64.

Lashof DA, Ahuja DR. (1990). Relative contributions of greenhouse gas emissions to global warming. *Nature* **344**: 529–531.

Lee SH, Kang H. (2015). The activity and community structure of total bacteria and denitrifying bacteria across soil depths and biological gradients in estuary ecosystem. *Appl Microbiol Biotechnol* **100**: 1999–2010.

Löffler FE, Sanford RA, Tiedje JM. (1996). Initial characterization of a reductive dehalogenase from *Desulfitobacterium chlororespirans* Co23. *Appl Environ Microbiol* **62**: 3809–13.

Lovley D. (2013). Dissimilatory Fe(III)- and Mn(IV)-reducing prokaryotes. In: Rosenberg E, DeLong EF, Lory S, Stackebrandt E, Thompson F (eds). *The Prokaryotes*. Springer Berlin Heidelberg: Berlin Heidelberg, pp 287–308.

Lovley DR, Holmes DE, Nevin KP. (2004). Dissimilatory Fe(III) and Mn(IV) reduction. In: Poole RK (ed) Vol. Volume 49. *Advances in Microbial Physiology*. Academic Press: London, pp 219–286.

Luckmann M, Mania D, Kern M, Bakken LR, Frostegard A, Simon J. (2014). Production and consumption of nitrous oxide in nitrate-ammonifying *Wolinella succinogenes* cells. *Microbiology* **160**: 1749–1759.

Luo Y, Su B, Currie WS, Dukes JS, Finzi A, Hartwig U, *et al.* (2004). Progressive nitrogen limitation of ecosystem responses to rising atmospheric carbon dioxide.

Bioscience **54**: 731–739.

Ma WK, Bedard-Haughn A, Siciliano SD, Farrell RE. (2008). Relationship between nitrifier and denitrifier community composition and abundance in predicting nitrous oxide emissions from ephemeral wetland soils. *Soil Biol Biochem* **40**: 1114–1123.

Manconi I, van der Maas P, Lens P. (2006). Effect of copper dosing on sulfide inhibited reduction of nitric and nitrous oxide. *Nitric Oxide* **15**: 400–407.

Marchler-Bauer A, Panchenko AR, Shoemaker BA, Thiessen PA, Geer LY, Bryant SH. (2002). CDD: A database of conserved domain alignments with links to domain three-dimensional structure. *Nucleic Acids Res* **30**: 281–283.

Matocha CJ, Dhakal P, Pyzola SM. (2012). The role of abiotic and coupled biotic/abiotic mineral controlled redox processes in nitrate reduction. In: *Advances in Agronomy*. Elsevier Inc.: San Diego, CA, pp 181–214.

Melton ED, Stief P, Behrens S, Kappler A, Schmidt C. (2014). High spatial resolution of distribution and interconnections between Fe- and N-redox processes in profundal lake sediments. *Environ Microbiol* **16**: 3287–3303.

Moraghan JT, Buresh RJ. (1977). Chemical reduction of nitrite and nitrous oxide by ferrous iron. *Soil Sci Soc Am J* **41**: 47–50.

Morales SE, Cosart T, Holben WE. (2010). Bacterial gene abundances as indicators of greenhouse gas emission in soils. *ISME J* **4**: 799–808.

Orellana LH, Rodriguez-R LM, Higgins S, Chee-Sanford JC, Sanford RA, Ritalahti KM, *et al.* (2014). Detecting nitrous oxide reductase (*nosZ*) genes in soil metagenomes: method development and implications for the nitrogen cycle. *MBio* **5**: 1–8.

Petrie L, North NN, Dollhopf SL, Balkwill DL, Kostka JE. (2003). Enumeration and characterization of iron(III)-reducing microbial communities from acidic subsurface sediments contaminated with uranium(VI). *Appl Environ Microbiol* **69**: 7467–7479.

Rakshit S, Matocha CJ, Haszler GR. (2005). Nitrate reduction in the presence of wüstite. *J Environ Qual* **34**: 1286–1292.

Ravishankara AR, Daniel JS, Portmann RW. (2009). Nitrous oxide (N_2O): The dominant ozone-depleting substance emitted in the 21st century. *Science* **326**: 123–125.

Roden EE, McBeth JM, Blöthe M, Percak-Dennett EM, Fleming EJ, Holyoke RR, *et al.* (2012). The microbial ferrous wheel in a neutral pH groundwater seep. *Front Microbiol* **3**: 1–18.

Sanford RA, Cole JR, Tiedje JM. (2002). Characterization and description of *Anaeromyxobacter dehalogenans* gen. nov., sp. nov., an aryl-halorespiring facultative anaerobic myxobacterium. *Appl Environ Microbiol* **68**: 893–900.

Sanford RA, Wagner DD, Wu Q, Chee-Sanford JC, Thomas SH, Cruz-García C, *et al.* (2012). Unexpected nondenitrifier nitrous oxide reductase gene diversity and abundance in soils. *Proc Natl Acad Sci U S A* **109**: 19709–14.

Shacklette HT, Boerngen J. (1984). Element concentrations in soils and other surficial materials of the conterminous United States.

Shi L, Squier TC, Zachara JM, Fredrickson JK. (2007). Respiration of metal (hydr)oxides by *Shewanella* and *Geobacter*: A key role for multihaem *c*-type cytochromes. *Mol Microbiol* **65**: 12–20.

Stein LY. (2011). Surveying N_2O-producing pathways in bacteria. In: Vol. 486. *Methods in Enzymology*. pp 131–152.

Stookey LL. (1970). Ferrozine-a new spectrophotometric reagent for iron. *Anal Chem* **42**: 779–781.

Tavaré S. (1986). Some probabilistic and statistical problems in the analysis of DNA sequences. In: Miura RM (ed). *Lectures on Mathematics in the Life Sciences*. American Mathematical Society: Providence, RI, pp 57–86.

Thamdrup B. (2000). Bacterial manganese and iron reduction in aquatic sediments. In: Vol. 16. *Advances in Microbial Ecology*. pp 41–84.

Thomas SH, Sanford R a, Amos BK, Leigh MB, Cardenas E, Löffler FE. (2010). Unique ecophysiology among U(VI)-reducing bacteria as revealed by evaluation of oxygen metabolism in *Anaeromyxobacter dehalogenans* strain 2CP-C. *Appl Environ*

Microbiol **76**: 176–83.

Thomas SH, Wagner RD, Arakaki AK, Skolnick J, Kirby JR, Shimkets LJ, *et al.* (2008). The mosaic genome of *Anaeromyxobacter dehalogenans* strain 2CP-C suggests an aerobic common ancestor to the delta-proteobacteria. *PLoS One* **3**: 1–12.

Wagner DD, Hug LA, Hatt JK, Spitzmiller MR, Padilla-Crespo E, Ritalahti KM, *et al.* (2012). Genomic determinants of organohalide-respiration in *Geobacter lovleyi*, an unusual member of the *Geobacteraceae*. *BMC Genomics* **13**: 1–17.

Wallenstein MD, Myrold DD, Firestone M, Voytek M. (2006). Environmental controls on denitrifying communities and denitrification rates: Insights from molecular methods. *Ecol Appl* **16**: 2143–2152.

Wei W, Isobe K, Nishizawa T, Zhu L, Shiratori Y, Ohte N, *et al.* (2015). Higher diversity and abundance of denitrifying microorganisms in environments than considered previously. *ISME J* **9**: 1954–1965.

Wilhelm E, Battino R, Wilcock RJ. (1977). Low-pressure solubility of gases in liquid water. *Chem Rev* **77**: 219–262.

Yilmaz P, Parfrey LW, Yarza P, Gerken J, Pruesse E, Quast C, *et al.* (2014). The SILVA and All-species Living Tree Project (LTP) taxonomic frameworks. *Nucleic Acids Res* **42**: D643–D648.

Yoon S, Nissen S, Park D, Sanford RA, Löffler FE. (2016). Nitrous oxide reduction kinetics distinguish bacteria harboring clade I NosZ from those harboring clade II NosZ. *Appl Environ Microbiol* **82**: 3793–3800.

Zhu-Barker X, Cavazos AR, Ostrom NE, Horwath WR, Glass JB. (2015). The importance of abiotic reactions for nitrous oxide production. *Biogeochemistry* **126**: 251–267.

Zhu X, Silva LCR, Doane TA, Horwath WR. (2013). Iron: The forgotten driver of nitrous oxide production in agricultural soil. *PLoS One* **8**: e60146.

Appendix: Tables

Table 2.1. Cell growth of *A. dehalogenans* during Fe(III) and NO_3^- reduction. qPCR data corresponding to Figures 2.1 and 2.4. The standard deviations of triplicate cultures are indicated in parentheses.

Corresponding Figure	Cells per mL			
	Initial*	After Fe^{2+} Production	After NO_3^-/NO_2^- Reduction	After N_2O Consumption
1A	4.8×10^3 (1.5×10^3)	5.6×10^6 (2.0×10^6)	6.0×10^7 (2.5×10^7)	3.3×10^7 (1.4×10^7)
1B	7.8×10^3 (3.2×10^3)	8.4×10^6 (3.9×10^6)	4.4×10^7 (6.5×10^6)	N/A
2A	2.2×10^4 ($1.4 \times 10^{\$}$)	4.3×10^6 (2.0×10^6)	2.1×10^6 (6.1×10^5)	1.4×10^7 (6.5×10^6)
2B	2.1×10^4 ($1.4 \times 10^{\$}$)	1.2×10^7 (9.4×10^6)	5.3×10^2 (6.6×10^2)	N/A

*Introduced with the inoculum.

Table 2.2. Complete RefSeq genomes with *narG*/*napA* and *nosZ*, but lacking *nirK*/*nirS*. These bacterial genomes contain a suite of denitrification genes similar to *A. dehalogenans* strain 2CP-C; that is, they have a NO_3^- reductase gene (*napA* and/or *narG*), a N_2O reductase gene (*nosZ*), and do not contain a NO-producing NO_2^- reductase gene (*nirK* or *nirS*). The ability to reduce ferric iron was derived from the literature.

Organism	Accession Number	Reduces Iron	Source of Isolate	Reference	NosZ Clade I or II**
Aeromonas media strain WS	GCF_000287215.2_ ASM28721v3	+	Cooling water systems	McLeod et al. 1998	I
Algibacter sp. strain HZ22	GCF_001310225.1_ ASM131022v1	-	Algae	Sun et al. 2016	II
Alkalilimnicola ehrlichii strain MLHE-1	GCF_000014785.1_ ASM1478v1	-	Soda lake	Oremland et al. 2002	I
Anaeromyxobacter dehalogenans strain 2CP-1	GCF_000022145.1_ ASM2214v1	+	Stream sediment	Sanford et al. 2002	II
Anaeromyxobacter dehalogenans strain 2CP-C	GCF_000013385.1_ ASM1338v1	+	Rain forest soil	Sanford et al. 2002	II
Anaeromyxobacter sp. strain Fw109-5	GCF_000017505.1_ ASM1750v1	+	Contaminated soils	Thomas et al. 2009	II
Anaeromyxobacter sp. strain K	GCF_000020805.1_ ASM2080v1	+			II
Azoarcus sp. strain BH72	GCF_000061505.1_ ASM6150v1	-	Rhizosphere of Kallar grass	Hurek et al. 1993	I
Azospirillum brasilense	GCF_000632475.1_ ASM63247v2	-	Plant roots of Crabgrass	Terrand and Kreig 1978	I
Campylobacter concisus strain ATCC 33237	GCF_001298465.1_ ASM129846v1	-*	Human mouth	Tanner et al. 1981	II
Campylobacter concisus strain 13826	GCF_000017725.1_ ASM1772v1	-*	Human mouth	Tanner et al. 1981	II
Campylobacter curvus strain 525.92	GCF_000017465.1_ ASM1746v1	-*			II
Campylobacter fetus subsp. fetus 04/554	GCF_000759485.1_ ASM75948v1	-*			II
Campylobacter fetus subsp. fetus 82-40	GCF_000015085.1_ ASM1508v1	-*	Human blood	Perez and Blaser 1985	II
Campylobacter fetus subsp. testudinum	GCF_000814265.1_ ASM81426v1	-*			II
Campylobacter fetus subsp. testudinum 03-427	GCF_000495505.1_ ASM49550v1	-*	Human blood	Fitzgerald et al. 2014	II

Table 2.2. Continued.

Organism	Accession Number	Reduces Iron	Source of Isolate	Reference	NosZ Clade I or II**
Campylobacter fetus subsp. testudinum Sp3	GCF_001484645.1_ ASM148464v1	-*	Snake	Fitzgerald et al. 2014	II
Campylobacter fetus subsp. venerealis 97/608	GCF_000759515.1_ ASM75951v1	-*			II
Campylobacter fetus subsp. venerealis str. 84-112	GCF_000967135.1_ CFV	-*	Bovine preputial secretion	et al. 1986; Clark et al.	II
Campylobacter gracilis	GCF_001190745.1_ ASM119074v1	-*	Human mouth	Tanner et al. 1981	II
Campylobacter iguaniorum strain 1485E	GCF_000736415.1_ ASM73641v1	-*	Reptile digestive tracts	Gilbert et al. 2016	II
Campylobacter iguaniorum strain 2463D	GCF_001483985.1_ ASM148398v1	-*	Reptile digestive tracts	Gilbert et al. 2016	II
Cellulophaga algicola strain DSM 14237	GCF_000186265.1_ ASM18626v1	-	Sea ice	Bowman 2000	II
Denitrovibrio acetiphilus strain DSM 12809	GCF_000597885.1_ ASM59788v1	-	Oil resevoir model column	Torsvik 2000	II
Desulfitobacterium dehalogenans strain ATCC 51507	GCF_000025725.1_ ASM2572v1	-*	Sediment in freshwater pond	al. 2010; Utkin et al.	II
Desulfitobacterium dichloroeliminans strain LMG P-21439	GCF_000243155.2_ ASM24315v3	-*	Soil	NCBI	II
Desulfitobacterium hafniense strain DCB-2	GCF_000243135.2_ ASM24313v3	+	Municipal sludge	n and Ahring	II
Desulfitobacterium hafniense strain Y51	GCF_000021925.1_ ASM2192v1	-*	Contaminated soil	Suyama et al. 2001	II
Desulfomonile tiedjei strain DSM 6799	GCF_000010045.1_ ASM1004v1	-*	Sewage sludge	DeWeerd et al. 1990	II
Dyadobacter fermentans strain DSM 18053	GCF_000266945.1_ ASM26694v1	-	Corn stems	Triplett 2000	II
Flammeovirgaceae bacterium strain 311 (*Cesiribacter roseus*)	GCF_000023125.1_ ASM2312v1	-	Desert sand	Liu et al. 2012	II
Haliscomenobacter hydrossis strain DSM 1100	GCF_000212735.1_ ASM21273v1	-	Activated Sludge	1995; van Veen et al.	II
Hoeflea sp. strain IMCC20628	GCF_001011155.1_ ASM101115v1	-			I
Leisingera methylohalidivorans strain DSM 14336	GCF_000511355.1_ ASM51135v1	-	Marine/Seawater	Schaefer et al. 2002	I
Magnetospira sp. strain QH-2	GCF_000968135.1_ ASM96813v1	-	Seawater pond	Zhu et al. 2010	II
Marinobacter sp. strain CP1	GCF_001266795.1_ ASM126679v1	-	Biocathode biofilm/seawater	Wang et al. 2015	I
Methylobacterium sp. strain 4-46	GCF_000019365.1_ ASM1936v1	-			I

Table 2.2. Continued.

Organism	Accession Number	Reduces Iron	Source of Isolate	Reference	NosZ Clade I or II**
Methylophaga nitratireducenticrescens	GCF_000260985.3_ ASM26098v2	-	Seawater treatment system	et al. 2013; Mauffrey et	I
Niabella soli strain DSM 19437	GCF_000243115.2_ ASM24311v3	-	Soil	Weon et al. 2008	II
Niastella koreensis strain GR20-10	GCF_000246855.1_ ASM24685v1	-	Soil	Weon et al. 2006	II
Psychromonas ingrahamii strain 37	GCF_000015285.1_ ASM1528v1	-	Sea ice core	Auman et al. 2006	I
Rhodoferax ferrireducens strain T118	GCF_000013605.1_ ASM1360v1	+	Subsurface sediments	Finneran et al. 2003	I
Rhodopseudomonas palustris strain BisB18	GCF_000013745.1_ ASM1374v1	-*	River sediment	Dailey 1986; Oda	I
Rhodopseudomonas palustris strain HaA2	GCF_000013365.1_ ASM1336v1	-*	Shallow pond	Dailey 1986; Oda	I
Rhodospirillum centenum strain SW	GCF_000016185.1_ ASM1618v1	-	Hot springs	Favinger et al. 1989	I
Runella slithyformis strain DSM 19594	GCF_000218895.1_ ASM21889v1	-	Freshwater lake	Williams 1978	II
Sulfurospirillum cavolei	GCF_001548055.1_ ASM154805v1	-	contaminated groundwater	al. 2007; Ross et al.	II
Sulfurospirillum multivorans strain DSM 12446	GCF_000568815.1_ ASM56881v1	-	Activated Sludge	Muramatsu et al. 1995	II
Thioalkalivibrio paradoxus strain ARh 1	GCF_000227685.2_ ASM22768v3	-	Soda lake	Sorokin et al. 2002	I
Vibrio tubiashii strain ATCC 19109	GCF_000772105.1_ ASM77210v1	-	Clam	al. 1965; Hada et al.	I
Zobellia galactanivorans	GCF_000973105.1_ ASM97310v1	-	Red algae	Barbeyron et al. 2001	II

*Iron reduction demonstrated by another member of the same genus.

**Clade I = Typical, clade II = Atypical (Jones et al. 2013; Sanford et al. 2012)

References for Table 2.2

Auman AJ, Breeze JL, Gosink JJ, Kämpfer P, Staley JT. (2006). *Psychromonas ingrahamii* sp. nov., a novel gas vacuolate, psychrophilic bacterium isolated from Arctic polar sea ice. *Int J Syst Evol Microbiol* **56**: 1001–1007.

Barbeyron T, L'Haridon S, Corre E, Kloareg B, Potin P. (2001). *Zobellia galactanovorans* gen. nov., sp. nov., a marine species of *Flavobacteriaceae* isolated from a red alga, and classification of [*Cytophaga*] *uliginosa* (ZoBell and Upham 1944) Reichenbach 1989 as *Zobellia uliginosa* gen. nov., comb. nov. *Int J Syst Evol Microbiol* **51**: 985–997.

Bowman JP. (2000). Description of *Cellulophaga algicola* sp. nov., isolated from the surfaces of Antarctic algae, and reclassification of *Cytophaga uliginosa* (ZoBell and Upham 1944) Reichenbach 1989 as *Cellulophaga uliginosa* comb. nov. *Int J Syst Evol Microbiol* **50**: 1861–1868.

Chelius MK, Triplett EW. (2000). *Dyadobacter fermentans* gen. nov., sp. nov., a novel Gram-negative bacterium isolated from surface-sterilized *Zea mays* stems. *Int J Syst Evol Microbiol* **50**: 751–758.

Christiansen N, Ahring BK. (1996). *Desulfitobacterium hafniense* sp. nov., an anaerobic, reductively dechlorinating bacterium. *Int J Syst Bacteriol* **46**: 442–448.

DeWeerd KA, Mandelco L, Tanner RS, Woese CR, Suflita JM. (1990). *Desulfomonile tiedjei* gen. nov. and sp. nov., a novel anaerobic, dehalogenating, sulfate-reducing bacterium. *Arch Microbiol* **154**: 23–30.

Favinger J, Stadtwald R, Gest H. (1989). *Rhodospirillum centenum*, sp. nov., a thermotolerant cyst-forming anoxygenic photosynthetic bacterium. *Antonie Van Leeuwenhoek* **55**: 291–296.

Finneran KT, Johnsen C V., Lovley DR. (2003). *Rhodoferax ferrireducens* sp. nov., a psychrotolerant, facultatively anaerobic bacterium that oxidizes acetate with the reduction of Fe(III). *Int J Syst Evol Microbiol* **53**: 669–673.

Fitzgerald C, Tu ZC, Patrick M, Stiles T, Lawson AJ, Santovenia M, *et al.* (2014). *Campylobacter fetus* subsp. *testudinum* subsp. nov., isolated from humans and reptiles. *Int J Syst Evol Microbiol* **64**: 2944–2948.

Hada HS, West P a., Lee J V., Stemmler J, Colwell RR. (1984). *Vibrio tubiashii* sp. nov.,

a pathogen of bivalve mollusks. *Int J Syst Bacteriol* **34**: 1–4.

He Q, Sanford RA. (2003). Characterization of Fe(III) reduction by chlororespiring *Anaeromxyobacter dehalogenans*. *Appl Environ Microbiol* **69**: 2712–2718.

Kämpfer P. (1995). Physiological and chemotaxonomic characterization of filamentous bacteria belonging to the genus *Haliscomenobacter*. *Syst Appl Microbiol* **18**: 363–367.

Kodama Y, Ha LT, Watanabe K. (2007). *Sulfurospirillum cavolei* sp. nov., a facultatively anaerobic sulfur-reducing bacterium isolated from an underground crude oil storage cavity. *Int J Syst Evol Microbiol* **57**: 827–831.

Kunapuli U, Jahn MK, Lueders T, Geyer R, Heipieper HJ, Meckenstock RU. (2010). *Desulfitobacterium aromaticivorans* sp. nov. and *Geobacter toluenoxydans* sp. nov., iron-reducing bacteria capable of anaerobic degradation of monoaromatic hydrocarbons. *Int J Syst Evol Microbiol* **60**: 686–695.

Larkin JM, Williams PM. (1978). *Runella slithyformis* gen. nov., sp. nov., a curved, nonflexible, pink bacterium. *Int J Syst Bacteriol* **28**: 32–36.

Liu M, Qi H, Luo X, Dai J, Peng F, Fang C. (2012). *Cesiribacter roseus* sp. nov., a pink-pigmented bacterium isolated from desert sand. *Int J Syst Evol Microbiol* **62**: 96–99.

Madsen T, Licht D. (1992). Isolation and characterization of an anaerobic chlorophenol-transforming bacterium. *Appl Environ Microbiol* **58**: 2874–2878.

Martineau C, Villeneuve C, Mauffrey F, Villemur R. (2013). *Hyphomicrobium nitrativorans* sp. nov., isolated from the biofilm of a methanol-fed denitrification system treating seawater at the Montreal Biodome. *Int J Syst Evol Microbiol* **63**: 3777–3781.

Mauffrey F, Martineau C, Villemur R. (2015). Importance of the two dissimilatory (Nar) nitrate reductases in the growth and nitrate reduction of the methylotrophic marine bacterium *Methylophaga nitratireducenticrescens* JAM1. *Front Microbiol* **6**: 1–11.

McLeod ES, Dawood Z, MacDonald R, Oosthuizen MC, Graf J, Steyn PL, *et al.* (1998). Isolation and identification of sulphite- and iron reducing, hydrogenase positive facultative anaerobes from cooling water systems. *Syst Appl Microbiol* **21**: 297–305.

Moody MD, Dailey HA. (1985). Ferric iron reductase of *Rhodopseudomonas sphaeroides*. *J Bacteriol* **163**: 1120–1125.

Myhr S, Torsvik T. (2000). *Denitrovibrio acetiphilus*, a novel genus and species of dissimilatory nitrate-reducing bacterium isolated from an oil reservoir model column. *Int J Syst Evol Microbiol* **50**: 1611–1619.

Oda Y, Larimer FW, Chain PSG, Malfatti S, Shin M V, Vergez LM, *et al.* Multiple genome sequences reveal adaptations of a phototrophic bacterium to sediment microenvironments.

Oremland RS, Hoeft SE, Santini JM, Bano N, Hollibaugh RA, Hollibaugh JT. (2002). Anaerobic oxidation of arsenite in Mono Lake water and by a facultative, arsenite-oxidizing chemoautotroph, Strain MLHE-1. *Appl Environ Microbiol* **68**: 4795–4802.

Perez-Perez GI, Blaser MJ, Bryner JH. (1986). Lipopolysaccharide structures of Campylobacter fetus are related to heat-stable serogroups. *Infect Immun* **51**: 209–212.

Perez Perez GI, Blaser MJ. (1985). Lipopolysaccharide characteristics of pathogenic campylobacters. *Infect Immun* **47**: 353–359.

Reinhold-Hurek B, Hurek T, Gillis M, Hoste B, Vancanneyt M, Kersters K, *et al.* (1993). *Azoarcus* gen. nov., Nitrogen-Fixing Proteobacteria Associated with Roots of Kallar Grass (*Leptochloa fusca* (L.) Kunth), and Description of Two Species, *Azoarcus indigens* sp. nov. and *Azoarcus communis* sp. nov. *Int J Syst Bacteriol* **43**: 574–584.

Ross DE, Marshall CW, May HD, Norman RS. (2016). Comparative genomic analysis of *Sulfurospirillum cavolei* MES reconstructed from the metagenome of an electrosynthetic microbiome. *PLoS One* **11**. e-pub ahead of print, doi: 10.1371/journal.pone.0151214.

Sanford RA, Cole JR, Tiedje JM. (2002). Characterization and description of Anaeromyxobacter dehalogenans gen. nov., sp. nov., an aryl-halorespiring facultative anaerobic myxobacterium. *Appl Environ Microbiol* **68**: 893–900.

Schaefer J, Goodwin K, McDonald I, Murrell JC, Oremland R. (2002). *Leisingera methylohalidivorans* gen. nov., sp. nov., a marine methylotroph that grows on

methyl bromide. *Int J Syst Evol Microbiol* **52**: 851–9.

Scholz-Muramatsu H, Neumann A, Meßmer M, Moore E, Diekert G. (1995). Isolation and characterization of *Dehalospirillum multivorans* gen. nov., sp. nov., a tetrachloroethene-utilizing, strictly anaerobic bacterium. *Arch Microbiol* **163**: 48–56.

Sorokin DY, Tourova TP, Lysenko AM, Mityushina LL, Gijs Kuenen J. (2002). *Thioalkalivibrio thiocyanoxidans* sp. nov. and *Thioalkalivibrio paradoxus* sp. nov., novel alkaliphilic, obligately autotrophic, sulfur-oxidzing bacteria capable of growth on thiocyanate, from soda lakes. *Int J Syst Evol Microbiol* **52**: 657–664.

Sun C, Fu G, Zhang C, Hu J, Xu L, Wang R, *et al.* (2016). Isolation and complete genome sequence of *Algibacter alginolytica* sp. nov., a novel seaweed-degrading *Bacteroidetes* bacterium with diverse putative polysaccharide utilization loci Liu S-J (ed). *Appl Environ Microbiol* **82**: 2975–2987.

Suyama A, Iwakiri R, Kai K, Tokunaga T, Sera N, Furukawa K. (2001). Isolation and characterization of *Desulfitobacterium* sp. strain Y51 capable of efficient dehalogenation of tetrachloroethene and polychloroethanes. *Biosci Biotechnol Biochem* **65**: 1474–1481.

Tanner ACR, Badger S, Lai CH, Listgarten MA, Visconti RA, Socransky SS. (1981). *Wolinella* gen. nov., *Wolinella succinogenes* (*Vibrio succinogenes* Wolin et al.) comb. nov., and description of *Bacteroides gracilis* sp. nov., *Wolinella recta*, sp. nov., *Campylobacter concisus* sp. nov., and *Eikenella corrodens* from humans with periodontal disease. *Int J Syst Bacteriol* **31**: 432–445.

Tarrand JJ, Krieg NR, Döbereiner J. (1978). A taxonomic study of the *Spirillum lipoferum* group, with descriptions of a new genus, *Azospirillum* gen. nov. and two species, *Azospirillum lipoferum* (Beijerinck) comb. nov. and *Azospirillum brasilense* sp. nov. *Can J Microbiol* **24**: 967–80.

Thomas SH, Padilla-Crespo E, Jardine PM, Sanford RA, Löffler FE. (2009). Diversity and distribution of *Anaeromyxobacter* strains in a uranium-contaminated subsurface environment with a nonuniform groundwater flow. *Appl Environ Microbiol* **75**: 3679–87.

Tubiash HS, Chanley PE, Leifson E. (1965). Bacillary necrosis, a disease of larval and

juvenile bivalve mollusks. I. Etiology and epizootiology. *J Bacteriol* **90**: 1036–1044.

Utkin I, Woese C, Wiegel J. (1994). Isolation and characterization of *Desulfitobacterium dehalogenans* gen. nov., sp. nov., an anaerobic bacterium which reductively dechlorinates chlorophenolic compounds. *Int J Syst Bacteriol* **44**: 612–619.

Van Veen WL, Van Der Kooij D, W A Geuze EC, Van Der Vlies AW, Veen V, Der Kooij V, *et al.* (1973). Investigations on the sheathed bacterium isolated from activated sludge. *Antonie Van Leeuwenhoek* **39**: 207–216.

Wang Z, Eddie BJ, Malanoski AP, Hervey IV WJ, Lin B, Strycharz-Glaven SM. (2015). Complete genome sequence of *Marinobacter* sp. CP1, isolated from a self-regenerating biocathod biofilm. *Genome Announc* **3**: 1–2.

Weon H-Y, Kim B-Y, Joa J-H, Kwon S-W, Kim W-G, Koo B-S. (2008). *Niabella soli* sp. nov., isolated from soil from Jeju Island, Korea. *Int J Syst Evol Microbiol* **58**: 467–9.

Zhu K, Pan H, Li J, Yu-Zhang K, Zhang S-D, Zhang W-Y, *et al.* (2010). Isolation and characterization of a marine magnetotactic spirillum axenic culture QH-2 from an intertidal zone of the China Sea. *Res Microbiol* **161**: 276–283.

Table 2.3. Theoretical growth yields per mole electrons. Growth yield on NO_2^- was calculated by flow cytometry with *Anaeromyxobacter* strain R. Growth yields of *A. dehalogenans* strain 2CP-C with Fe(III) and N_2O were used from previously published values (He and Sanford 2003 and Yoon et al. 2016, respectively).

Process	Reduction Half Reaction	Growth yield (# cells/mole e-)[a]	Reference
NO_2^- Reduction	$0.16\ NO_2^- + 1\ e^- + 4.33\ H^+ \rightarrow 0.16\ NH_4^+ + 0.33\ H_2O$	2×10^{13}	Personal Correspondence[b]
Fe(III) Reduction	$Fe^{3+} + 1\ e^- \rightarrow Fe^{2+}$	6.0×10^{12}	27
N_2O Reduction	$0.5\ N_2O + 1e^- + 1\ H^+ \rightarrow 1/2N_2 + H_2O$	2.4×10^{13}	17
Chemodenitrification		1.5×10^{13}	Theoretical calculation[c]

[a]Based on published numbers (1.4 mg biomass/mmole Fe(III) and 11.2 mg biomass/mmole N_2O) and a weight of 2.4×10^{-13} grams per bacterial cell.

[b]Personal correspondence with Rob Sanford. Determined by flow cytometry with *Anaeromyxobacter* strain R.

[c]Based on the reduction of 0.5 moles Fe^{3+} and 0.25 moles N_2O (produced by reaction between NO_2^- and Fe[II]).

Appendix: Figures

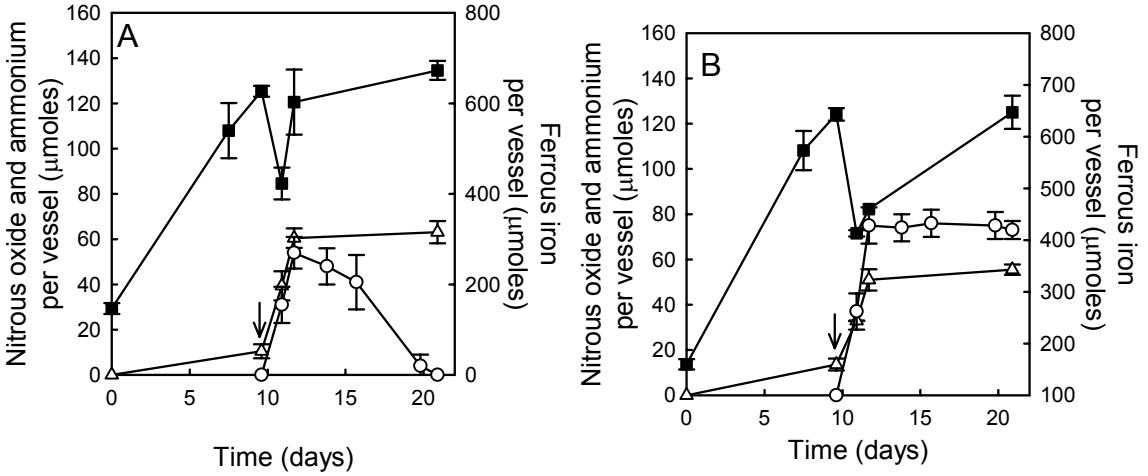

Figure 2.1. Abiotic production of N_2O after NO_3^- addition to *A. dehalogenans* cultures. Error bars represent the standard deviation of three replicate cultures. Ferrous iron (closed squares), N_2O-N (open circles), and NH_4^+ (open triangles). **(A)** *A. dehalogenans* grown on 1,000 μmoles acetate and 700 μmoles ferric citrate. NO_3^- (100 μmoles) was added on Day 10 (indicated by arrow). **(B)** Same as (A) except acetylene (10% of headspace) was included.

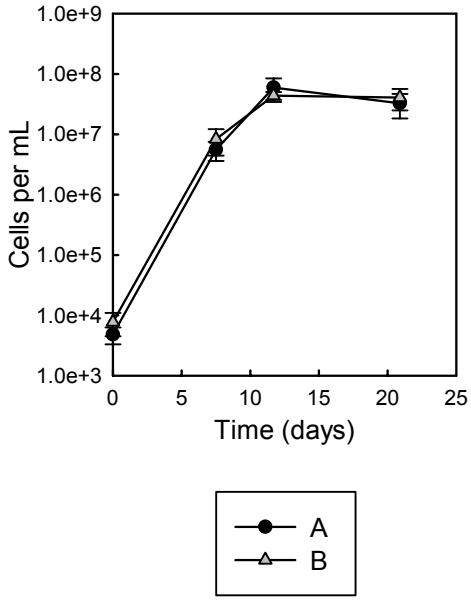

Figure 2.2. Cell numbers of *A. dehalogenans* cultures grown with ferric citrate and NO_3^-. Corresponds to Figure 2.1. Error bars represent the standard deviation of three replicate cultures. *A. dehalogenans* was grown on 1,000 μmoles acetate and 700 μmoles ferric citrate. 100 μmoles of NO_3^- were added on Day 8. Corresponds to Figure 1A (closed circles) and Figure 1B (gray triangles).

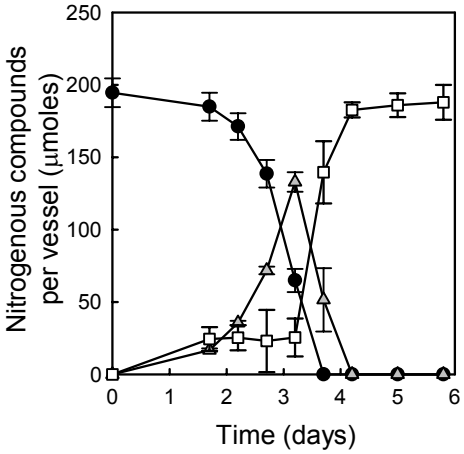

Figure 2.3. Cultures of *A. dehalogenans* grown with 1,000 µmoles acetate and 200 µmoles NO_3^- in the absence of ferric citrate. Averages of three replicate cultures are shown. Bars indicate the standard error. Small amounts (approximately 2 µmoles per vessel) of N2O-N were measured after four days (not shown). Only duplicate cultures were measured after four days. NO_3^- (closed circles); NO_2^- (gray triangles); NH_4^+ (open squares).

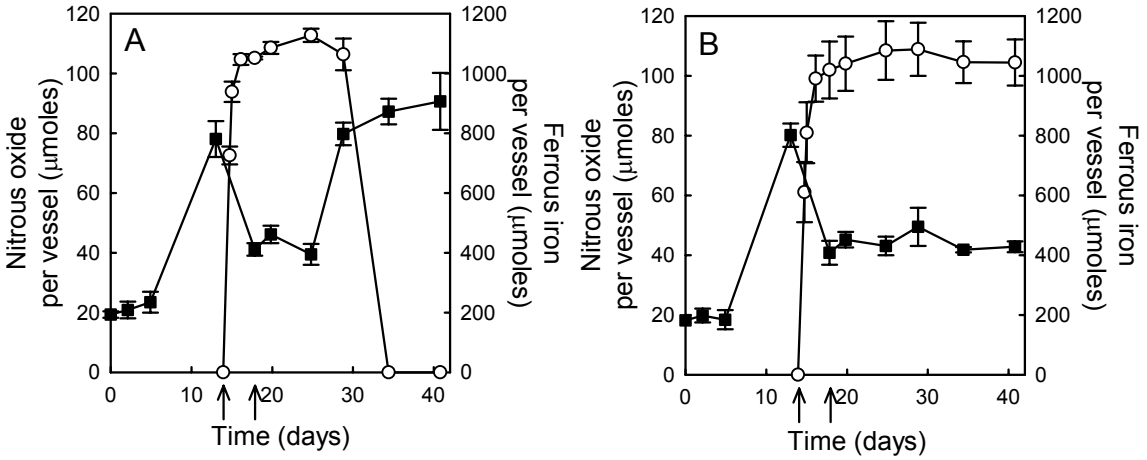

Figure 2.4. Abiotic production of N_2O after NO_2^- addition to *A. dehalogenans* cultures. Error bars represent the standard deviation of three replicate cultures. Ferrous iron (closed squares) and N_2O-N (open circles). (**A**) Cultures of *A. dehalogenans* were grown on 100 µmoles acetate and 900 µmoles ferric citrate. On Day 14, 100 µmoles NO_2^- was added (indicated by the first arrow). On Day 18, an additional 200 µmoles acetate was added (indicated by the second arrow). (**B**) Cultures treated the same as A except they were autoclaved prior to NO_2^- addition. H.K., heat-killed.

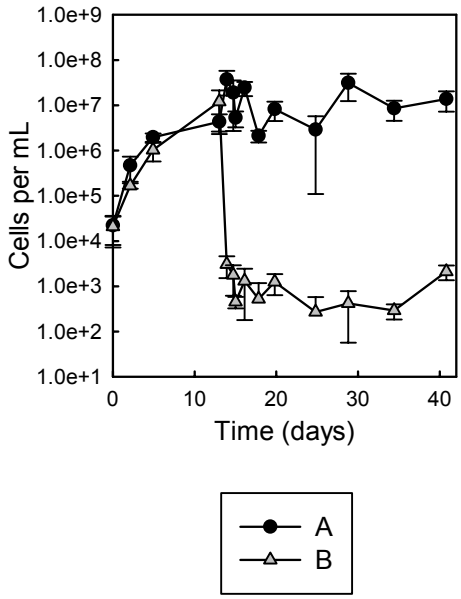

Figure 2.5. Cell numbers of *A. dehalogenans* cultures grown with ferric citrate and NO_2^-. Corresponds to Figure 2.4. Error bars represent the standard deviation of three replicate cultures. (**A**) Closed circles: Cultures of *A. dehalogenans* were grown on 100 µmoles acetate and 900 µmoles ferric citrate. On Day 14, 100 µmoles NO_2^- was added. On Day 18, an additional 200 µmoles acetate was added. (**B**) Gray triangles: Cultures treated the same as A except heat-killed prior to NO_2^- addition.

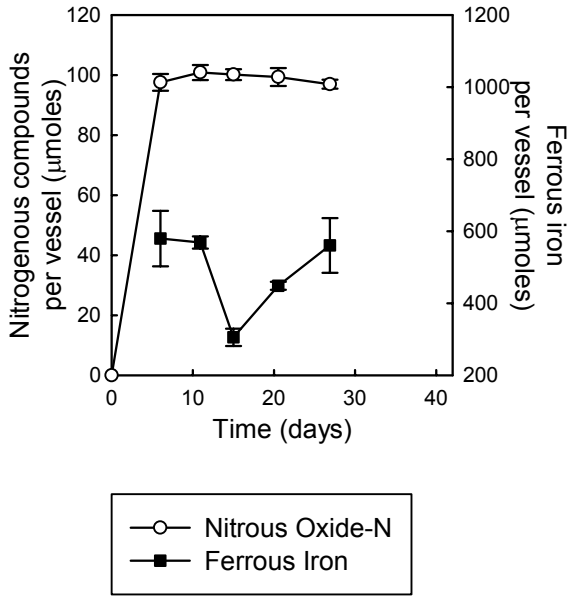

Figure 2.6. Abiotic reaction between NO_2^- and Fe(II). Abiotic (no inoculum) control consisting of 800 µmoles ferrous chloride in the same medium and with the same NO_2^- and acetate additions as in Figure 2A and 2B.

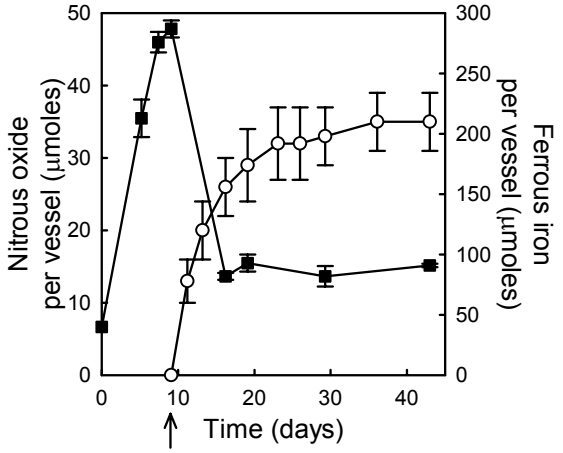

Figure 2.7. Cultures of *A. dehalogenans* grown with 1,000 µmoles acetate and ferric oxyhydroxide. 100 µmoles NO_2^- was added on Day 9 (indicated by the arrow). Ferrous iron (closed squares) and N_2O-N (open circles). Error bars represent the standard deviation of two replicate cultures.

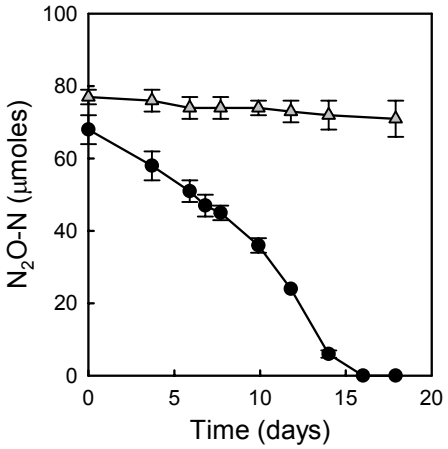

Figure 2.8. N_2O reduction by *A. dehalogenans* in the presence and absence of 0.2 mM sulfide. N_2O shown for cultures with (gray triangles) and without (closed circles) 0.2 mM sulfide. The average of three replicates are shown for the treatment with sulfide, and the average of two replicates is shown for the treatment without sulfide.

Figure 2.9. Maximum likelihood phylogenetic tree of the 16S rRNA genes from selected RefSeq bacterial genomes with NO_3^- reductase and N_2O reductase genes, but lacking *nirK*/*nirS.* All intergeneric nodes with bootstrap values < 50% are marked with red circles. Branches are colored by class. Four archaeal sequences were included as outgroups. Each node is labeled with the estimated number of *c*-type cytochromes (with the number of *c*-type cytochromes with more than four heme-binding domains in parentheses), a plus sign if that organism is capable of Fe(III) reduction, which *nosZ* clade the genome contains (I or II), and a symbol representing the source of the isolate. The absence of a plus sign for iron reduction indicates that it is unknown (most frequently, untested) and the absence of a symbol for the source indicates that the source is unknown. The scale bar corresponds to the number of nucleotide substitutions per site. References for the isolation of the organisms are located in Table 2.2. The Venn Diagram shows the proportion of the analyzed RefSeq genomes containing *nirK*/*nirS*, *napA*/*narG*, and/or *nosZ*. Out of the 4,739 genomes analyzed, 2,567 had either a *napA* or a *narG* gene, 634 had a *nirK* or a *nirS* gene, and 394 had a *nosZ* gene. *Isolated from an alkaline lake.

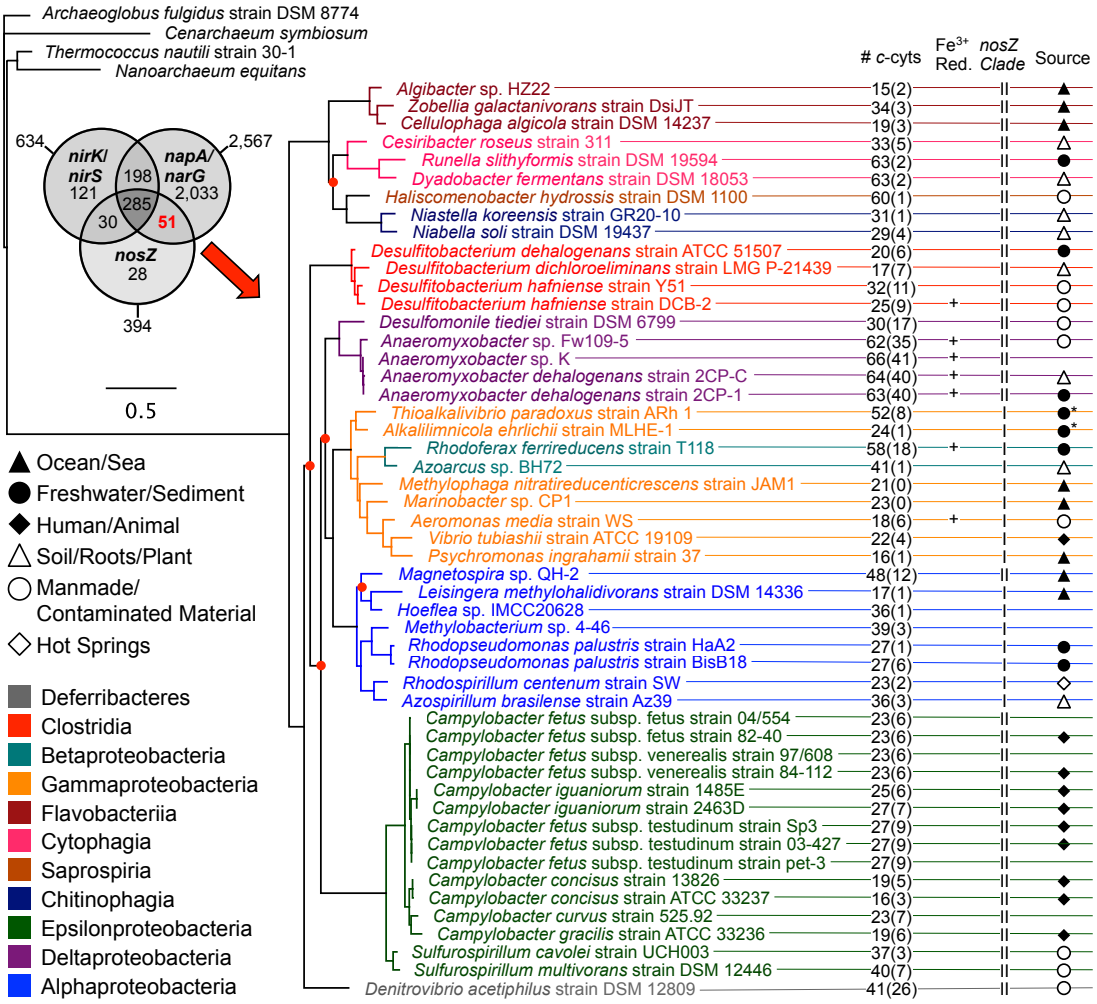
Archaeoglobus fulgidus strain DSM 8774
Cenarchaeum symbiosum
Thermococcus nautili strain 30-1
Nanoarchaeum equitans
634
nirK/ nirS 121
198
napA/ narG 2,033
2,567
285
30
51
nosZ 28
394
0.5
c-cyts
Fe3+ Red.
nosZ Clade
Source
Algibacter sp. HZ22 15(2) II
Zobellia galactanivorans strain DsiJT 34(3) II
Cellulophaga algicola strain DSM 14237 19(3) II
Cesiribacter roseus strain 311 33(5) II
Runella slithyformis strain DSM 19594 63(2) II
Dyadobacter fermentans strain DSM 18053 63(2) II
Haliscomenobacter hydrossis strain DSM 1100 60(1) II
Niastella koreensis strain GR20-10 31(1) II
Niabella soli strain DSM 19437 29(4) II
Desulfitobacterium dehalogenans strain ATCC 51507 20(6) II
Desulfitobacterium dichloroeliminans strain LMG P-21439 17(7) II
Desulfitobacterium hafniense strain Y51 32(11) II
Desulfitobacterium hafniense strain DCB-2 25(9) + II
Desulfomonile tiedjei strain DSM 6799 30(17) II
Anaeromyxobacter sp. Fw109-5 62(35) + II
Anaeromyxobacter sp. K 66(41) + II
Anaeromyxobacter dehalogenans strain 2CP-C 64(40) + II
Anaeromyxobacter dehalogenans strain 2CP-1 63(40) + II
Thioalkalivibrio paradoxus strain ARh 1 52(8) I
Alkalilimnicola ehrlichii strain MLHE-1 24(1) I
Rhodoferax ferrireducens strain T118 58(18) + I
Azoarcus sp. BH72 41(1) I
Methylophaga nitratireducenticrescens strain JAM1 21(0) I
Marinobacter sp. CP1 23(0) I
Aeromonas media strain WS 18(6) + I
Vibrio tubiashii strain ATCC 19109 22(4) I
Psychromonas ingrahamii strain 37 16(1) I
Magnetospira sp. QH-2 48(12) II
Leisingera methylohalidivorans strain DSM 14336 17(1) I
Hoeflea sp. IMCC20628 36(1) I
Methylobacterium sp. 4-46 39(3) I
Rhodopseudomonas palustris strain HaA2 27(1) I
Rhodopseudomonas palustris strain BisB18 27(6) I
Rhodospirillum centenum strain SW 23(2) I
Azospirillum brasilense strain Az39 36(3) I
Campylobacter fetus subsp. fetus strain 04/554 23(6) II
Campylobacter fetus subsp. fetus strain 82-40 23(6) II
Campylobacter fetus subsp. venerealis strain 97/608 23(6) II
Campylobacter fetus subsp. venerealis strain 84-112 23(6) II
Campylobacter iguaniorum strain 1485E 25(6) II
Campylobacter iguaniorum strain 2463D 27(7) II
Campylobacter fetus subsp. testudinum strain Sp3 27(9) II
Campylobacter fetus subsp. testudinum strain 03-427 27(9) II
Campylobacter fetus subsp. testudinum strain pet-3 27(9) II
Campylobacter concisus strain 13826 19(5) II
Campylobacter concisus strain ATCC 33237 16(3) II
Campylobacter curvus strain 525.92 23(7) II
Campylobacter gracilis strain ATCC 33236 19(6) II
Sulfurospirillum cavolei strain UCH003 37(3) II
Sulfurospirillum multivorans strain DSM 12446 40(7) II
Denitrovibrio acetiphilus strain DSM 12809 41(26) II
Ocean/Sea
Freshwater/Sediment
Human/Animal
Soil/Roots/Plant
Manmade/ Contaminated Material
Hot Springs
Deferribacteres
Clostridia
Betaproteobacteria
Gammaproteobacteria
Flavobacteriia
Cytophagia
Saprospiria
Chitinophagia
Epsilonproteobacteria
Deltaproteobacteria
Alphaproteobacteria

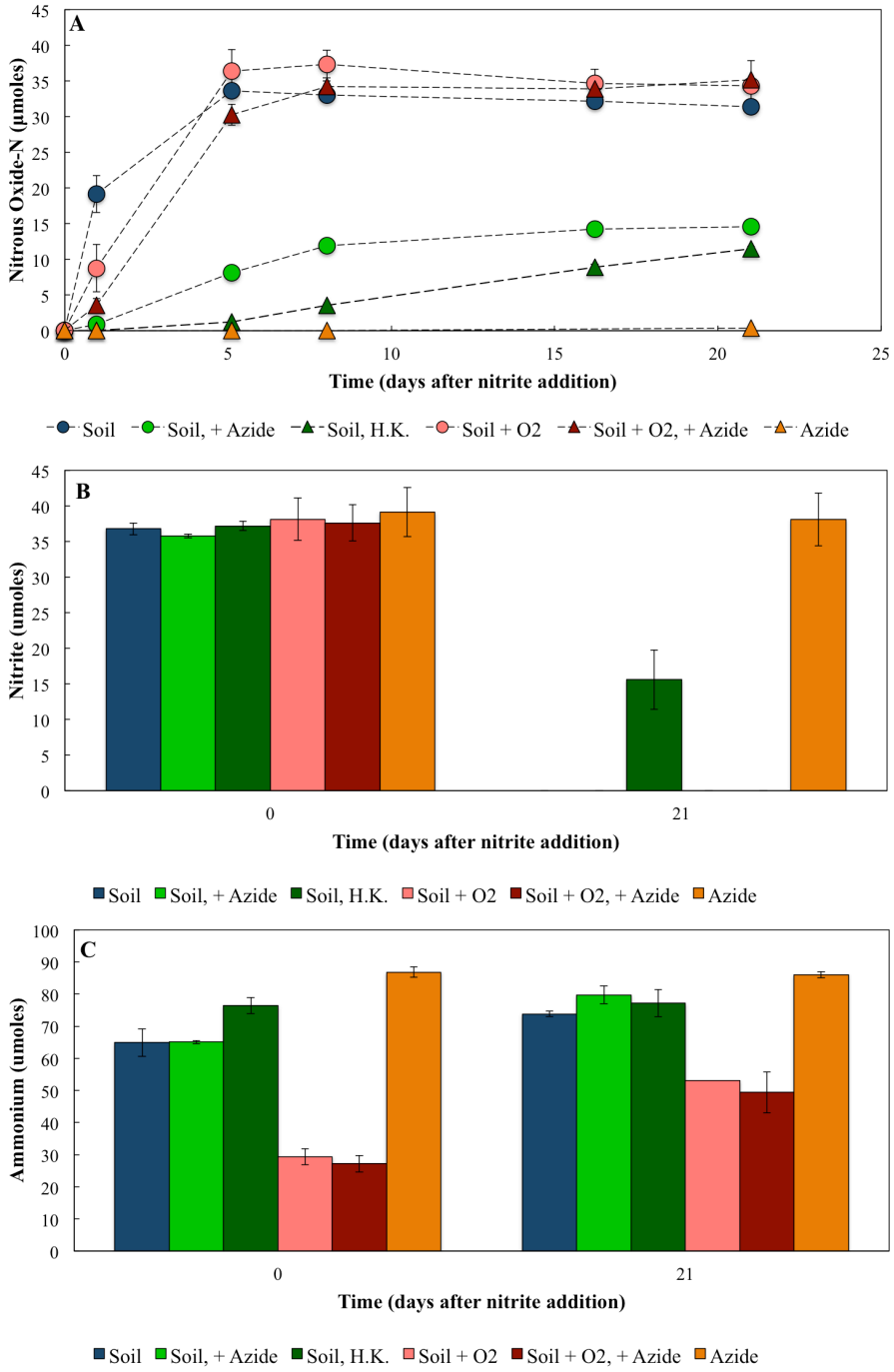

Figure 2.10. Chemodenitrification in Illinois soil microcosms. The reduction of 30 µmoles NO_2^- in microcosms containing 20 g Illinois agricultural soil. All were incubated two weeks before NO_2^- addition, and acetylene was added 1-2 days before NO_2^-. The average of two replicate cultures are shown for each point/bar, and error bars show standard deviation. (A) N_2O-N. (B) NO_2^-. (C) NH_4^+. H.K. indicates microcosms that were heat-killed before NO_2^- addition. +Azide indicates that 3 mM sodium azide was added before NO_2^- addition. +O_2 indicates that microcosms were exposed to O_2 until NO_2^- addition; after NO_2^- addition cultures were sealed.

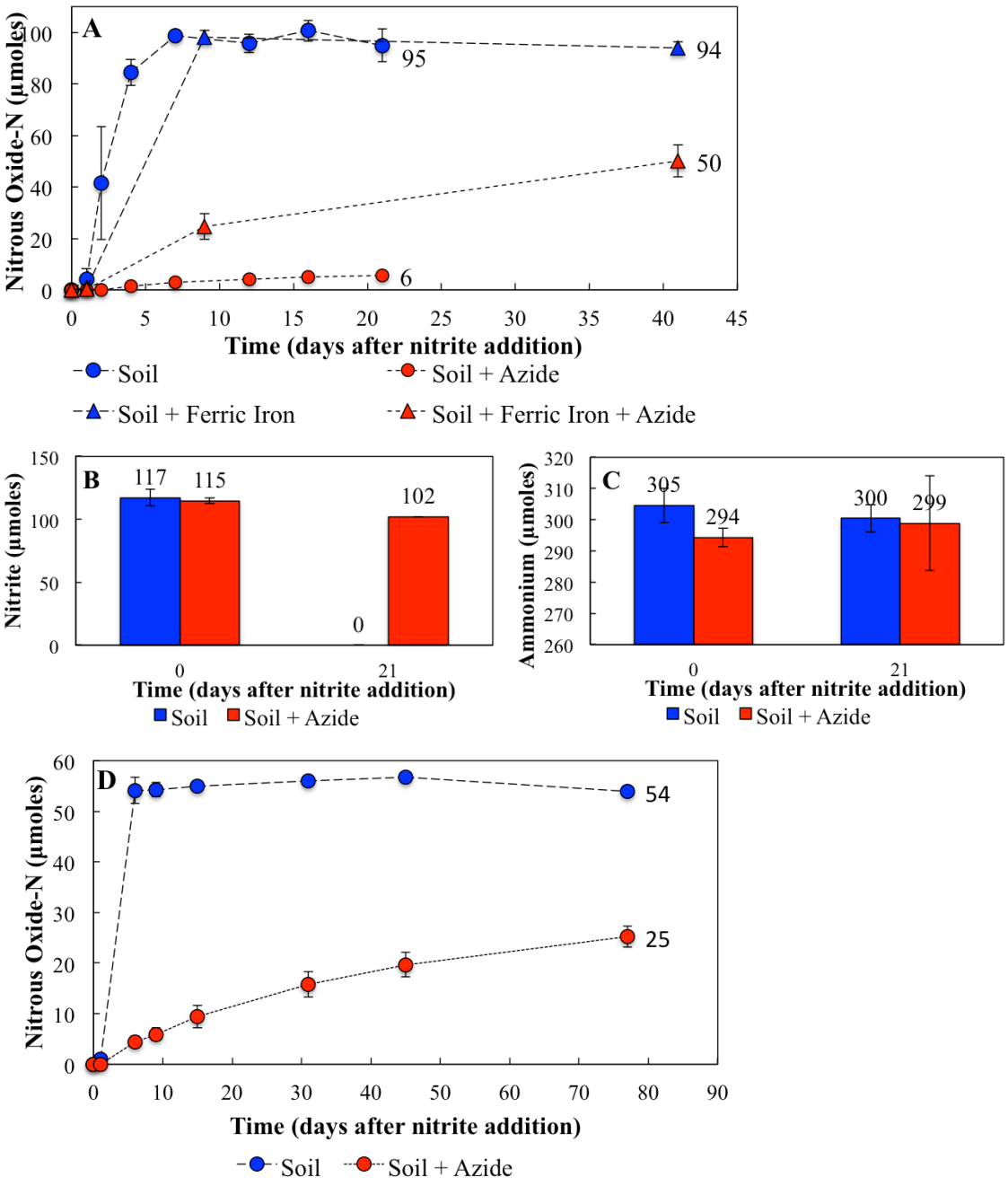

Figure 2.11. Chemodenitrification in Illinois and Puerto Rico soil microcosms. The reduction of 100 µmoles NO_2^- in microcosms containing 5 g Illinois (A-C) or 1 g Puerto Rico (D) soils. All were incubated at least two weeks before NO_2^- addition, and acetylene was added 1-2 days before NO_2^-. The average of 2 replicate cultures is shown for each bar/point, and error bars show the standard deviation. +Azide indicates that 3 mM sodium azide was added before NO_2^- addition. (A) N_2O production in microcosms containing Illinois soil with or without 5 mM poorly crystalline ferric oxyhydroxide. (B) NO_2^- mass for no-iron added microcosms from A. (C) NH_4^+ mass for no-iron added microcosms from A. (D) N_2O production in microcosms containing Puerto Rico soil.

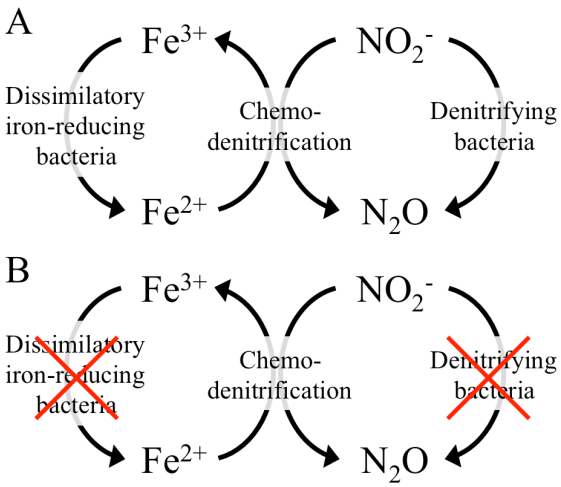

Figure 2.12. Schematic of NO_2^- reduction to N_2O in the presence (A) and absence (B) of live cells. Processes affected by killing live cells (i.e., by azide or autoclaving) are indicated by a red X.

Chapter 3: Sulfide Inhibition of Nitrate and Nitrous Oxide Reduction by *Anaeromyxobacter dehalogenans* strain 2CP-C and Ramifications for Chemodenitrification Potential

Abstract

N turnover in natural environments is important to climate change, eutrophication, agriculture, and human health. N fertilizers (e.g., ammonium [NH_4^+] and nitrate [NO_3^-]) are converted to nitrous oxide (N_2O) by microorganisms in agricultural soils, and the overuse of N-fertilizers has led to N_2O becoming the dominant greenhouse gas. Understanding the mechanisms for NO_3^- removal and retention is important for predicting the fate of N fertilizers and guiding climate change models and agricultural practices. Extensive research has focused on the fate of NO_3^-, especially on environmental and biological factors that influence denitrification and respiratory ammonification. Multiple studies have shown that sulfide slows NO_3^- reduction and causes an accumulation of intermediates, such as nitrite (NO_2^-). Additionally, trace metals are known to influence the extent of NO_3^- reduction. Abiotic factors that influence N flux affect the retention of N in soils, as NO_3^-, N_2O, and N_2 are lost from soil but NH_4^+ is retained in soil. Further research is needed to understand the mechanisms behind the effects of sulfide and trace metals on NO_3^- reduction, and the potential synergistic effects of sulfide and trace metals. In the present study, the effects of sulfide and molybdenum (an essential cofactor for NO_3^- reductases) on NO_3^-, NO_2^-, and N_2O reduction and intermediate accumulation were tested in pure cultures of the common soil bacterium *Anaeromyxobacter dehalogenans* strain 2CP-C. NO_3^- reduction rates and intermediate NO_2^- concentrations decreased with increasing sulfide concentrations, and NO_3^- reduction was completely inhibited by 0.4 mM sulfide. N_2O reduction was inhibited by 0.2 mM sulfide. Increasing the molybdenum (Mo) concentration from 0.15 μM to 1.5 mM partially alleviated the inhibition of NO_3^- reduction by sulfide, and experiments performed at the optimal concentration of 1.5 mM Mo revealed that sulfide sequestration of Mo was responsible for decreased NO_3^- reduction rates. Finally, the presence of 0.2 mM sulfide was demonstrated to prevent the reaction between intermediate NO_2^- and ferrous iron during NO_3^- reduction, due to decreased release of NO_2^-. These findings show that sulfide and trace metals are important for abiotic and biotic processes in the N-cycle and influence the end products of NO_3^- reduction.

Introduction

The N cycle is highly modular; i.e., while many organisms contain complete pathways, others only perform single pathway steps (Graf *et al.*, 2014; Stein and Klotz, 2016). This modularity may be advantageous if an organism specifically benefits from a single process (Stein and Klotz, 2016) or if an intermediate is toxic, since segregating pathway steps into different cells relieves that toxicity by decreasing the accumulation of intermediates (Lilja and Johnson, 2016). NO_2^- is a key intermediate in several N cycling pathways: denitrification, nitrification, respiratory ammonification and anaerobic NH_4^+ oxidation (Figure 1.1). Some respiratory ammonifiers and denitrifiers release NO_2^- temporarily before complete reduction to NH_4^+ or gaseous products (i.e. N_2 or N_2O), respectively, while others do not release measurable concentrations of NO_2^- (Betlach and Tiedje, 1981; Tiedje, 1988). The release of NO_2^- can have important ecological impacts, since it is toxic (Klüber and Conrad, 1998; Philips *et al.*, 2002), can be utilized by other organisms (e.g., denitrifiers, respiratory ammonifiers, and nitrifiers) and can react abiotically with other compounds (e.g., with ferrous iron) (Moraghan and Buresh, 1977). The amount of NO_2^- accumulated during NO_3^- reduction may influence the extent to which these phenomena occur.

A variety of abiotic factors influence the end products and the rate of dissimilatory NO_3^- reduction and denitrification. These abiotic factors include oxygen concentration, pH, sulfide content, the NO_3^-:NO_2^- ratio, the carbon:nitrogen ratio, and soil moisture (i.e., water-filled pore space) (Broadbent and Clark, 1965; Stevens *et al.*, 1998; Aelion and Warttinger, 2009; Yoon *et al.*, 2014, 2015). NO_2^- accumulates in some natural environments under alkaline and neutral conditions (Cleemput and Samater, 1996; Kelso *et al.*, 1997; Philips *et al.*, 2002; Shen *et al.*, 2003; Gelfand and Yakir, 2008). High pH, high NH_4^+ concentrations, and a variety of other environmental factors were shown to be correlated with NO_2^- accumulation (Stevens *et al.*, 1998; Philips *et al.*, 2002; Shen *et al.*, 2003). One hypothesis for the cause of NO_2^- accumulation is that different steps of denitrification and nitrification have different enzymatic rates (Gelfand and Yakir, 2008; Betlach and Tiedje, 1981; Philips *et al.*, 2002). Additionally, the N-cycle is highly modular and organisms with NO_3^- reductases but lacking NO_2^- reductases likely contribute to NO_2^- accumulation as well (Tiedje, 1988; Philips *et al.*, 2002).

The trace metals molybdenum (Mo), copper, and iron are essential to the function of enzymes involved in respiratory ammonification and denitrification (Figure 3.1) and thus have the ability to influence NO_2^- accumulation in the environment. Recently, Mo concentrations was shown to correlate with NO_3^- removal and NO_2^- accumulation at a site contaminated with high concentrations of NO_3^- and in *Pseudomonas* cultures (Thorgersen *et al.*, 2015). Mo is the key element for the molybdopterin cofactor in both the periplasmic and membrane-bound NO_3^- reductases (Moreno-Vivián *et al.*, 1999; González *et al.*, 2006) and molybdenum is actively transported into the cell as molybdate by a molybdate transporter (Hagen, 2011). Studies show that the concentration of trace metals (including Mo) in the environment are much lower (i.e., nanomolar concentrations) than that which is optimal for microbial growth (i.e., μM concentrations) (Glass and Orphan, 2012; Glass *et al.*, 2012). Increased concentrations of Mo increase NO_3^- reduction rates, and if the Mo concentration is high enough (i.e., 0.1-120 mM for *Pseudomonas* strains), toxic concentrations of NO_2^- accumulate (Thorgersen *et al.*, 2015). This further supports the hypothesis that enzyme kinetics plays a role in intermediate NO_2^- accumulation, and suggests that trace metal concentration is a limiting factor in natural environments.

Sulfide contributes to the shortage of trace metals that are integral to N-cycling reactions. Sulfide forms metal-sulfide complexes that are less bioavailable than free metal, decreasing the activity of N-cycling enzymes (Gonzalez-Gil *et al.*, 1999; Jansen *et al.*, 2007). The addition of sulfide slows denitrification and causes an accumulation of NO_2^- and/or N_2O (Sørensen *et al.*, 1980; Gould and McCready, 1982; Senga *et al.*, 2006; Tugtas and Pavlostathis, 2007). The addition of copper overcomes sulfide inhibition of N_2O reduction, suggesting that sulfide precipitates copper and reduces the bioavailability of copper (Manconi *et al.*, 2006). The concentration of sulfur in US soils is 800-48,000 ppm (Shacklette and Boerngen, 1984), and oxidized sulfur compounds can be reduced to sulfide under reducing conditions; thus sulfide may be present in reduced soils and precipitate important trace metals.

Less is known about synergistic effects of sulfide and Mo on NO_2^- reduction and NO_2^- accumulation. It is known that sulfide negatively impacts NO_3^- reduction rates and leads to accumulation of denitrification and respiratory ammonification intermediates,

whereas Mo enhances NO_3^- reduction rates (Thorgersen *et al.*, 2015). However, the literature lacks clear evidence linking the effects of sulfide and Mo. Considering what is reported about trace metals and sulfide, and the relationship between copper bioavailability and sulfide, it was predicted that a similar phenomenon would be observed with Mo and sulfide. The present study tests the hypothesis that the presence of sulfide slows or inhibits NO_3^- reduction because sulfide reacts with Mo, which becomes biologically unavailable either for molybdate entry into the cell or for incorporation in the NO_3^- reductase. *A. dehalogenans*, a common soil bacterium, was chosen for study due to its ability to reduce NO_3^- to NH_4^+ via NO_2^- as an intermediate, and the role *A. dehalogenans* plays in chemodenitrification. Since the NO_2^- reductase in *A. dehalogenans* uses an iron-containing cofactor, it was also hypothesized that sulfide would affect NO_2^- reduction. However, iron is more abundant in the growth medium used to cultivate *A. dehalogenans*, so the NO_2^- reductase should be less affected by sulfide than the NO_3^- reductase (Figure 3.1; Table 3.1). Thus it was predicted that a decrease in NO_3^- reduction rate ($rate_1$) and a lesser or nonexistent decrease in NO_2^- reduction rate ($rate_2$) would cause an accumulation of NO_2^- (Figure 3.2). Furthermore, the effects of sulfide on chemodenitrification were studied, to test if the abiotic reaction between Fe(II) and NO_2^- depends on the transient accumulation of NO_2^-.

To address these hypotheses, *A. dehalogenans* strain 2CP-C was cultivated with NO_3^- in the presence of a range of Mo and sulfide concentrations and monitored NO_3^- and NO_2^- concentrations. The effects of sulfide on N_2O reduction were also tested. In Chapter 2, chemodenitrification was demonstrated when NO_3^- was added to iron-reducing cultures of *A. dehalogenans*. Here, the effects of sulfide on chemodenitrification were tested by repeating some of the experiments from Chapter 2 in the presence of sulfide. The following results demonstrate an inhibitory effect of sulfide on NO_3^-, NO_2^-, and N_2O reduction, an increase in intermediate (i.e., NO_2^-) accumulation, and a resulting decrease in chemodenitrification potential. This chapter reveals potential environmental controls on the chemodenitrifier phenomena observed in Chapter 2, and further areas for study are suggested in the discussion.

Materials and Methods

Culture Conditions

Anaeromyxobacter dehalogenans strain 2CP-C was grown anaerobically in a defined mineral salts medium (Löffler *et al.*, 1996) with the following modifications: bicarbonate was replaced with 50 mM HEPES (4-[2-hydroxyethyl]-1-piperazineethanesulfonic acid), phosphate was reduced from 1.47 mM to 0.29 mM, L-cysteine was decreased from 0.2 mM to 0.1 mM, and the headspace was 100% N_2. Sulfide was omitted except where indicated. The medium was adjusted to a pH of 7.2 by the drop-wise addition of a 10 M sodium hydroxide solution. The medium was dispensed in 100 mL aliquots into 160 mL serum bottles, sealed with rubber stoppers, then autoclaved. Although autoclaving HEPES buffer is unadvisable due to the production of radicals, *A. dehalogenans* grew robustly in this medium, and no difference in NO_2^- accumulation was observed when bicarbonate-buffered medium and HEPES-buffered medium was compared directly (data not shown). For chemodenitrification experiments, unmodified bicarbonate-buffered medium was utilized (Löffler *et al.*, 1996). For experiments in which NH_4^+ was quantified, NH_4^+ concentrations were adjusted to 3 mM to allow accurate measurement. Sulfide was added from filter-sterilized, anoxic sodium sulfide stock solutions that were prepared with washed crystals, with the exception of a few experiments. In experiments where sulfide was not added from stocks solutions, sulfide concentrations are indicated with the '≤' symbol since concentrations were likely lower than that reported due to the presence of other sulfuric compounds on the surface of the sodium sulfide nonahydrate crystals. The concentration of sulfide was measured in experiments testing the optimum concentration of Mo, and confirmed to be between 0.08 and 0.11 mM in all "0.1 mM" sulfide treatments. Mo was added as sodium molybdate dihydrate from anoxic, autoclaved stock solutions made in milliQ water with 79 mM hydrochloric acid. The pH of medium after adding the stock solution was checked and ensured to be unaffected by the HCl in the stock solution. Acetate (10 mM) was included in the medium preparation and vitamins (Wolin *et al.*, 1963) were added from a filter-sterilized, anoxic stock solution to individual bottles after autoclaving. NO_3^-, ferric citrate, and/or N_2O were included in medium preparation or added from sterile, anoxic stocks (with the exception of N_2O, which was added from an Aldrich Chemistry N_2O

[99%] gas canister). The ferric citrate stock solution was prepared as described in Chapter 2. Anaerobic culture techniques were utilized in all experiments. The same conditions used for cultures were used to grow the seed cultures (i.e., cultures used to inoculate experimental cultures). All experiments were done in triplicate unless indicated otherwise.

Analytical and Statistical Methods

N_2O, acetate, NO_3^-, NO_2^-, and ferrous iron were measured as described in Chapter 2. Total accumulated NO_2^- was determined by plotting NO_2^- mass vs. time, and finding the area under the curve in SigmaPlot 12. NO_3^- reduction rates were determined by plotting NO_3^- mass vs. time and finding the slope (the absolute value was used). Sulfide was measured with a colorimetric assay (Cord-Ruwisch, 1985). Anoxic samples (500 µL) were withdrawn with a syringe and added immediately to 500 µL of a copper reagent consisting of 50 mM HCl and 5mM $CuSO_4$. The reaction produced the blue-colored CuS, which was measured on a spectrophotometer at 480 nm. Standards were prepared by adding washed crystals of sodium sulfate nonahydrate to anoxic water, and performing serial dilutions in anoxic water. All statistical comparisons were done by performing a paired 2-tailed student t-test. Significance values are indicated by asterisks, and the number of asterisks corresponds to the P-value (as indicated in figure legends).

Results

Sulfide slows NO_3^- reduction and increases NO_2^- accumulation

To test the effect of sulfide on NO_3^- and NO_2^- reduction, cultures of *A. dehalogenans* strain 2CP-C were grown with 10 mM acetate and 1 mM NO_3^- with or without 0.1 mM sulfide. Cultures completely reduced NO_3^- with measurable concentrations of NO_2^- as the intermediate (Figure 3.3). When sulfide was excluded from the medium, nearly all (91% ± 4%) of the NO_3^- accumulated as NO_2^- before NO_2^- was consumed. However, when approximately 0.1 mM sulfide was included, NO_3^- removal took more time (over two days longer) and less NO_2^- accumulated. The rate of NO_3^- reduction during logarithmic growth was 49 ± 1 µmoles/day for sulfide-free cultures and

39 ± 10 μmoles/day for sulfide+ cultures. After the maximum NO_2^- levels were reached for both the sulfide+ and sulfide- amended treatments, subsequent NO_2^- reduction was slower in cultures containing sulfide (Figure 3.3a). The area under the NO_2^- curve indicates that although NO_2^- removal was slower in the presence of sulfide, the total accumulated NO_2^- was still less than in the controls without sulfide (Figure 3.3b). In several repeats of this experiment, NO_2^- accumulation was also observed to be lower or sometimes non-existent in the presence of sulfide (data not shown). The addition of approximately 0.4 mM sulfide completely inhibited NO_3^- reduction (data not shown).

The age of the seed culture (i.e., early log phase, late log phase, and late stationary phase) was tested to determine if that also influenced NO_3^- reduction rates and NO_2^- accumulation rates. Although cultures reduced NO_3^- faster when inoculated from late log phase, similar concentrations of NO_2^- accumulated in each treatment (data not shown). The type of buffer (bicarbonate or HEPES buffer) also did not affect NO_2^- accumulation (data not shown). *A. dehalogenans* requires a reduced source of sulfur in order to grow, so the effect of adding other sulfur sources was tested. The addition of 0.4 mM cysteine did not affect the level of NO_2^- accumulation, indicating the effects seen with sulfide additions were not caused by an increase in sulfur sources in the medium (data not shown). Additionally, *A. dehalogenans* strain 2CP-C does not grow in the absence of cysteine even when sulfide is included in the medium indicating that sulfide may not be utilized for sulfur assimilation (personal observation).

The optimal concentration of Mo for NO_3^- reduction is 1.5 mM

Cultures of *A. dehalogenans* strain 2CP-C were grown on NO_3^- with 0.15, 15, 150, or 1500 μM sodium molybdate dihydrate. The Mo concentration typically used in studies with *A. dehalogenans* strain 2CP-C is 0.15 μM (Sanford *et al.*, 2002, 2012). Sulfide was either excluded or included at a concentration of 0.1 mM. In cultures both with and without sulfide, the time for full NO_3^- reduction decreased as Mo concentrations increased (Figure 3.4a). NO_3^- reduction rates were not calculated due to the coarse time course. The addition of 0.1 mM sulfide consistently increased the time for full NO_3^- as compared to the sulfide-free controls (Figure 3.4a). Sulfide measurements confirmed the presence of 0.1 (±0.02) mM sulfide in the sulfide treatments (data not shown). The

maximum NO_2^- accumulated appeared to be lower for sulfide treatments; however, no statistics are shown since the timescale of measurements is too coarse for such an analysis (Figure 3.4b). To test if concentrations higher than 1.5 mM molybdate further enhance NO_3^- reduction, an additional experiment was performed in which 1.5 mM and 15 mM molybdate was tested. *A. dehalogenans* strain 2CP-C cultures grown with either 1.5 mM Mo or 15 mM Mo did not show a significant difference in time for NO_3^- reduction or maximum NO_2^- accumulation (Figure 3.5). Based on the data shown in Figures 3.4 and 3.5, 1.5 mM molybdate was chosen for subsequent experiments testing the effects of sulfide and Mo on NO_3^- reduction and NO_2^- accumulation.

The addition of Mo alleviates NO_3^- reduction inhibition by sulfide

In order to test if the effects of sulfide on NO_3^- reduction are caused by an interaction with Mo, the following experiments were performed at an optimal concentration (1.5 mM) of Mo. This was done so that two concentrations of Mo could be tested alongside a range of sulfide concentrations, without any effects from Mo (i.e., two concentrations of Mo that yielded the same NO_3^- reduction rates were utilized). Sulfide was added in varied concentrations (0, 0.1, 0.3, and 0.6 mM) and Mo was increased to 3.0 mM in some cultures in order to assess if increasing Mo concentrations could remove negative effects caused by sulfide. The addition of 0.1 mM sulfide did not affect NO_3^- reduction rates or NO_2^- accumulation in the presence of 1.5 mM Mo (data not shown). The addition of 0.3 mM sulfide and 0.6 mM sulfide to cultures of *A. dehalogenans* resulted in decreased NO_3^- reduction rates (Figure 3.6). Increasing the concentration of Mo to 3.0 mM reduced the amount of time needed for complete NO_3^- consumption by 1.5 days in the 0.6 mM sulfide treatment, but had little effect in the 0.3 mM sulfide treatment. The NO_3^- reduction rate was significantly slower than the sulfide-free control in both the 0.3 mM sulfide treatment ($P < 0.01$) and the 0.6 mM sulfide treatment ($P < 0.05$) (Figure 3.6b). Increasing Mo from 1.5 mM to 3.0 mM significantly increased the NO_3^- reduction rate in the 0.3 mM sulfide treatments ($P < 0.05$) but did not significantly affect the 0.6 mM sulfide treatments or control.

Interactions between Mo and sulfide increase NO_2^- accumulation

In sulfide-free controls, increasing the Mo from 1.5 mM to 3.0 mM did not affect NO_2^- accumulation (Figure 3.7a). Since adding 0.3 or 0.6 mM sulfide delayed NO_3^- reduction (Figure 3.6a), the appearance of NO_2^- was also delayed in sulfide treatments (Figure 3.7a). The addition of 0.6 mM sulfide significantly decreased the maximum concentration of NO_2^- measured ($P < 0.005$) (Figure 3.7b). Both 0.3 mM and 0.6 mM sulfide significantly decreased the total amount of accumulated NO_2^- as measured by determining the area under the NO_2^- curve (Figure 3.7b). Increasing Mo from 1.5 mM to 3.0 mM did not significantly affect NO_2^- accumulation in sulfide-free controls, but significantly increased NO_2^- accumulation in both 0.3 and 0.6 mM sulfide treatments (Figure 3.7b).

Sulfide inhibits N_2O reduction by *A. dehalogenans* strain 2CP-C

Like molybdenum, copper is also present in trace concentrations (0.01 μM) in the media used to culture *A. dehalogenans* strain 2CP-C. The N_2O reductase requires copper as a cofactor. To test if sulfide affects N_2O reduction similarly to NO_3^- reduction, cultures of *A. dehalogenans* strain 2CP-C were grown with N_2O as the electron acceptor in the presence and absence of approximately 0.2 mM sulfide. N_2O was consumed in the absence but not in the presence of sulfide (see Figure 2.8 in Chapter 2). This consumption was observed in a number of replicate experiments (data not shown) and anecdotally described by other lab members.

Sulfide prevents chemodenitrification during NO_3^- reduction

To determine the effect of sulfide on chemodenitrifier denitrification (i.e. denitrification as a result of combined abiotic and biotic reactions), NO_3^- or NO_2^- was added to *A. dehalogenans* cultures that had reduced ferric citrate as an electron acceptor in the presence of approximately 0.2 mM sulfide. Cultures of *A. dehalogenans* strain 2CP-C with 10 mM acetate and 12 mM ferric citrate were incubated until 1,000 μmoles ferric iron was reduced to ferrous iron, at which point NO_3^- or NO_2^- was added to the cultures. Cultures that received NO_3^- reduced NO_3^- to NH_4^+, but did not produce N_2O (Figure 3.8a). Acetylene was added to controls to inhibit N_2O reduction. NO_2^- addition

resulted in non-stoichiometric reduction to N_2O both in the presence and absence of acetylene (Figures 3.9b and 3.9c). N_2O was not consumed even in the absence of acetylene (Figure 3.8b).

Discussion

Sulfide decreases NO_3^- reduction rates and NO_2^- accumulation due to an interaction with Mo

Previous literature indicates that sulfide affects NO_3^- reduction rates and end products. Sulfide is known to sequester trace metals, rendering them less biologically available. In the studies described above, the sulfide reduces the rate of NO_3^- reduction by the respiratory ammonifier *A. dehalogenans* strain 2CP-C and is ultimately inhibitory at concentrations of approximately 0.4 mM sulfide when only 0.15 µM Mo is present (Figure 3.3; data not shown). At higher concentrations of Mo (e.g., 1.5 mM), *A. dehalogenans* can reduce NO_3^- in the presence of 0.6 mM sulfide (Figure 3.6a).

Increasing concentrations of Mo increased the NO_3^- reduction rate, while increasing the concentration of sulfide decreased the NO_3^- reduction rate (Figure 3.4a). The concentration typically used to culture *A. dehalogenans* is 0.15 µM (Table 3.1) and is shown here to be suboptimal for NO_3^- reduction. This evidence alone does not demonstrate an interaction between Mo and sulfide (i.e., it does not rule out independent effects of Mo and sulfide). In order to determine if the effects of sulfide and Mo were independent or if sulfide interacts directly with Mo, the Mo concentration was adjusted to an optimal concentration for NO_3^- reduction. When the tested Mo concentration range has no effect on NO_3^- reduction alone, combined Mo and sulfide treatments can be tested to determine their synergistic effect on NO_3^- reduction. Surprisingly, the NO_3^- reduction rate increased with Mo concentration until Mo was at a millimolar (1.5 mM) concentration (Figure 3.4), at which increased concentrations of Mo (i.e., 15 mM Mo) did not affect the NO_3^- reduction rate (Figure 3.5). This concentration is surprisingly high; however, the bioavailability of Mo after addition of Mo to the medium was not tested, and further research is required to determine if a component in sulfide-free medium also sequesters

Mo. It seems likely the concentration of bioavailable Mo was in actuality less than 1.5 mM.

When Mo was adjusted to an optimal concentration (1.5 mM), *A. dehalogenans* was able to grow in the presence of sulfide concentrations that otherwise inhibited growth (Figure 3.6). The addition of 0.6 mM sulfide decreased the NO_3^- reduction rate, but increasing Mo to 3.0 mM decreased the amount of total time for NO_3^- reduction (Figure 3.6). This indicates that the decreased NO_3^- reduction rates were caused by a removal of bioavailable Mo by sulfide. The accumulated NO_2^- (as measured by maximum NO_2^- observed and area under the NO_2^- curve) decreased with increasing sulfide concentrations, but increased with added Mo (Figure 3.7). The decrease in bioavailable Mo resulted in a slower $rate_1$ (Figure 3.2) but did not impact $rate_2$ (or at least, impacted $rate_2$ less than $rate_1$). Interestingly, the NO_3^- reduction rate was not significantly higher in the 3.0 mM Mo and 0.6 mM sulfide treatment than in the 1.5 mM Mo and 0.6 mM sulfide treatment, even though the time to complete NO_3^- consumption was much lower. However, with more frequent measurements, the NO_3^- reduction rate could have been more accurate and possibly reflected a significant difference.

It is important to note that in the presence of 0.6 mM sulfide, NO_2^- reduction rates were also affected (Figure 3.7a). Iron is required for the NH_4^+-forming NO_2^- reductase (NrfA) encoded on the genome of *A. dehalogenans* (Figure 3.1). Since the concentration of trace iron is a magnitude higher than Mo in the medium used for these experiments (Table 3.1), it was hypothesized that sequestration by sulfide would not affect NO_2^- reduction as greatly as NO_3^- reduction. Although sulfide decreased NO_2^- reduction rates, NO_2^- accumulation was still significantly lower in sulfide treatments (Figure 3.7b).

The ability of sulfide to complex Mo and decrease NO_2^- accumulation during respiratory ammonification has important consequences for N turnover in the environment. Since the experiments described here were performed in pure cultures, any NO_2^- released into the medium was subsequently utilized by *A. dehalogenans*. However, it is possible that in a natural environment, a competing microorganism may be able to utilize the NO_2^- more quickly than *A. dehalogenans*. Additionally, NO_2^- serves as a regulator between denitrification and respiratory ammonification (Yoon *et al.*, 2015) and

the amount of NO_2^- released from the cell may influence the extent of chemodenitrification, as discussed in the following section.

Sulfide determines the potential for chemodenitrification

Previous experiments demonstrated that *A. dehalogenans* completely reduces NO_3^- to N_2 in the presence of ferrous iron due to an abiotic reaction between NO_2^- and ferrous iron (Chapter 2; Table 3.2). However, if NO_2^- is not released from the cell, it may not react as readily with ferrous iron. When sulfide was included in the medium, NO_3^- was reduced to NH_4^+ rather than reacting with ferrous iron (Figure 3.8a), suggesting that sulfide prevents chemodenitrification. Thus the presence or absence of ferrous iron and sulfide dramatically changed the final product of NO_3^- reduction by *A. dehalogenans* (Table 3.2). When NO_2^- was added directly to iron-reducing cultures, N_2O was still produced, indicating that NO_2^- still reacts with ferrous iron under these conditions (Figures 3.9b and 3.9c). N_2O was stable both in the presence and absence of acetylene (Figures 3.9b and 3.9c), which is consistent with the observation that sulfide inhibits N_2O reduction by *A. dehalogenans* (Figure 2.8).

Although decreased NO_3^- reduction rates in the presence of sulfide is consistent with previous observations, the decreased NO_2^- accumulation contradicts several environmental studies that observed increased NO_2^- accumulation in the presence of sulfide (Tugtas and Pavlostathis, 2007; Aelion and Warttinger, 2009). There are several possible explanations for the contradiction. First of all, the ability to quickly remove NO_2^- by *A. dehalogenans* may not be shared by all soil communities. This explanation does not seem likely, considering the wide diversity of bacteria found in soils. Alternatively, those environments may have limiting concentrations of bioavailable iron (which is limited in natural environments) and limited copper for assimilation into NarK NO_2^- reductases, thus decreasing $rate_2$ (Figure 3.1). In the present experiments, 7.5 μM iron chloride was included in the medium, and additional ferrous iron was available in iron reduction experiments, so iron was assumed to not be limiting. Additionally, *A. dehalogenans* does not depend on copper for NO_2^- reduction. Copper is at a low concentration (0.01 μM) in the medium, and thus is presumed to be more sensitive to sulfide sequestration, as evidenced by the inhibition of N_2O reduction in the presence of 0.2 mM sulfide (Figures

2.8 and 3.8). This suggests that environments containing low concentrations of bioavailable iron and copper would see an increase in NO_2^- accumulation due to sequestering of iron and copper by sulfide. In Chapter 2 it was demonstrated that gene content and the presence of iron reduction are important factors determining chemodenitrification potential. In this section, it is shown that the concentrations of sulfide and bioavailable Mo, copper, and iron are also important (Figure 3.9). Each step in denitrification and respiratory ammonification is affected by specific metal-containing cofactors that are limiting in different environments. The findings presented here demonstrate a mechanism by which sulfide alters both N-turnover rates and end-products of NO_3^- reduction, suggesting that sulfide plays an important role in N-turnover in the environment.

Limitations and future directions

The experiments described above tested the effects of sulfide on copper-dependent processes (i.e., N_2O reduction) and Mo-dependent processes (i.e., NO_3^- reduction) but did not test the effect of sulfide on NO_2^- reduction in detail. Although the concentration of iron is a magnitude higher than that of Mo and copper (Table 3.1), the amount of sulfide (0.6 mM) added should theoretically be enough to sequester the iron in the medium. Indeed, negative effects of sulfide on NO_2^- reduction rates were observed when 0.6 mM sulfide was added to NO_3^--reducing cultures (Figure 3.7a). Further experiments with *A. dehalogenans* growing on NO_2^- as the sole electron acceptor are recommended to distinguish the effects of sulfide on NO_2^- release from cells and on NO_2^- reduction rates by the NO_2^- reductase.

When testing the effect of sulfide on microbial-mediated chemodenitrification, bicarbonate buffer was utilized (Figure 3.8). Since other experiments were performed with HEPES buffer (Figures 3.3-3.8), it would be most thorough to repeat the chemodenitrification experiment shown in Figure 3.8 with a HEPES-buffered medium. However, since buffer type did not affect the amount of NO_2^- accumulated (data not shown), it is not expected that buffer type will cause a different outcome. Additionally, the experiments in Figure 3.8 were performed with non-optimal analytical techniques (i.e., there was an overlapping peak with NO_3^-), leading to inaccurate quantification of

NO_3^- concentrations. It would also be interesting to grow *A. dehalogenans* with ferric iron in the presence of sulfide and elevated levels of Mo, then add NO_3^-, to see if the inhibition of chemodenitrifier denitrification by sulfide can be relieved by added Mo. This is expected, since added Mo alleviated the effects of sulfide inhibition of NO_2^- accumulation in cultures without ferric citrate (Figure 3.6).

The genome of *A. dehalogenans* strain 2CP-C encodes the genes for two NO_3^- reductases: *narG* (encoding a membrane-bound NO_3^- reductase) and *napA* (encoding a periplasmic NO_3^- reductase. It is possible that the relative expression of each of these affects the concentration of NO_2^- released into the medium. If that is the case, measuring the protein expression of NarG and NapA and determining what conditions influence their expression will shed further light on environmental conditions that influence the chemodenitrifier lifestyle.

References

Aelion CM, Warttinger U. (2009). Low sulfide concentrations affect nitrate transformations in freshwater and saline coastal retention pond sediments. *Soil Biol Biochem* **41**: 735–741.

Betlach MR, Tiedje JM. (1981). Kinetic explanation for accumulation of nitrite, nitric oxide, and nitrous oxide during bacterial denitrification. *Appl Environ Microbiol* **42**: 1074–1084.

Broadbent FE, Clark F. (1965). Denitrification. In: Bartholomew W V., Clark FE (eds). *Soil Nitrogen*. American Society of Agronomy, Inc.: Madison, Wisconsin, pp 344–359.

Cleemput O Van, Samater AH. (1996). Nitrite in soils: accumulation and role in the formation of gaseous N compounds. *Fertil Res* **45**: 81–89.

Cord-Ruwisch R. (1985). A quick method for the determination of dissolved and precipitated sulfides in cultures of sulfate-reducing bacteria. *J Microbiol Methods* **4**: 33–36.

Gelfand I, Yakir D. (2008). Influence of nitrite accumulation in association with seasonal patterns and mineralization of soil nitrogen in a semi-arid pine forest. *Soil Biol Biochem* **40**: 415–424.

Glass JB, Axler RP, Chandra S, Goldman CR, Sañudo-Wilhelmy S. (2012). Molybdenum limitation of microbial nitrogen assimilation in aquatic ecosystems and pure cultures. e-pub ahead of print, doi: 10.3389/fmicb.2012.00331.

Glass JB, Orphan VJ. (2012). Trace metal requirements for microbial enzymes involved in the production and consumption of methane and nitrous oxide. *Front Microbiol* **3**: 1–20.

Gonzalez-Gil G, Kleerebezem R, Lettinga G. (1999). Effects of nickel and cobalt on kinetics of methanol conversion by methanogenic sludge as assessed by on-line CH_4 monitoring. *Appl Environ Microbiol* **65**: 1789–1793.

González PJ, Correia C, Moura I, Brondino CD, Moura JJG. (2006). Bacterial nitrate reductases: Molecular and biological aspects of nitrate reduction. *J Inorg Biochem* **100**: 1015–1023.

Gould WD, McCready RGL. (1982). Denitrification in several Alberta soils: Inhibition by sulfur anions. *Can J Soil Sci* **62**: 333–342.

Graf DRH, Jones CM, Hallin S. (2014). Intergenomic comparisons highlight modularity of the denitrification pathway and underpin the importance of community structure for N_2O emissions. *PLoS Biol* **9**: 1–20.

Hagen WR. (2011). Cellular uptake of molybdenum and tungsten. *Coord Chem Rev* **255**: 1117–1128.

Jansen S, Gonzalez-Gil G, Van Leeuwen HP. (2007). The impact of Co and Ni speciation on methanogenesis in sulfidic media—Biouptake versus metal dissolution. *Enzyme Microb Technol* **40**: 823–830.

Kelso BHL, Smith R V., Laughlin RJ, Lennox SD. (1997). Dissimilatory nitrate reduction in anaerobic sediments leading to river nitrite accumulation. *Appl Environ Microbiol* **63**: 4679–4685.

Klüber HD, Conrad R. (1998). Inhibitory effects of nitrate, nitrite, NO, and N_2O on methanogenesis by *Methanosarcina barkeri* and *Methanobacterium bryantii*. *FEMS Microbiol Ecol* **25**: 331–339.

Lilja EE, Johnson DR. (2016). Segregating metabolic processes into different microbial cells accelerates the consumption of inhibitory substrates. *ISME J* **10**: 1568–1578.

Löffler FE, Sanford RA, Tiedje JM. (1996). Initial characterization of a reductive dehalogenase from *Desulfitobacterium chlororespirans* Co23. *Appl Environ Microbiol* **62**: 3809–13.

Manconi I, van der Maas P, Lens P. (2006). Effect of copper dosing on sulfide inhibited reduction of nitric and nitrous oxide. *Nitric Oxide* **15**: 400–407.

Moraghan JT, Buresh RJ. (1977). Chemical reduction of nitrite and nitrous oxide by ferrous iron. *Soil Sci Soc Am J* **41**: 47–50.

Moreno-Vivián C, Cabello P, Martínez-Luque M, Blasco R, Castillo F. (1999). Prokaryotic nitrate reduction: Molecular properties and functional distinction among bacterial nitrate reductases. *J Bacteriol* **181**: 6573–6584.

Philips S, Laanbroek HJ, Verstraete W. (2002). Origin, causes and effects of increased nitrite concentrations in aquatic environments. *Rev Environ Sci Bio/Technology* **1**: 115–141.

Sanford RA, Cole JR, Tiedje JM. (2002). Characterization and description of *Anaeromyxobacter dehalogenans* gen. nov., sp. nov., an aryl-halorespiring facultative anaerobic myxobacterium. *Appl Environ Microbiol* **68**: 893–900.

Sanford RA, Wagner DD, Wu Q, Chee-Sanford JC, Thomas SH, Cruz-García C, *et al.* (2012). Unexpected nondenitrifier nitrous oxide reductase gene diversity and abundance in soils. *Proc Natl Acad Sci U S A* **109**: 19709–14.

Senga Y, Mochida K, Fukumori R, Okamoto N, Seike Y. (2006). N 2 O accumulation in estuarine and coastal sediments: The influence of H 2 S on dissimilatory nitrate reduction. e-pub ahead of print, doi: 10.1016/j.ecss.2005.11.021.

Shen QR, Ran W, Cao ZH. (2003). Mechanisms of nitrite accumulation occurring in soil nitrification. *Chemosphere* **50**: 747–753.

Sørensen J, Tiedje JM, Firestone RB. (1980). Inhibition by sulfide of nitric and nitrous oxide reduction by denitrifying *Pseudomonas fluorescens*. *Appl Environ Microbiol* **39**: 105–108.

Stein LY, Klotz MG. (2016). The nitrogen cycle. *Curr Biol* **26**: R94–R98.

Stevens RJ, Laughlin RJ, Malone JP. (1998). Soil pH affects the processes reducing nitrate to nitrous oxide and di-nitrogen. *Soil Biol Biochem* **30**: 1119–1126.

Thorgersen MP, Lancaster WA, Vaccaro BJ, Poole FL, Rocha AM, Mehlhorn T, *et al.* (2015). Molybdenum availability Is key to nitrate removal in contaminated groundwater environments. *Appl Environ Microbiol* **81**: 4976–4983.

Tiedje JM. (1988). Ecology of denitrification and dissimilatory nitrate reduction to ammonium. In: Zehnder AJB (ed). *Biology of Anaerobic Microorganisms*. John Wiley & Sons, Inc.: New York City, pp 179–244.

Tugtas AE, Pavlostathis SG. (2007). Effect of sulfide on nitrate reduction in mixed methanogenic cultures. *Biotechnol Bioeng* **97**: 1448–1459.

Wolin EA, Wolin MJ, Wolfe RS. (1963). Formation of methane by bacterial extracts. *J Biol Chem* **238**: 2882–2886.

Yoon S, Cruz-García C, Sanford R, Ritalahti KM, Löffler FE. (2014). Denitrification versus respiratory ammonification: environmental controls of two competing dissimilatory NO_3^-/NO_2^- reduction pathways in *Shewanella loihica* strain PV-4. *ISME J* 1093–1104.

Yoon S, Sanford R, Löffler FE. (2015). Nitrite control over dissimilatory nitrate/nitrite reduction pathways in *Shewanella loihica* strain PV-4. *Appl Environ Microbiol* **81**:

Appendix: Tables

Table 3.1. Concentration of trace metals in medium. Trace metals shown in Figure 3.1 are highlighted by orange (iron), blue (molybdenum), and green (copper).

Compound	Conc. (µM)
$FeCl_2$ x 4 H_2O	7.54
$CoCl_2$ x 6 H_2O	0.69
$MnCl_2$ x 4 H_2O	0.51
$ZnCl_2$	0.51
H_3BO_3	0.10
Na_2MoO_4 x 2 H_2O	0.15
$NiCl_2$ x 6 H_2O	0.10
$CuCl_2$ x 2 H_2O	0.01

Table 3.2. End products of NO_3^-/NO_2^- reduction in *A. dehalogenans* strain 2CP-C cultures under different iron and sulfide conditions.

Compound	6-8 mM Ferrous Iron	0.2 mM Sulfide	End Product
NO_3^-	+	+	NH_4^+
NO_2^-	+	+	N_2O
NO_3^-	+	-	N_2/NH_4^+
NO_2^-	+	-	N_2
NO_3^-/NO_2^-	-	+/-	NH_4^+

Appendix: Figures

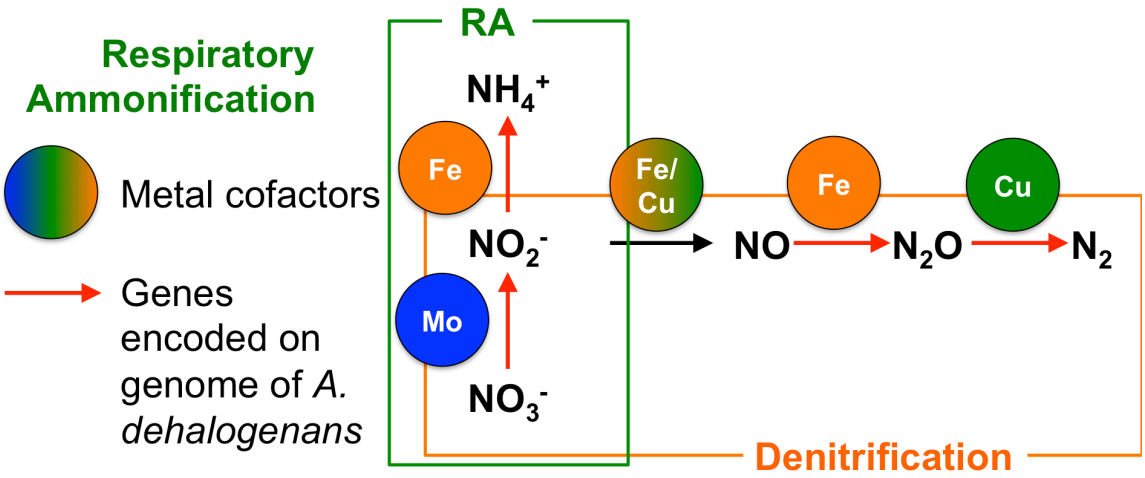

Figure 3.1. NO_3^- reduction pathways and required trace metals for N-cycle enzymes. Genes on the genome of *A. dehalogenans* strain 2CP-C are indicated by red arrows. Note: NO_2^- reduction to nitric oxide can be performed by NirS (which contains iron) or NirK (which contains copper).

Figure 3.2. NO_3^- reduction by *A. dehalogenans* and associated rates.

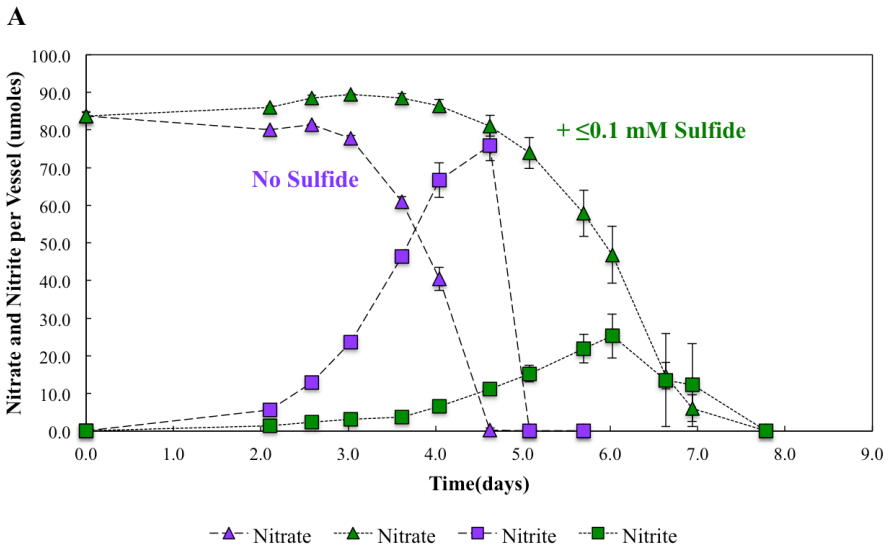

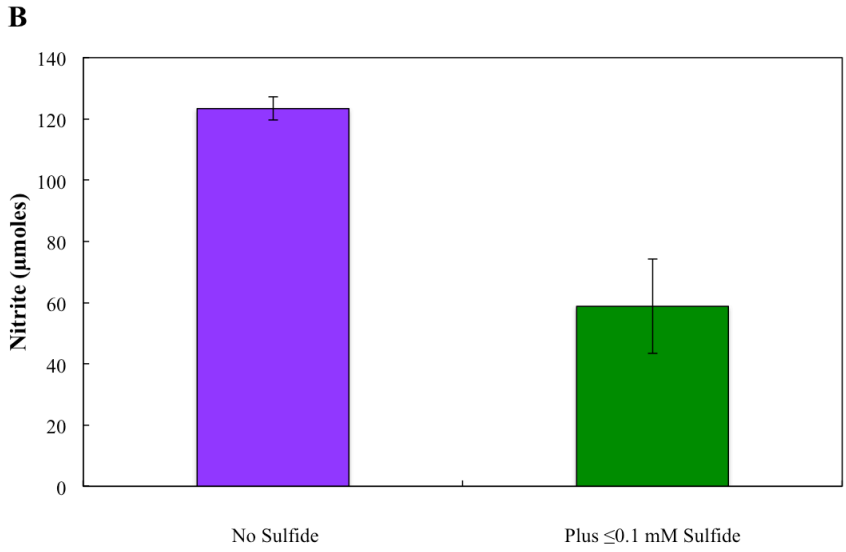

Figure 3.3 *A. dehalogenans* strain 2CP-C cultures with 10 mM acetate and 1 mM NO_3^- in the presence or absence of ≤0.1 mM sulfide. (A) Total NO_3^- and NO_2^- per vessel. (B) Area under the NO_2^- curves from part A. Each point and bar represents the average of three replicate cultures, and error bars show the standard deviation.

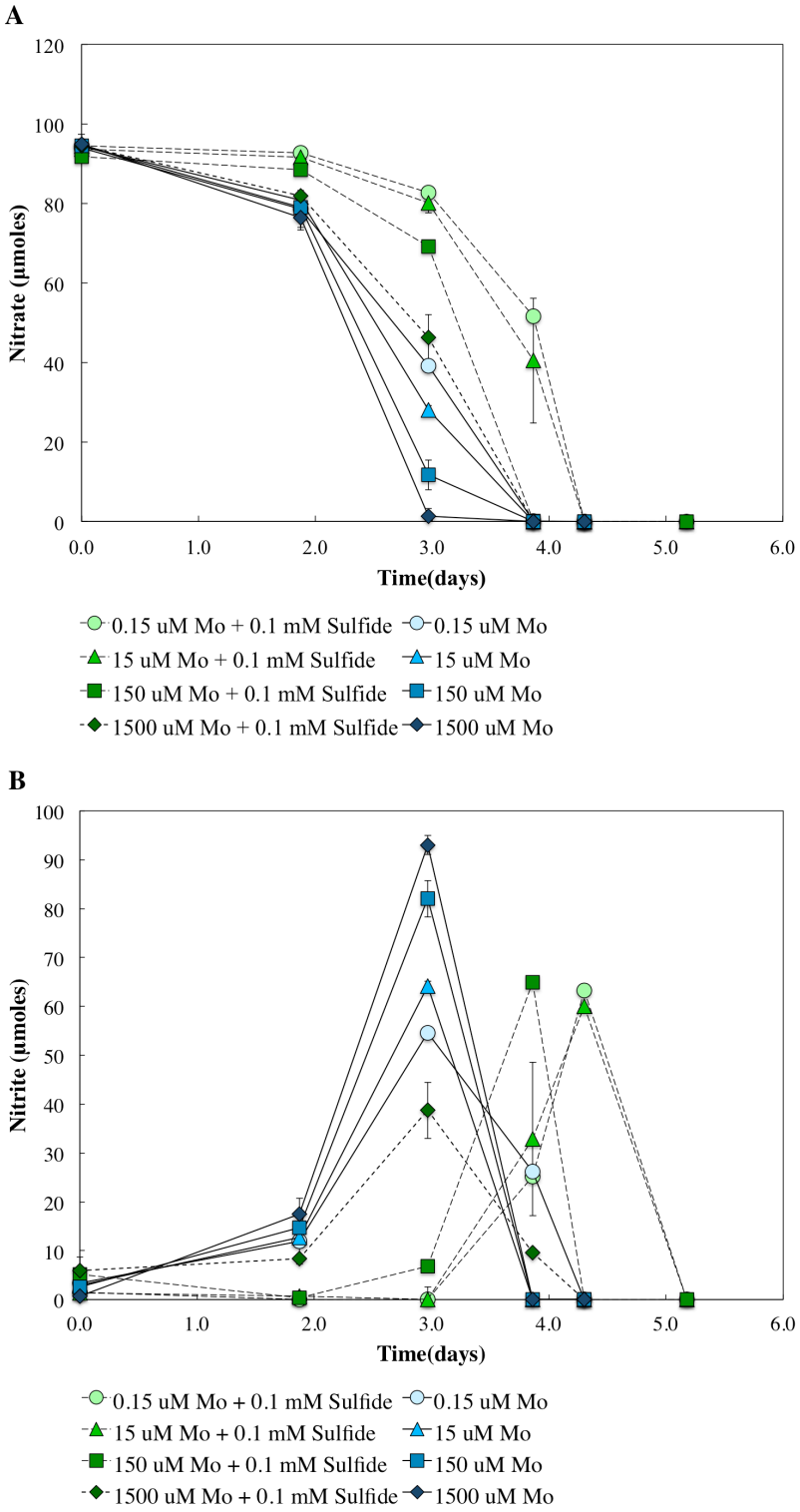

Figure 3.4 Effect of molybdenum on NO_3^- reduction. *A. dehalogenans* strain 2CP-C cultures with 10 mM acetate, 1 mM NO_3^-, and different concentrations of molybdate in the presence or absence of 0.1 mM sulfide. (A) Total NO_3^- per vessel. (B) Total NO_2^- per vessel. Each point represents the average of two replicate cultures, and error bars show the standard deviation.

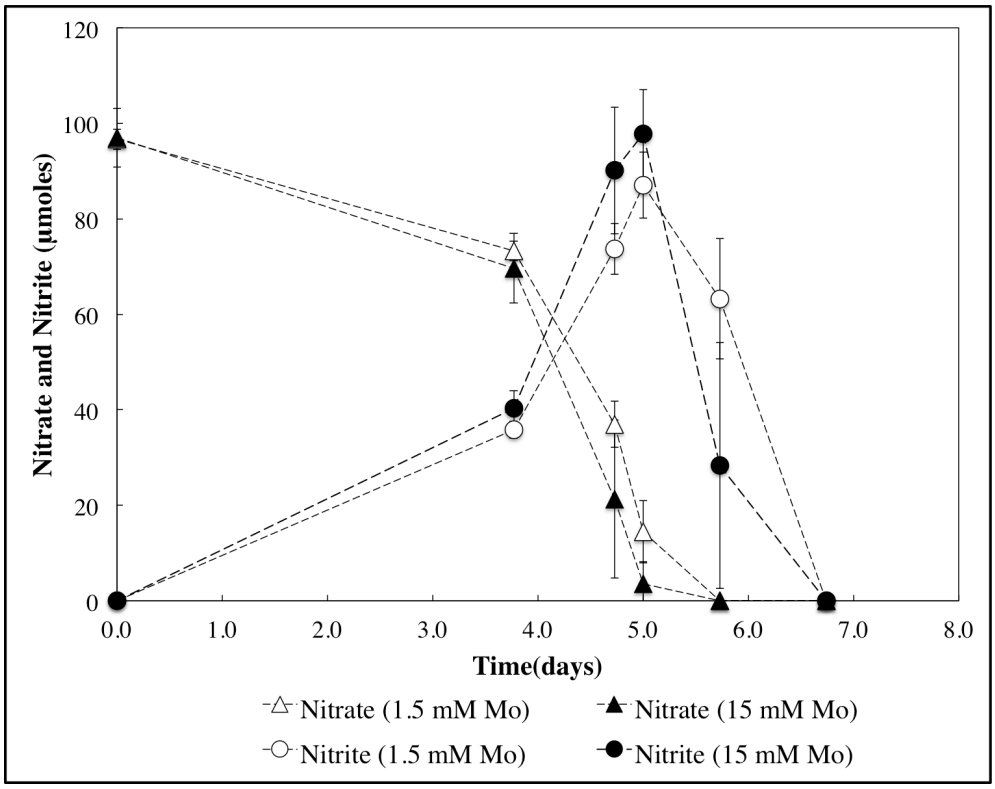

Figure 3.5. Effect of >1.5 mM molybdenum on NO_3^- reduction. *A. dehalogenans* strain 2CP-C cultures with 10 mM acetate, 1 mM NO_3^-, and either 1.5 mM molybdate or 15 mM molybdate. Each point represents the average of three replicate cultures, and error bars show the standard deviation.

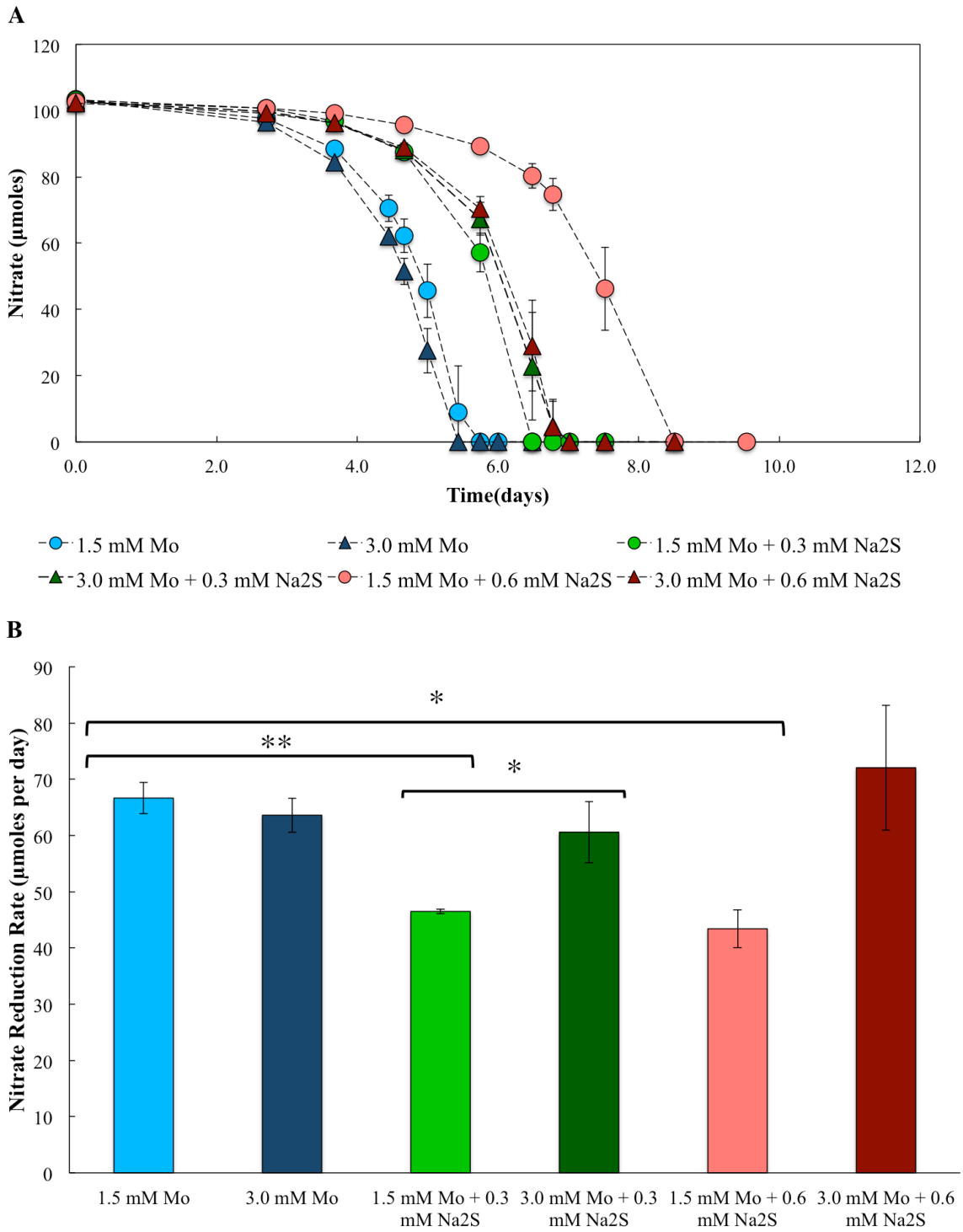

Figure 3.6 *A. dehalogenans* strain 2CP-C cultures with 10 mM acetate, 1 mM NO_3^-, and varied concentrations of molybdate and sulfide. Each point or bar represents the average of three replicate cultures, and error bars show the standard deviation. (B) NO_3^- reduction rates from (A). Asterisks indicate the significance based on a 2-tailed student t-test. * $p < 0.05$ ** $p < 0.01$

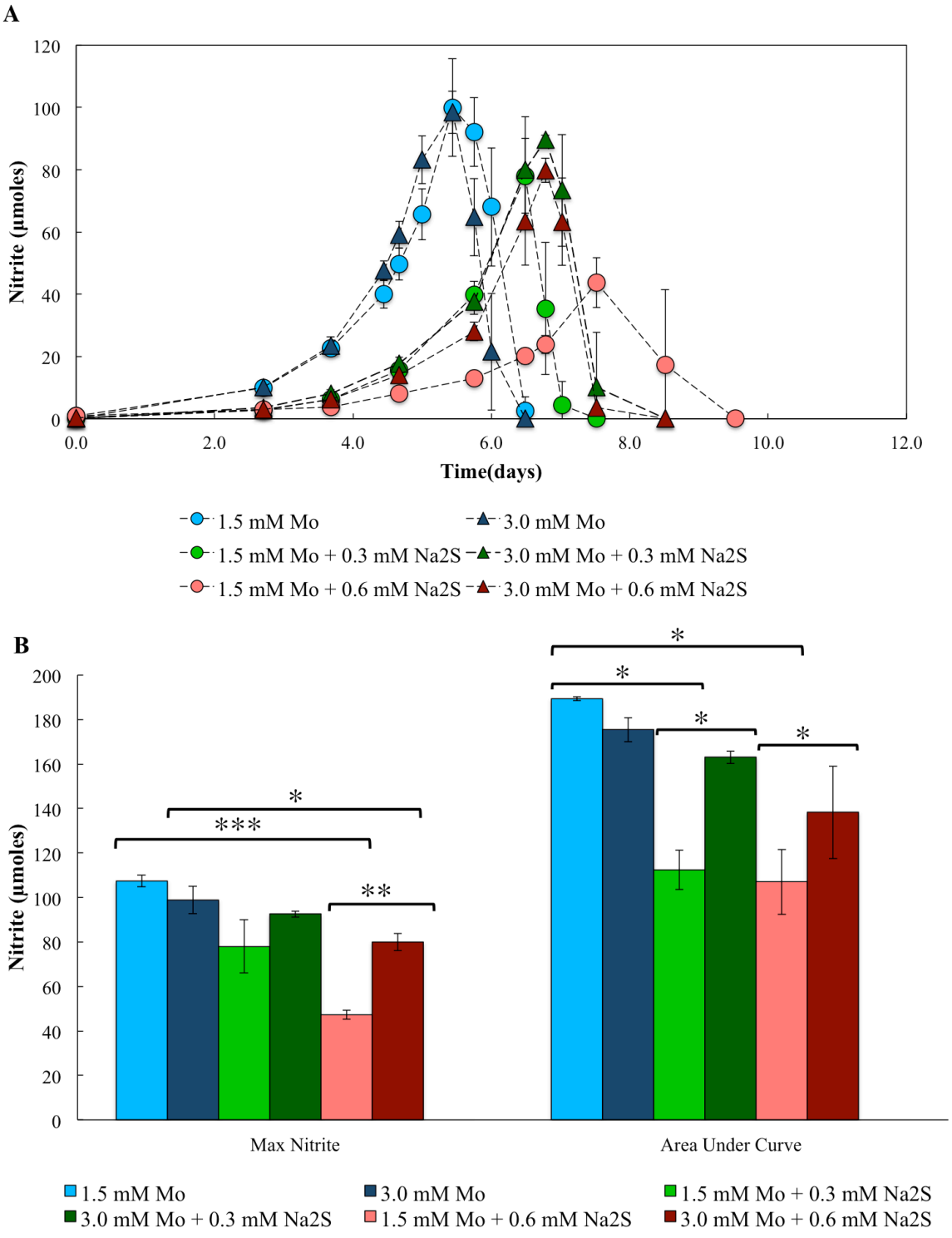

Figure 3.7. Effect of molybdenum concentration on NO_2^- accumulation. NO_2^- concentrations from experiment shown in Figure 3.6. Each bar or point represents the average of three replicate cultures, and error bars show the standard deviation. (B) Maximum NO_2^- measured and the area under the NO_2^- curve. Asterisks indicate the significance based on a 2-tailed student t-test. * $p < 0.05$ ** $p < 0.01$ *** $p < 0.005$

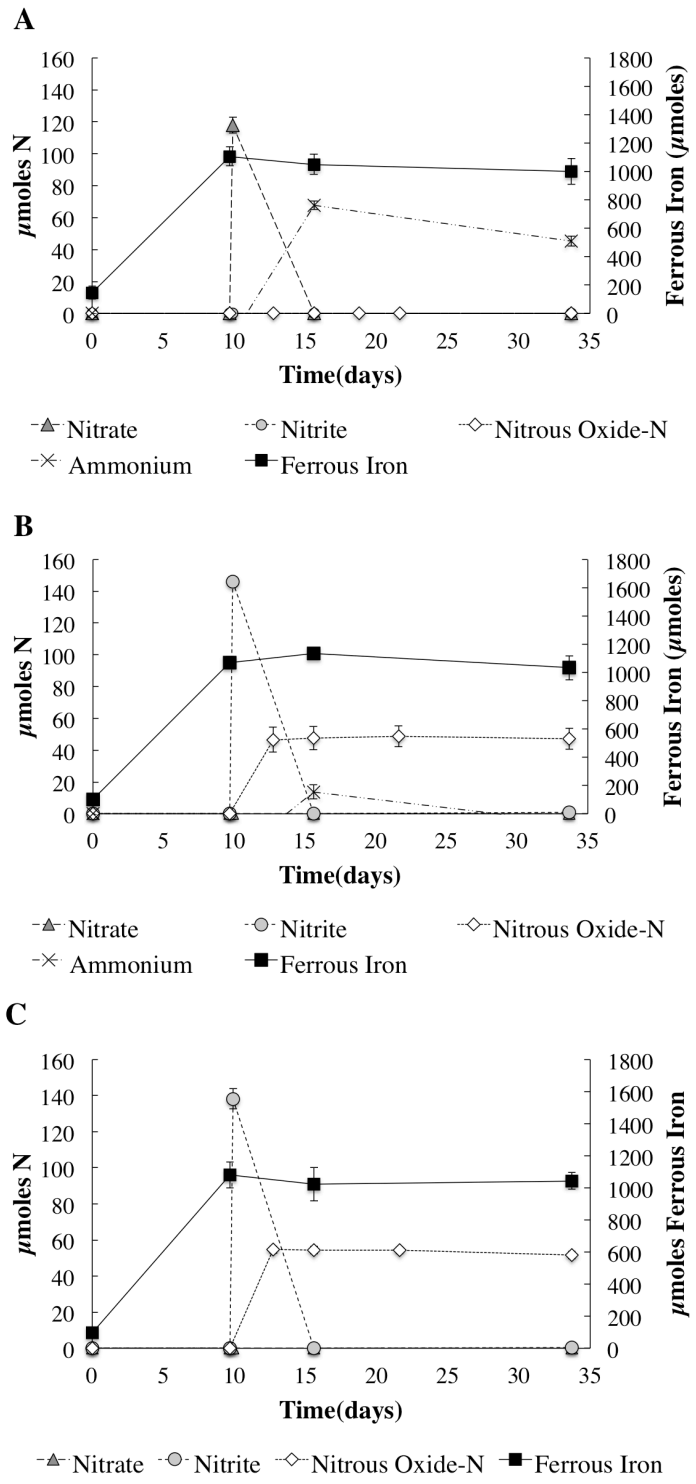

Figure 3.8. Effect of sulfide on chemodenitrification. Cultures reducing ferric citrate with NO_3^- or NO_2^- additions in the presence of ≤0.2 mM sulfide. (A) Cultures grown with ferric citrate; 100 µmoles NO_3^- added on day 10. (B) Cultures grown with ferric citrate; 100 µmoles NO_2^- added on day 10. (C) Same as B except headspace included 10% acetylene gas. Each point represents the average of three replicate cultures, and error bars show the standard deviation.

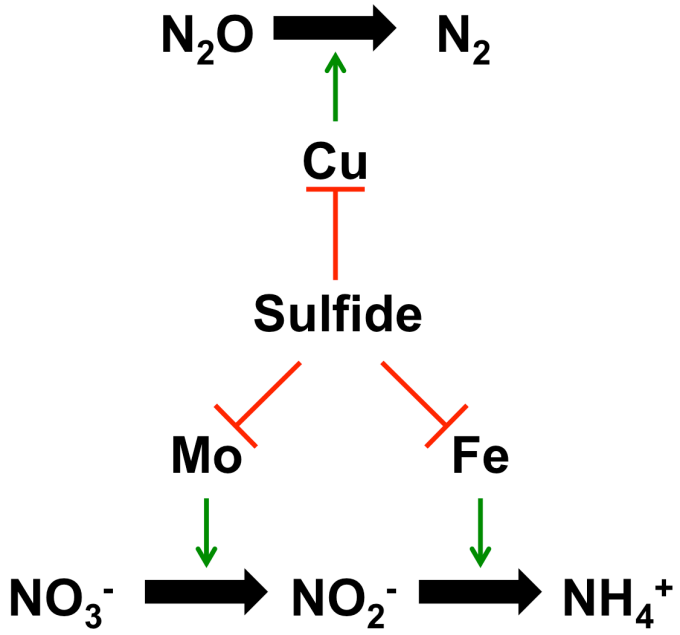

Figure 3.9. Effects of sulfide on N-cycling by *A. dehalogenans*. Green arrows indicate a positive relationship and red lines indicate a negative effect (i.e., sequestration).

Chapter 4: Oxygen Detoxification and Utilization by *Anaeromyxobacter dehalogenans*

Abstract

Microoxic concentrations of oxygen (O_2) occur naturally in many environments, and microorganisms have evolved mechanisms to utilize a range of O_2 concentrations. Aerobes possess low-affinity cytochrome *c* oxidases (e.g., cytochrome aa_3) to respire high levels (i.e., 21%) of O_2, while microaerophiles possess high-affinity oxidases (e.g., cytochrome cbb_3) to respire low levels of O_2. Many facultative anaerobes possess both high- and low-affinity oxidases, enabling them to utilize both low and high levels of O_2. *Anaeromyxobacter dehalogenans* is a microaerophilic soil bacterium that is well adapted to fluctuating redox conditions, as this organism utilizes many different electron acceptors including microoxic concentrations of O_2. The genome of *A. dehalogenans* encodes both cytochrome aa_3 and cytochrome cbb_3, and *A. dehalogenans* was classified as a facultative anaerobe due to the ability to grow in microoxic and anoxic conditions. The presence of cytochrome aa_3 genes on the genomes of organisms incapable of respiration with 21% O_2 suggests another role for cytochrome aa_3, such as O_2 detoxification. In the present study the role of cytochrome aa_3 is examined and previous O_2 growth studies are expanded upon with *A. dehalogenans* strain 2CP-C. *A. dehalogenans* was cultured with varying concentrations of O_2 (2-21%) and growth rates were measured by optical density measurements. Proteins were extracted from cells grown with 5, 15, and 21% O_2 and analyzed via LC-MS/MS. Contrary to past studies, robust aerobic growth by *A. dehalogenans* with classical aerobic growth methods (i.e., rapid shaking in baffled flasks) was observed. The subunit II of cytochrome aa_3 subunit was expressed under all three concentrations of O_2, suggesting that *A. dehalogenans* utilizes low-affinity cytochrome *c* oxidases for aerobic growth. Several reactive oxygen species (ROS)-detoxifying proteins were detected, including a relatively high abundance of rubrerythrin. Additionally, a number of other *c*-type cytochromes were expressed in all three conditions, including the two hypothetical proteins Adeh_2966 and Adeh_2967, which were not detected during growth with other electron acceptors (except NO_3^-) and warrant further investigation. The findings presented here support the classification of *A. dehalogenans* as a facultative anaerobe, and demonstrate further metabolic flexibility (i.e., growth with 21% O_2) in this versatile microorganism.

Introduction

The Earth's atmosphere is composed of 21% oxygen (i.e., 0.21 pO_2), and oxygen (O_2) is essential to many organisms on Earth. However, O_2 is poorly soluble in water, and many natural environments have a gradient of O_2 concentrations from 21% O_2 to anoxia (Brune *et al.*, 2000; Morris and Schmidt, 2013). Examples of O_2 gradients include marine snow, soil particles, plants, digestive tracts of mammals and insects, sediments, and plant roots (Morris and Schmidt, 2013; Brune *et al.*, 2000). The interface between oxic and anoxic environments is crucial to biogeochemical processes and contaminant turnover, because reduced compounds (e.g., Fe[II], Mn[II], and U[IV]) can be reoxidized at the oxic/anoxic interface (Wu *et al.*, 2007; Roden *et al.*, 2012). The ability of an organism to survive the influx of O_2 may lend an ecological advantage in these environments. For example, hexavalent uranium (U[VI]) can be reduced to U(IV) by a number of iron-reducing bacteria such as *Anaeromyxobacter* and *Geobacter* species. However, *Anaeromyxobacter dehalogenans* species are able to tolerate O_2 and increase in numbers after the influx of O_2 , whereas *Geobacter lovleyi* cell numbers remain constant or decrease (Thomas *et al.*, 2010). Further studies under microoxic conditions will shed light on the ecophysiology of microorganisms that thrive in oxic gradients.

Microorganisms have a variety of relationships to O_2, and are frequently categorized as obligate aerobes, microaerophiles, facultative anaerobes, nanaerobes, aerotolerant anaerobes, and obligate anaerobes (Ludwig, 2004; Morris and Schmidt, 2013). Generally speaking, aerobes have a positive relationship between growth substrate turnover and O_2 concentration, while anaerobes have a negative relationship. Microaerophiles have a peak substrate turnover rate at a microoxic concentration of O_2 and decreasing substrate turnover as O_2 concentrations increase or decrease (Ludwig, 2004). These terms are sometimes used incorrectly or with different definitions; this dissertation will use the definitions as outlined in Morris and Schmidt 2013. Many microorganisms have enzymes that defend against reactive oxygen species (ROS). These can include superoxide dismutase ($O_2^- + O_2^- + H^+ \rightarrow H_2O_2 + O_2$), peroxidase ($H_2O_2 + NADH + H^+ \rightarrow 2H_2O + NAD^+$), catalase ($H_2O_2 + H_2O_2 \rightarrow 2H_2O + O_2$), rubrerythrin ($H_2O_2 + NADH + H^+ \rightarrow 2H_2O + NAD^+$), and rubredoxin (Polyglucose + $NADH + H^+ \rightarrow$ glucose + NAD^+ [i.e., for *D. vulgaris*]) (Thomas *et al.*, 2008; Madigan *et al.*, 2015). A

key defining feature between aerobes, facultative anaerobes, and microaerophiles is the terminal electron accepting enzyme utilized by these organisms. The final enzyme in the electron transport chain is a *c*-type cytochrome, which catalyzes the reduction of O_2 to water. The type of terminal enzyme distinguishes the type of respiration of an organism. Before an explanation of cytochrome types is made, however, the nomenclature of cytochromes must be made clear. A cytochrome is a heme-containing protein that transfers electrons. In a "*c*-type cytochrome," the heme is covalently bound to the protein via the CxxCH motif (Meyer, 1996). However, the CxxCH motif is also found in many other types of proteins and the presence of a CxxCH domain alone does not indicate that a protein is a cytochrome (Meyer, 1996). Heme is a prosthetic group that has an iron atom (which undergoes oxidation-reduction reactions) in a porphyrin, and can have a variety of functional groups. Depending on the different functional groups, heme has different designations. Cytochromes are named after these hemes, such that "cytochrome *c*" contains heme C, cytochrome aa_3 contains two of heme A, cytochrome cbb_3 contains two of heme C and a heme B, and so forth (although some contain additional hemes not included in the name). Aerobic organisms utilize low-affinity terminal oxidases such as cytochrome aa_3, whereas microaerophiles utilize high-affinity terminal oxidases such as cytochrome cbb_3 and cytochrome *bd* (Morris and Schmidt, 2013). Cytochrome cbb_3 has a high affinity for O_2 and appears to have evolved within the Proteobacteria for the purpose of microaerophilic metabolism; however, it has been hypothesized to serve as a redox sensor as well (Pitcher and Watmough, 2004). On the other hand, cytochrome aa_3 is used for O_2 respiration at ambient concentrations of O_2, and its presence in the genome of anaerobes is sometimes unexplained. Some facultative anaerobes have both high- and low-affinity oxidases, allowing growth in oxic and microoxic conditions.

Anaeromyxobacter dehalogenans strains have been classified several different ways since their description in 1994. Before the genus was described, the first isolate (later to be named *A. dehalogenans* strain 2CP-1) was described as a "facultative anaerobe" due to its ability to grow with approximately 0.07 pO_2 (Cole *et al.*, 1994). The inability of strain 2CP-1 to grow in open containers was speculated to be caused by a dependency on CO_2 in the headspace (Cole *et al.*, 1994). Later the genus *Anaeromyxobacter* was described along with *A. dehalogenans* strains 2CP-1, 2CP-3, and

2CP-C, and these strains were also described as facultative anaerobes that utilize low levels of O_2 (i.e., 0.05 pO_2 on plates and 0.006 pO_2 in broth) and grow poorly with air (Sanford *et al.*, 2002). A myxobacterium capable of anaerobic growth was a novel finding, since members of the myxobacteria were previously shown to be obligate aerobes. Since *Anaeromyxobacter* branches deeply in the Myxococcales order, Thomas et al. proposed that the anaerobic lifestyle is due to convergent evolution (2008). Further studies with *A. dehalogenans* strain 2CP-C showed growth at up to 18% O_2 and a negative correlation between growth and O_2 concentration (Thomas *et al.*, 2010). Growth was inconsistent at a pO_2 of 0.21, and strain 2CP-C was classified as a microaerophile (Thomas *et al.*, 2010). Interestingly, the genome of *A. dehalogenans* strain 2CP-C contains the genes for both cytochrome aa_3 and cytochrome cbb_3 (Figure 4.1). Cytochrome aa_3 is associated with an aerobic lifestyle, yet *A. dehalogenans* did not grow with ambient levels of O_2 (Thomas *et al.*, 2008, 2010). It was suggested that cytochrome aa_3 may be utilized as a non-respiratory enzyme for detoxification of O_2 and ROS (Thomas *et al.*, 2008, 2010); however, currently the function of cytochrome aa_3 in *A. dehalogenans* is unknown. Further research is needed to determine if *A. dehalogenans* expresses cytochrome aa_3 and if *A. dehalogenans* utilizes cytochrome aa_3 for aerobic respiration.

The genome of another facultative anaerobe, *Shewanella oneidensis* MR-1, encodes cytochrome aa_3, cbb_3, and *bd*, and the role of these cytochrome *c* oxidases were examined. Studies of *Shewanella oneidensis* MR-1 showed different abundance patterns of transcripts and proteins for O_2 respiration genes (Zhou *et al.*, 2013; Le Laz *et al.*, 2014, 2016). When transcript abundance was measured, cytochrome cbb_3 and a *bd*-type oxidase were expressed under oxic conditions, while cytochrome aa_3 was only present at low levels in all conditions tested and not considered to be physiologically important (Zhou *et al.*, 2013). Measurements of protein abundance showed expression of cbb_3 and the *bd*-type oxidase and the absence of cytochrome aa_3 as well (Le Laz *et al.*, 2014). Transcript measurements showed greater expression of cytochrome cbb_3 at low levels of O_2 than in high levels of O_2 (Zhou *et al.*, 2013), while protein measurements demonstrated similar levels of cytochrome cbb_3 protein at both low and high concentrations of O_2 (Le Laz *et al.*, 2014). Differences in the *bd*-type oxidase expression observed with transcript

abundance under oxic and microoxic conditions were more significant when measured by protein abundance than with transcript abundance. A later study demonstrated the expression of cytochrome aa_3 under carbon-limiting and oxic conditions (Le Laz *et al.*, 2016). These studies demonstrated that while cytochrome cbb_3 may be utilized for microaerophilic growth, it also appears to play a role in aerobic growth, and cytochrome aa_3 may only be expressed during aerobic growth with carbon is limiting. Whether this is specific to *S. oneidensis* or if it applies to other microorganisms remains to be seen. These studies also demonstrate that the measurement of transcript and protein abundances yield different results; since transcripts are not always translated into protein, measuring proteins directly may give a more accurate snapshot of the metabolic potential in a cell. Proteomic analyses have been employed at contaminated sites, lending insight into the strategies used by microbial communities to respond to toxic contaminants (Lacerda *et al.*, 2007; Halter *et al.*, 2011; Chourey *et al.*, 2013; Yun *et al.*, 2016). As mentioned previously, O_2 plays an important role in contaminant turnover at contaminated sites. Identifying the conditions in which cytochromes aa_3 and cbb_3 are expressed and measuring their abundance at contaminated sites may reveal the relationship between O_2 and microbial community responses to contaminants. If microbial communities express cytochrome aa_3 is under oxic conditions and cytochrome cbb_3 is under microoxic conditions, these cytochromes could serve as molecular markers for O_2 intrusion into a site. *A. dehalogenans* serves as a useful model organism for studying the expression of cytochromes aa_3 and cbb_3 since *A. dehalogenans* is adapted for life in fluctuating redox conditions (Thomas *et al.*, 2010) and proteomic studies have been successfully conducted with *A. dehalogenans* (Chao *et al.*, 2010; Nissen *et al.*, 2012).

Based on the ability of *A. dehalogenans* strain 2CP-C to respire O_2 in microoxic but not oxic conditions, it was hypothesized that *A. dehalogenans* utilizes cytochrome aa_3 as a non-respiratory enzyme to decrease the level of O_2 to a lower concentration at which *A. dehalogenans* can use cytochrome cbb_3 for oxygen respiration (Figure 4.2). An alternative hypothesis is that *A. dehalogenans* utilizes cytochrome aa_3 to respire O_2 under oxic conditions, and that aerobic growth has not yet been recognized in this organism. Other alternatives include the utilization of cytochrome aa_3 for microaerophilic growth,

or the possibility that the cytochrome aa_3 gene is a remnant from an ancestor in the Myxococcales and no longer functions to respire O_2. In order to test the hypothesis that *A. dehalogenans* does not couple growth to respiration of 21% O_2 and uses cytochrome aa_3 in a non-respiratory fashion to lower the O_2 concentration, pure-culture studies with varied concentrations of O_2 were performed and growth and protein expression were measured. This chapter reveals new metabolic capabilities for *A. dehalogenans*.

Materials and Methods

Culture Conditions

Anaeromyxobacter dehalogenans strain 2CP-C was grown in a defined mineral salts medium (Löffler *et al.*, 1996) in which bicarbonate was replaced with 50 mM HEPES (4-[2-hydroxyethyl]-1-piperazineethanesulfonic acid) and sulfide was omitted. The medium was adjusted to a pH of 7.2 by the drop-wise addition of a 10 M sodium hydroxide solution. The medium was dispensed in 100 mL aliquots into 160 mL serum bottles, sealed with rubber stoppers, then autoclaved. For open vessel experiments (i.e., in Erlenmeyer flasks with or without baffles) with 5, 10, or 15% O_2, bottles and flasks were taken into a microoxic chamber (Coy Laboratory Products, Grass Lake, MI) with an atmosphere of 5, 10, or 15 % O_2 (±0.1%) and bottles were opened and poured into sterile flasks. Flasks were capped with sterile aluminum foil, and media were allowed to equilibrate for at least one hour while shaking before inoculation. Cultures were inoculated from cultures growing on the same concentration of O_2. Cultures grown with 5-21% O_2 were slowly transferred with increasing concentrations of O_2. All "open" cultures were grown at room temperature and with shaking at 160 rpm. For "closed" cultures that received O_2 flushing, fish pumps were connected to the headspace via 22 gauge needles to actively flush ambient air into the bottles (Figure 4.3), and cultures were incubated at 30ºC with shaking at 110 rpm.

Protein extraction and SDS-PAGE

To extract proteins for sodium dodecyl sulfate polyacrylamide gel electrophoresis (SDS-PAGE), 6 mL of cultures were removed and placed on ice. Samples were

centrifuged at 2,050 g at 4˚C for 20 minutes. Cell pellets were resuspended in 300 µL Laemmli buffer, boiled for 5-10 minutes, and briefly centrifuged. A 12% polyacrylamide gel was prepared by pouring a separating gel and a stacking gel into a large format Bio-Rad electrophoresis chamber. The separating gel was allowed to solidify under a layer of butanol-saturated water before pouring the separating gel. The separating gel was prepared by mixing 12 mL of 30% acrylamide/0.8% bisacrylamide, 7.5 mL of 4x Tris-Cl/SDS (pH 8.8), 10.5 mL milliQ water, 100 µL 10% w/v ammonium persulfate, and 20 µL tetramethylethylenediamine (TEMED). The stacking gel was prepared by mixing 1.3 mL 30% acrylamide/0.8% bisacrylamide, 2.5 mL of 4x Tris-Cl/SDS (pH 6.8), 6 mL milliQ water, 50 µL of 10% ammonium persulfate, and 10 µL TEMED. Solutions for the stacking and separating gels were degassed under a vacuum before pouring. 50-100 µL of samples were ran on the gel for 4-5 hours at 150-200 V. To stain heme-containing proteins, gels were slowly shaken in the dark in a 30 mL 3,3',5,5'-tetramethylbenzidine (TMBZ) solution for 1 hour, then developed for 5 or more minutes with 204 µL of 30% H_2O_2. The TMBZ solution was prepared by vigorously vortexing 0.013 g TMBZ and 9 mL methanol, then mixing with 21 mL of 0.25 M sodium acetate (pH 5.0).

Analytical and bioinformatic procedures

Acetate was measured as described in Chapter 2. Optical density was measured by removing 300 µL of culture and measuring in a Biotek Synergy 2 microplate reader at a wavelength of 600 nm. Growth rate was calculated by plotting the natural log-transformed optical density versus time, and calculating the slope of the linear portion. O_2 in the headspace of cultures was quantified by injecting 1 mL gas headspace samples into an Agilent 3000A Micro GC with an Agilent Molecular Sieve 5Å column (Agilent Technologies, Santa Clara, CA), a thermal conductivity detector, and argon as the carrier gas. The column pressure and temperature were 30 psi and 110°C, respectively. O_2 concentration in the headspace is reported as percentage or partial pressure (e.g. 21% or pO_2 of 0.21 for atmospheric air). Standards were made by injecting pure O_2 into sealed, anoxic bottles at concentrations of 0-25%. Cells for protein analysis were removed from cultures during log phase at an O.D. of approximately 0.12 to 0.16. Proteins were analyzed via coupled liquid chromatography and mass spectrometry (LC-MS/MS) as

previously described (Sharma *et al.*, 2012; Chourey *et al.*, 2013) and are normalized to total protein (normalized spectral counts [nSpc]). Protein BLAST and Conserved Domain Database (CDD) searches were performed via the online interfaces (https://blast.ncbi.nlm.nih.gov/Blast.cgi?PAGE=Proteins and https://www.ncbi.nlm.nih.gov/Structure/cdd/wrpsb.cgi, respectively).

Results

A. dehalogenans grows under oxic (21% O_2) conditions

It was hypothesized that *A. dehalogenans* does not gain growth at 21%, but rather expresses proteins that lower the concentration of O_2 to a tolerable concentration (Figure 4.2). To test the first part of this hypothesis, closed cultures of *A. dehalogenans* were grown with 10% O_2 in closed bottles, and subjected to 21% O_2 during log phase for 2 hours, 5 hours, or continuously (Figure 4.4). No apparent interruption in growth (as measured by optical density) or acetate utilization was observed. O_2 was consumed and growth was observed until acetate was depleted (Figure 4.4b, c, and d), with the exception of a control that was not subjected to 21% O_2 (Figure 4.4a). Independent, replicate experiments showed similar trends (data not shown). The expression of heme-containing proteins was measured by SDS-PAGE and heme-staining before and after exposure to 21% O_2, and differences in band patterns were not observed (data not shown); however, an abundance of bands were visible and were difficult to count or distinguish.

Since no growth defect was observed after the addition of 21% O_2, the growth of *A. dehalogenans* under oxic conditions (i.e., with 21% O_2) was further tested by growing cultures in open vessels (i.e., Erlenmeyer flasks rather than serum bottles). *A. dehalogenans* grew with 5, 10, 15, and 21% O_2 coupled to the oxidation of acetate (Figure 4.5). Cultures grown in flasks with and without baffles did not show stark differences, although cultures grown with 5% O_2 grew faster in baffled flasks than in non-baffled flasks (Figure 4.5a). When growth curves were adjusted to remove differences in lag phase (i.e., graphed with lag phase adjusted to equal time periods), different growth patterns were observed. Growth rates were similar, ranging from 0.012 ±

0.001 h^- to 0.018 ± 0 (Figure 4.6b). The maximum O.D. ranged from 0.20 to 0.36 (Figure 4.6a). Cultures grown with 10 and 15% O_2 grew to a lower overall O.D. (0.238 ± 0.063 and 0.247 ± 0.012, respectively) than cultures grown with 5 or 21% O_2 (0.337 ± 0.012 and 0.365 ± 0.002, respectively) (Figure 4.6c). Independent replicate cultures grown with 10% O_2 demonstrated a maximum O.D. of 0.201 ± 0.025, confirming a lower maximum O.D. for growth with 10% O_2 (data not shown).

***A. dehalogenans* expresses cytochrome *aa*$_3$ oxidase subunits during aerobic growth**

Protein abundances were measured for cultures grown at 5, 15, and 21% O_2. 806 proteins were detected for 5% O_2-grown cultures, 1,628 proteins were detected for 15% O_2-grown cultures, and 1,357 proteins were detected for 21%-grown cultures. *A. dehalogenans* has two gene clusters encoding cytochrome *aa*$_3$ (4 subunits each) and one gene cluster encoding cytochrome *cbb*$_3$ (2 subunits) (Figure 4.1). The expression of genes (as measured by protein abundance) in the cytochrome oxidase gene clusters for cytochrome *aa*$_3$ and cytochrome *cbb*$_3$ was examined more closely. The gene clusters as previously described in Figure S8 of Thomas et al. 2008 were used as a reference and only the cytochrome *c* oxidase subunits are shown in Figure 4.1. For the first cytochrome *aa*$_3$ gene cluster, 8 out of 12 proteins was expressed in at least one of the three O_2 concentration treatments, and three proteins were expressed with 5, 15, and 21% O_2 (Figure 4.7a). For the second cytochrome *aa*$_3$ gene cluster, 9 of the 14 proteins were expressed, and 7 proteins were expressed in all three O_2 treatments (Figure 4.7b). Although expression of other genes in the cytochrome *aa*$_3$ gene clusters was observed, of the genes encoding cytochrome *aa*$_3$ subunits (Adeh_0803-Adeh_0806 and Adeh_2272-Adeh_2275), only Adeh_0803 (subunit II) and Adeh_2275 (subunit I) were detected, and only Adeh_0803 was detected in all three treatments (Figure 4.7a and b). Adeh_2275 was only detected with 21% O_2, and only at an abundance of 8.05 spectral counts (Figure 4.7b). Three other putative *c*-type cytochromes in these gene clusters, Adeh_0795, Adeh_2285, and Adeh_2277 were also expressed. No proteins in the cytochrome *cbb*$_3$ gene cluster were detected in any of the conditions tested. In a separate study, proteins were assessed in anoxic *A. dehalogenans* cultures with ferric citrate, manganese oxide, NO_3^-, or fumarate, or microoxic cultures with 2.5%, 5%, or 9% O_2 (Silke Nissen, ORNL,

personal communication). Cultures were grown in closed serum bottles, and cells were removed for protein analysis when substrates had been depleted. Since these experiments were performed in closed systems, the concentration of O_2 was much lower during protein sampling than the initial starting O_2 concentration (i.e., much lower than 2.5, 5, or 9% O_2). Adeh_1172 (cytochrome *cbb*$_3$ oxidase subunit II) was expressed in all conditions, including closed cultures of *A. dehalogenans* grown with 2.5, 5, and 9% O_2 (Nissen, personal communication).

The expression of other *c*-type cytochromes was also assessed in cultures with 5, 15, and 21% O_2. Adeh_2966 and Adeh_2967 were expressed in higher abundance (over 2-fold) in the 21% O_2 treatment as compared to the 5% treatment (Figure 4.7c). Interestingly, in experiments performed by Silke Nissen, Adeh_2966 was only detected in NO_3^-- and O_2-grown cultures, and Adeh_2967 was only detected in O_2-grown cultures (personal communication). Both are annotated as hypothetical proteins. A protein BLAST search with Adeh_2966 yielded hypothetical proteins, and the best match in the NCBI Conserved Domain Database (CDD) was to the TIGR03805 model (an uncharacterized protein family). Adeh_2967 matched hypothetical proteins and cytochromes, and did not match any conserved domains in the CDD.

A. dehalogenans in the three treatments expressed proteins utilized for ROS detoxification. While expression of most ROS-detoxification proteins was below 16 normalized spectral counts (nSpc), Adeh_1952 (superoxide dismutase), Ade_0828 (thiol peroxidase), Adeh_2075 (rubrerythrin), and Adeh_0765 (rubrerythrin) were all more highly expressed (i.e., above 100 nSpc) (Figure 4.8). Most notable was the expression of Adeh_0765, which encodes rubrerythrin; expression in the 5% O_2 cultures was above 5,000 nSpc, and expression in 15% and 21% O_2 cultures was above 1,000 nSpc.

Discussion

Contrary to past studies, *A. dehalogenans* respires 21% O_2

A. dehalogenans strain 2CP-C has been classified as both a facultative anaerobe (Sanford *et al.*, 2002) and as a microaerophile (Thomas *et al.*, 2010). Previously *A. dehalogenans* demonstrated inconsistent growth with 21% O_2, and growth was dependent

on limiting mixing (i.e., with slow shaking or stationary cultures). The data here show growth coupled to the respiration of O_2 at 5, 10, 15, and 21% O_2 concentrations, with no observable growth defects at 21% O_2 (Figures 4.4 and 4.5). The ability to grow both anaerobically with alternative electron acceptors and with ambient levels of O_2, coupled with the presence of both low- and high-affinity cytochrome *c* oxidases, supports the classification of *A. dehalogenans* as a facultative anaerobe as defined by Morris and Schmidt (2013). The classification of "facultative anaerobe" typically includes microorganisms that can respire oxic concentrations of O_2, and is perhaps a more appropriate description of *A. dehalogenans* than "microaerophile." Past studies demonstrated that *A. dehalogenans* increased in numbers in soil exposed to water containing 281-375 μM dissolved O_2 (Thomas *et al.*, 2010), further evidence for aerobic growth. The data presented here demonstrate that organisms that respire 21% O_2 may have long lag phases or take long periods of time to adjust to fully ambient levels of O_2. It is possible that previous experiments showing growth defects of *A. dehalogenans* under oxic conditions did not provide enough time for *A. dehalogenans* to adjust to increased O_2 concentrations. When newly discovered bacteria are tested for growth on ambient concentrations of O_2, cultures are not always allowed to slowly adjust through incremental increases of O_2 concentration (as was done in the present study). Continual cultivation in anoxic conditions may cause an organism to adapt to anoxia. Gradual reintroduction of O_2 to other microorganisms with cytochrome aa_3 that are classified as strict anaerobes or microaerophiles may reveal other unknown facultative anaerobes.

A. dehalogenans expresses a low-affinity oxidase subunit (cytochrome aa_3) during O_2 respiration

While growing with 5, 15, and 21% O_2, *A. dehalogenans* expressed the cytochrome aa_3 subunit II (Adeh_0803) (Figure 4.7), suggesting that *A. dehalogenans* uses low-affinity cytochrome *c* oxidases for O_2 respiration. Interestingly, Adeh_0803 was also expressed with 2, 5, and 9% O_2 in closed vessels (Silke Nissen, personal communication), suggesting that cytochrome aa_3 may be expressed even when low O_2 concentrations are present. It is not clear if a fully functional cytochrome aa_3 is formed, however, since only subunit II was expressed, and the other three subunits (Adeh_0804,

Adeh_0805, and Adeh_0806) were not expressed, including the catalytic subunit I (Adeh_0804). Further evidence is required to definitively support the hypothesis that cytochrome *aa*$_3$ is expressed and functional. However, cytochrome *aa*$_3$ is typically associated with aerobic O_2 respiration. While the possibility that *A. dehalogenans* utilizes cytochrome *aa*$_3$ for O_2 detoxification cannot be ruled out, the utilization of cytochrome *aa*$_3$ to respire O_2 is a more parsimonious theory.

In comparison, none of the subunits of cytochrome *cbb*$_3$ were expressed in the conditions tested. However, previous studies by Silke Nissen demonstrated expression of cytochrome *cbb*$_3$ in closed cultures with O_2. This suggests that in the present study, the headspace concentrations of O_2 (5, 15, and 21% O_2) and thorough mixing (i.e., shaking cultures) created high enough dissolved O_2 concentrations that a high-affinity oxidase was not required. Cytochrome *cbb*$_3$ was also expressed by ferric citrate-, manganese oxide-, NO_3^--, and fumarate-reducing cells (personal communication; Nissen *et al.* 2012), indicating that this protein is expressed under anoxic and microoxic conditions. Furthermore, fumarate-grown cells quickly reduce microoxic concentrations of O_2 (Thomas *et al.*, 2010), demonstrating that *A. dehalogenans* is primed for microoxic O_2 reduction even while growing under anoxic conditions. The constitutive anaerobic expression of cytochrome *cbb*$_3$ shows that *A. dehalogenans* is adapted to life at oxic-anoxic interfaces. However, it is not known if cytochrome *cbb*$_3$ expressed by *A. dehalogenans* has another function, and further research is required to determine if cytochrome *cbb*$_3$ reduces other electron acceptors.

In addition to known O_2-reducing cytochromes, the expression ROS-detoxification proteins and of the cytochromes Adeh_2966 and Adeh_2967 was observed. It is not surprising that ROS-detoxification proteins were expressed under with 5, 15, and 21% O_2; however, it is interesting to note that *A. dehalogenans* expresses a high abundance (over 60x compared to the cytochrome *c* oxidase abundance) of rubrerythrin. Rubrerythrin catalyzes the reduction of hydrogen peroxide to water. It appears that rubrerythrin is especially important to ROS detoxification under oxic conditions; however, it is unknown why this ROS-detoxification protein would be more highly expressed during growth with 5% O_2 than with 15 and 21% O_2 (Figure 4.8b). Adeh_2966 and Adeh_2967, two hypothetical proteins, were also expressed in the

presence of O_2 in Silke Nissen's studies, and with the exception of Adeh_2966 expression with NO_3^-, were only expressed under oxic conditions. Further research is needed to determine the role of these proteins of unknown function.

Overall, it was demonstrated that *A. dehalogenans* is a facultative anaerobe that respires 21% O_2 and expresses cytochrome aa_3 subunit II in oxic conditions. The data fail to support the hypothesis that cytochrome aa_3 is utilized for O_2 detoxification or to lower the O_2 concentration in a non-respiratory fashion; the most parsimonious hypothesis is that *A. dehalogenans* possesses a cytochrome aa_3 oxidase for the purpose of 21% O_2 respiration coupled to growth. Over 1,300 proteins were expressed during growth with 21% O_2, and further data analysis may reveal other interesting protein expression patterns. For example, Adeh_2966 and Adeh_2967 were expressed under oxic conditions, and have unknown functions. The role of expressed proteins with unknown functions may inspire future studies with *A. dehalogenans*.

Limitations and future directions

Some important considerations limit the impact of this study. Proper controls (e.g., oxygen-free controls) were not included, so accurate comparison of protein abundance in the absence and presence of O_2 is not possible. However, previous protein analysis by Silke Nissen (which included many O_2-free treatments) was compared to the present analysis to provide insight. Additionally, although replicate cultures were sampled for protein analysis, only one replicate each of 5, 15, and 21% cultures were fully analyzed by LC-MS/MS. Pending further funding and collaborative opportunity, the remaining replicates should be analyzed in order to determine the statistical power of the observations.

Our results conflict with previous studies that reported inconsistent growth under ambient levels of O_2 (Sanford *et al.*, 2002; Thomas *et al.*, 2010). There are several possible explanations as to why observed robust growth of *A. dehalogenans* was observed at 5-21% O_2. Since *A. dehalogenans* cultures were transferred slowly with increasing concentrations of O_2, the possible selection for a mutant of *A. dehalogenans* cannot be ruled out. If that mutation was in cytochrome aa_3 subunit I (Adeh_0804) or cytochrome cbb_3, it may explain why these proteins were not detected, since the

identification of proteins via LC-MS/MS relies on a known sequence of each protein. It is also possible that *A. dehalogenans* loses unnecessary traits during long cultivation in the lab, and that continual cultivation in anoxic conditions in past experiments yielded mutants of *A. dehalogenans* incapable of aerobic growth. Alternatively, it may take extensive time for *A. dehalogenans* to adjust to oxic conditions. Initial long lag phases have been observed in cultures of *A. dehalogenans* with other electron acceptors such as N_2O (Figure 2.8) and 21% O_2 (personal observation; Thomas *et al.* 2010), suggesting that with some electron acceptors, *A. dehalogenans* is slow to express the necessary proteins for growth. After further electron acceptor addition, lag phases decrease (e.g., Figure 2.8). Thomas et al. inoculated O_2 cultures from dense fumarate-grown cultures, so the cells utilized in that study were not likely metabolically geared for 21% O_2 respiration at ambient concentrations of O_2 (2010).

Another surprising result was the absence of cytochrome *cbb*$_3$ expression during growth with lower (i.e. 5%) concentrations of O_2. It is possible that cytochrome *cbb*$_3$ was expressed but not detected by LC-MS/MS. However, this seems unlikely, since subunit II of cytochrome *cbb*$_3$ (Adeh_1172) was detected in previous studies employing the same LC-MS/MS techniques (Nissen *et al.*, 2012). Another potential explanation is that the lowest concentration of O_2 tested was not low enough for the expression of a high-affinity cytochrome *c* oxidase. Previous studies demonstrated a Michaelis constant (K_M) of 0.1-1.0 μM for the cytochrome *aa*$_3$ from *Escherichia coli* and 7 nM for the cytochrome *cbb*$_3$ from *Bradyrhizobium japonicum* (Morris and Schmidt, 2013; Ludwig, 2004; Pitcher and Watmough, 2004); thus it has been suggested that "microaerobic growth conditions" are below 1 μM (Ludwig, 2004). The lowest concentration of O_2 tested here was pO_2 of 5%, and the highest concentration tested was 21%, equivalent to approximately 68 and 285 μM dissolved O_2 in the liquid phase, respectively. The possibility that cytochrome *cbb*$_3$ is expressed at lower concentrations is supported by other studies in which Adeh_1172 was expressed during growth with lower concentrations of O_2 (Nissen, personal communication). However, several studies have demonstrated that cytochrome *cbb*$_3$ may play a role in nitric oxide turnover (Forte *et al.*, 2001; Hamada *et al.*, 2014). Since Adeh_1172 is expressed under anoxic conditions (e.g., during metal respiration

[Nissen *et al.* 2012]), further detailed studies are required to elucidate the function of cytochrome cbb_3 in *A. dehalogenans*.

LC-MS/MS was chosen to enumerate proteins since the SDS-PAGE and heme stain did not demonstrate any difference in protein band patterns. The lack of band changes may be due to the over abundance of *c*-type cytochromes (i.e., 64 *c*-type cytochromes) possessed by *A. dehalogenans*, since many bands were observed and it was difficult to distinguish individual bands. Additionally, SDS-PAGE was performed with proteins from closed cultures that were exposed to 21% O_2 by fish pumps. Despite the presence of 21% O_2 in the headspace, these cells may not have been fully exposed to 21% O_2 since they were in sealed serum bottles and slowly shaken, in contrast with the 5-21% O_2 experiments (in which open baffled flasks were used). Future studies should continue to use more targeted approaches, such as LC-MS/MS or Western blotting.

Acknowledgements

I would like to acknowledge Karuna Chourey (Oak Ridge National Laboratory) for extracting proteins, running LC-MS/MS, and analyzing the LC-MS/MS results. I would also like to acknowledge Dr. Silke Nissen for her shared partnership on this project and for providing her LC-MS/MS data.

References

Brune A, Frenzel P, Cypionka H. (2000). Life at the oxic-anoxic interface: microbial activities and adaptations. *FEMS Microbiol Rev* **24**: 691–710.

Chao TC, Kalinowski J, Nyalwidhe J, Hansmeier N. (2010). Comprehensive proteome profiling of the Fe(III)-reducing myxobacterium *Anaeromyxobacter dehalogenans* 2CP-C during growth with fumarate and ferric citrate. *Proteomics* **10**: 1673–1684.

Chourey K, Nissen S, Vishnivetskaya T, Shah M, Pfiffner S, Hettich RL, *et al.* (2013). Environmental proteomics reveals early microbial community responses to biostimulation at a uranium- and nitrate-contaminated site. *Proteomics* **13**: 2921–2930.

Cole JR, Cascarelli AL, Mohn WW, Tiedje JM. (1994). Isolation and characterization of a novel bacterium growing via reductive dehalogenation of 2-chlorophenol. *Appl Environ Microbiol* **60**: 3536–42.

Forte E, Urbani A, Saraste M, Sarti P, Brunori M, Giuffrè A. (2001). The cytochrome cbb_3 from *Pseudomonas stutzeri* displays nitric oxide reductase activity. *Eur J Biochem* **268**: 6486–6491.

Halter D, Cordi A, Gribaldo S, Gallien S, Goulhen-Chollet F, Heinrich-Salmeron A, *et al.* (2011). Taxonomic and functional prokaryote diversity in mildly arsenic-contaminated sediments. *Res Microbiol* **162**: 877–887.

Hamada M, Toyofuku M, Miyano T, Nomura N. (2014). cbb3-type cytochrome c oxidases, aerobic respiratory enzymes, impact the anaerobic life of Pseudomonas aeruginosa PAO1. *J Bacteriol* **196**: 3881–3889.

Lacerda CMR, Choe LH, Reardon KF. (2007). Metaproteomic analysis of a bacterial community response to cadmium exposure. *Proteome Res* **6**: 1145–1152.

Le Laz S, Kpebe A, Bauzan M, Lignon S, Rousset M, Brugna M. (2014). A biochemical approach to study the role of the terminal oxidases in aerobic respiration in *Shewanella oneidensis* MR-1. *PLoS One* **9**. e-pub ahead of print, doi: 10.1371/journal.pone.0086343.

Le Laz S, Kpebe A, Bauzan M, Lignon S, Rousset M, Brugna M. (2016). Expression of terminal oxidases under nutrient-starved conditions in Shewanella oneidensis: detection of the A-type cytochrome c oxidase. *Sci Rep* **6**: 1–11.

Löffler FE, Sanford RA, Tiedje JM. (1996). Initial characterization of a reductive dehalogenase from *Desulfitobacterium chlororespirans* Co23. *Appl Environ Microbiol* **62**: 3809–13.

Ludwig RA. (2004). Microaerophilic bacteria transduce energy via oxidative metabolic gearing. *Res Microbiol* **155**: 61–70.

Madigan M, Martinko JM, Bender KS, Buckley DH, Stahl DA. (2015). Brock Biology of Microorganisms. 14th ed. Pearson.

Meyer TE. (1996). Evolution and Classification of *c*-Type Cytochromes. In: Scott RA, Mauk AG (eds). *Cytochrome c*. University Science Books: Sausalito, CA, pp 33–99.

Morris RL, Schmidt TM. (2013). Shallow breathing: bacterial life at low O2. *Nat Rev Microbiol* **11**: 205–12.

Nissen S, Liu X, Chourey K, Hettich RL, Wagner DD, Pfiffner SM, *et al.* (2012). Comparative *c*-type cytochrome expression analysis in *Shewanella oneidensis* strain MR-1 and *Anaeromyxobacter dehalogenans* strain 2CP-C grown with soluble and insoluble oxidized metal electron acceptors. *Biochem Soc Trans* **40**: 1204–10.

Pitcher RS, Watmough NJ. (2004). The bacterial cytochrome cbb_3 oxidases. *Biochim Biophys Acta* **1655**: 388–99.

Roden EE, McBeth JM, Blöthe M, Percak-Dennett EM, Fleming EJ, Holyoke RR, *et al.* (2012). The microbial ferrous wheel in a neutral pH groundwater seep. *Front Microbiol* **3**: 1–18.

Sanford RA, Cole JR, Tiedje JM. (2002). Characterization and description of *Anaeromyxobacter dehalogenans* gen. nov., sp. nov., an aryl-halorespiring facultative anaerobic myxobacterium. *Appl Environ Microbiol* **68**: 893–900.

Sharma R, Dill BD, Chourey K, Shah M, VerBerkmoes NC, Hettich RL. (2012). Coupling a detergen lysis/cleanup methodology with intact protein fractionation for enhanced proteome characterization. *J Proteome Res* **11**. http://pubs.acs.org.proxy.lib.utk.edu:90/doi/pdf/10.1021/pr300709k (Accessed March 23, 2017).

Thomas SH, Sanford R a, Amos BK, Leigh MB, Cardenas E, Löffler FE. (2010). Unique ecophysiology among U(VI)-reducing bacteria as revealed by evaluation of oxygen

metabolism in *Anaeromyxobacter dehalogenans* strain 2CP-C. *Appl Environ Microbiol* **76**: 176–83.

Thomas SH, Wagner RD, Arakaki AK, Skolnick J, Kirby JR, Shimkets LJ, *et al.* (2008). The mosaic genome of *Anaeromyxobacter dehalogenans* strain 2CP-C suggests an aerobic common ancestor to the delta-proteobacteria. *PLoS One* **3**: 1–12.

Wu W-M, Carley J, Luo J, Ginder-Vogel MA, Cardenas E, Leigh MB, *et al.* (2007). In situ bioreduction of uranium (VI) to submicromolar levels and reoxidation by dissolved oxygen. *Environ Sci Technol* **41**: 5716–5723.

Yun J, Malvankar NS, Ueki T, Lovley DR. (2016). Functional environmental proteomics: Elucidating the role of a *c*-type cytochrome abundant during uranium bioremediation. *ISME J* **10**: 310–320.

Zhou G, Yin J, Chen H, Hua Y, Sun L, Gao H. (2013). Combined effect of loss of the caa_3 oxidase and Crp regulation drives *Shewanella* to thrive in redox-stratified environments. *ISME J* **7**: 1752–63.

Appendix: Figures

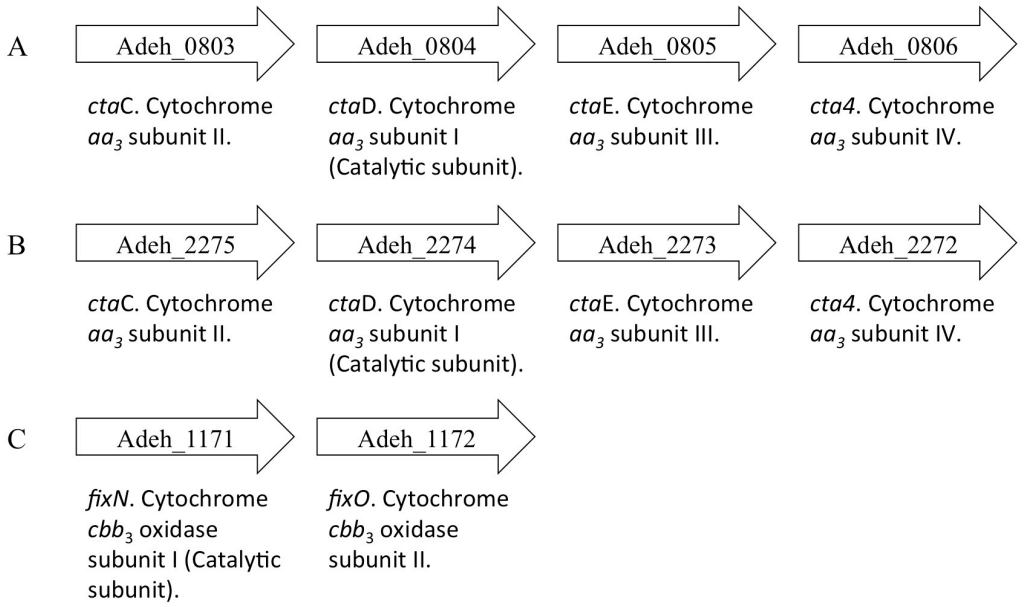

Figure 4.1. Cytochrome *c* oxidase subunits gene locus identities and description. (A) and (B) show genes with similarity to cytochrome aa_3. genes (C) Genes with similarity to cytochrome cbb_3 genes. Arrow size is not proportionate to gene size. Adapted from Thomas et al. 2008 Figure S8.

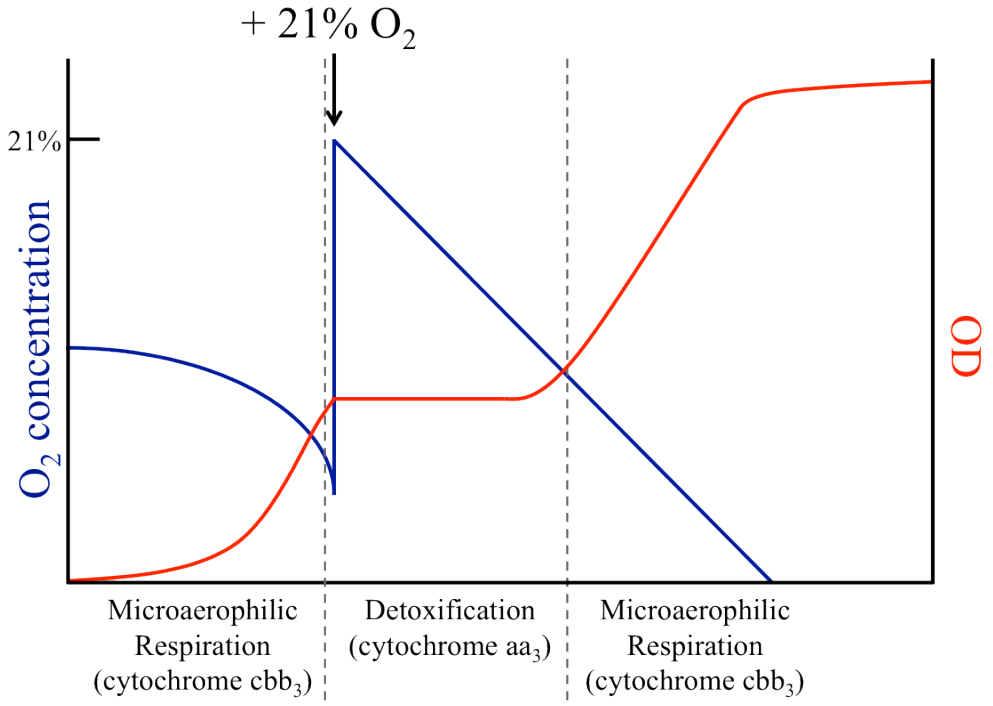

Figure 4.2. Schematic of the hypothesis that *A. dehalogenans* utilizes cytochrome aa_3 as a non-respiratory enzyme to decrease the level of oxygen to a lower concentration of oxygen at which *A. dehalogenans* can respire oxygen with cytochrome cbb_3.

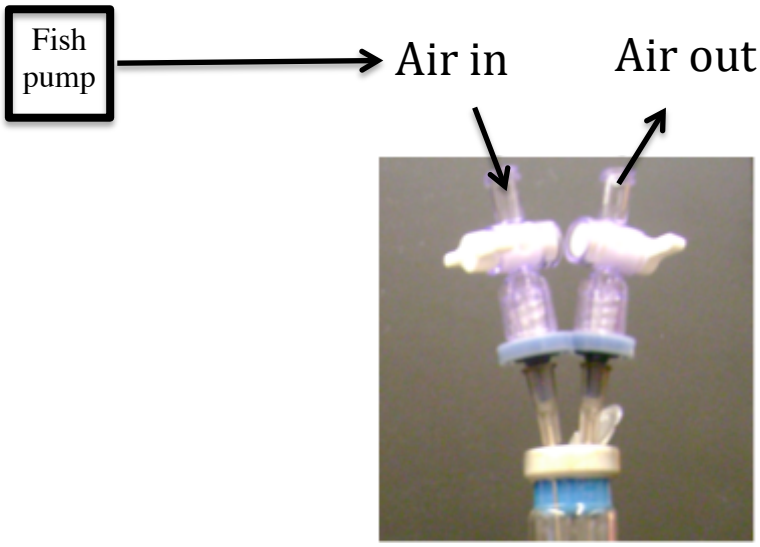

Figure 4.3. Setup of cultures with fish pump. Fish pumps were connected to a stopcock via plastic tubing, which was connected to a 22 gauge needle. The needle was inserted into the stopper. A stopcock and needle was utilized as the outflow.

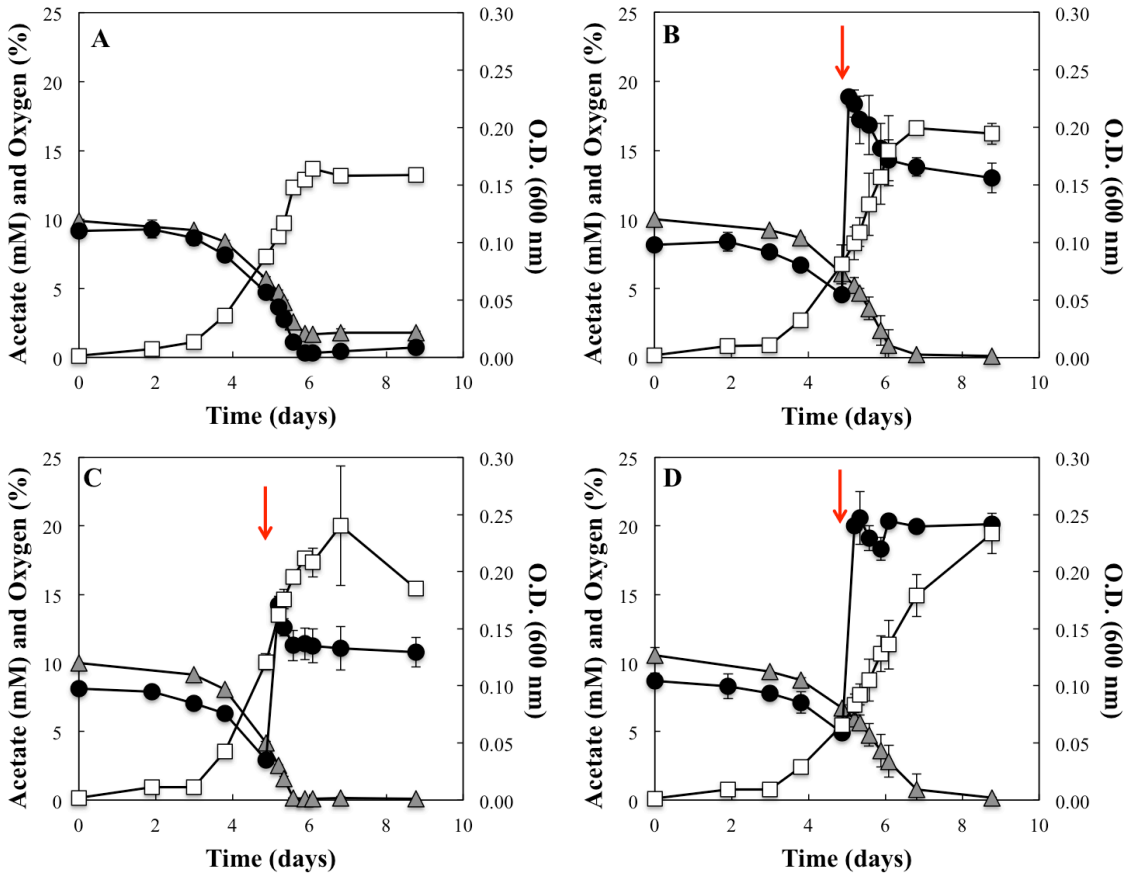

Figure 4.4. Effect of 21% O_2 exposure on *A. dehalogenans* growth. Closed cultures of *A. dehalogenans* grown with 10% O_2. On day 4.8, air (21% oxygen) was pumped into the bottles (as indicated by the red arrows) for 0 hours (A), 2 hours (B), 5 hours (C), or continuously (D). Acetate (gray triangles), oxygen (closed circles), optical density (open squares).

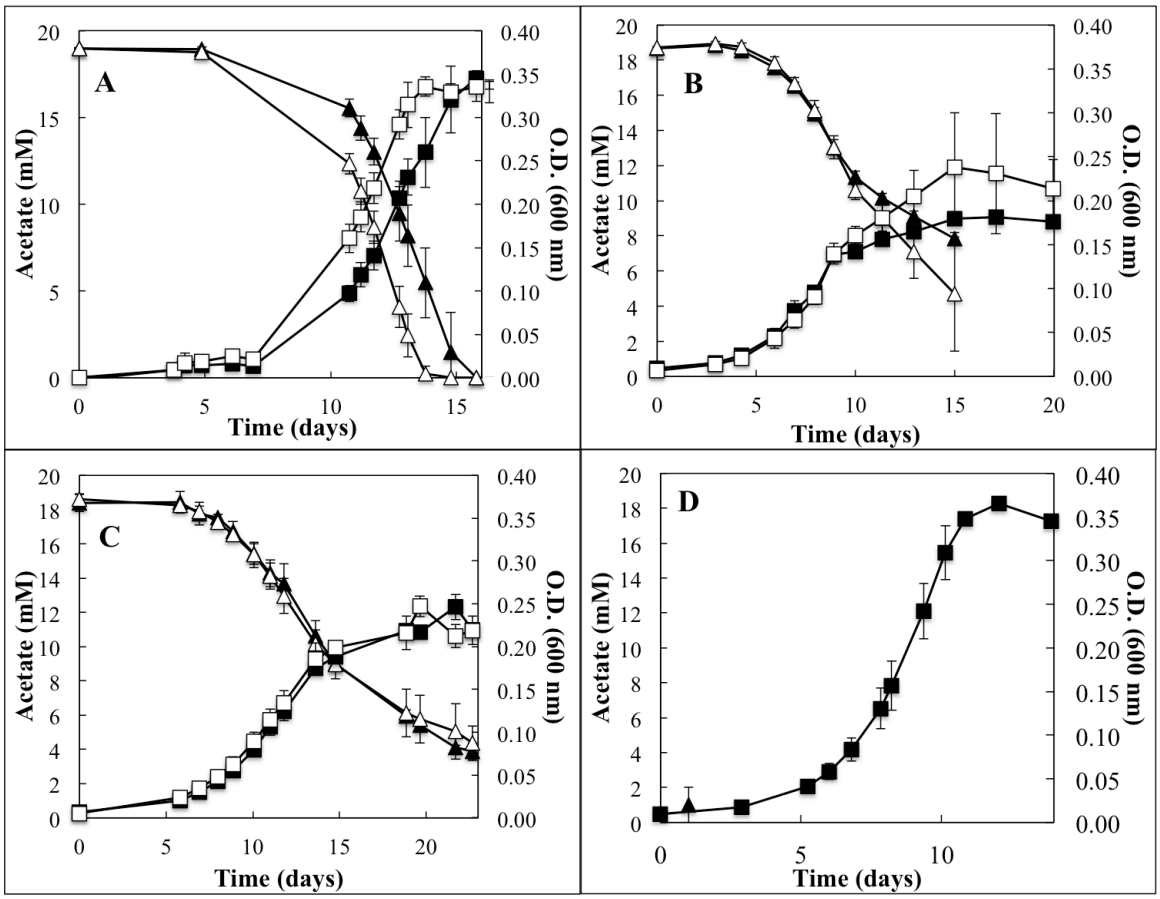

Figure 4.5. Aerobic growth of *A. dehalogenans*. Open cultures of *A. dehalogenans* in Erlenmeyer flasks with (open symbols) or without (closed symbols) baffles. Grown in an atmosphere of 5% O_2 (A), 10% O_2 (B), 15% O_2 (C) or 21% O_2 (D). Acetate (triangles) and optical density (squares).

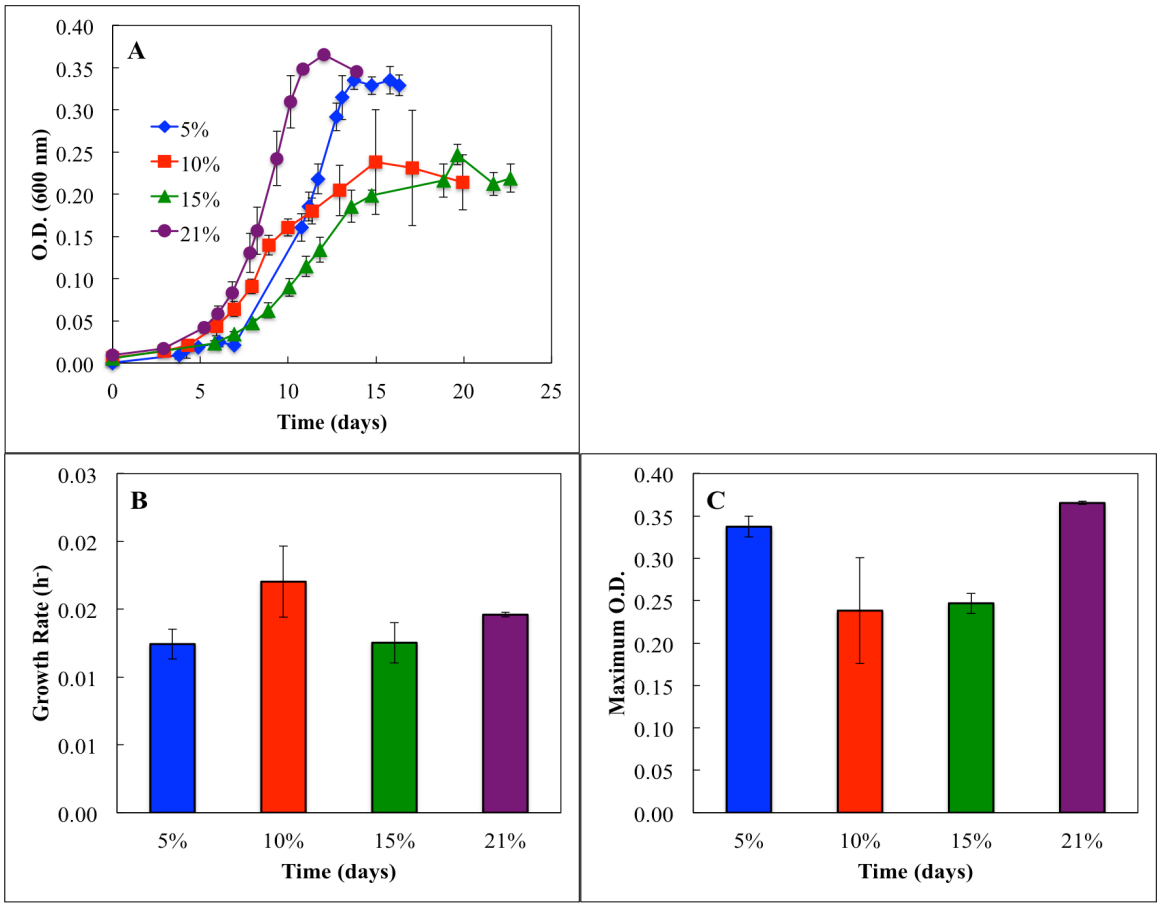

Figure 4.6. Aerobic growth rates. Open cultures of *A. dehalogenans* in Erlenmeyer flasks with baffles from Figure 5.4. (A) O.D. values from Figure 5.4, with values adjusted to remove differing lag phases. (B) Growth rate corresponding to A. (C) Maximum O.D. observed in *A. dehalogenans* cultures.

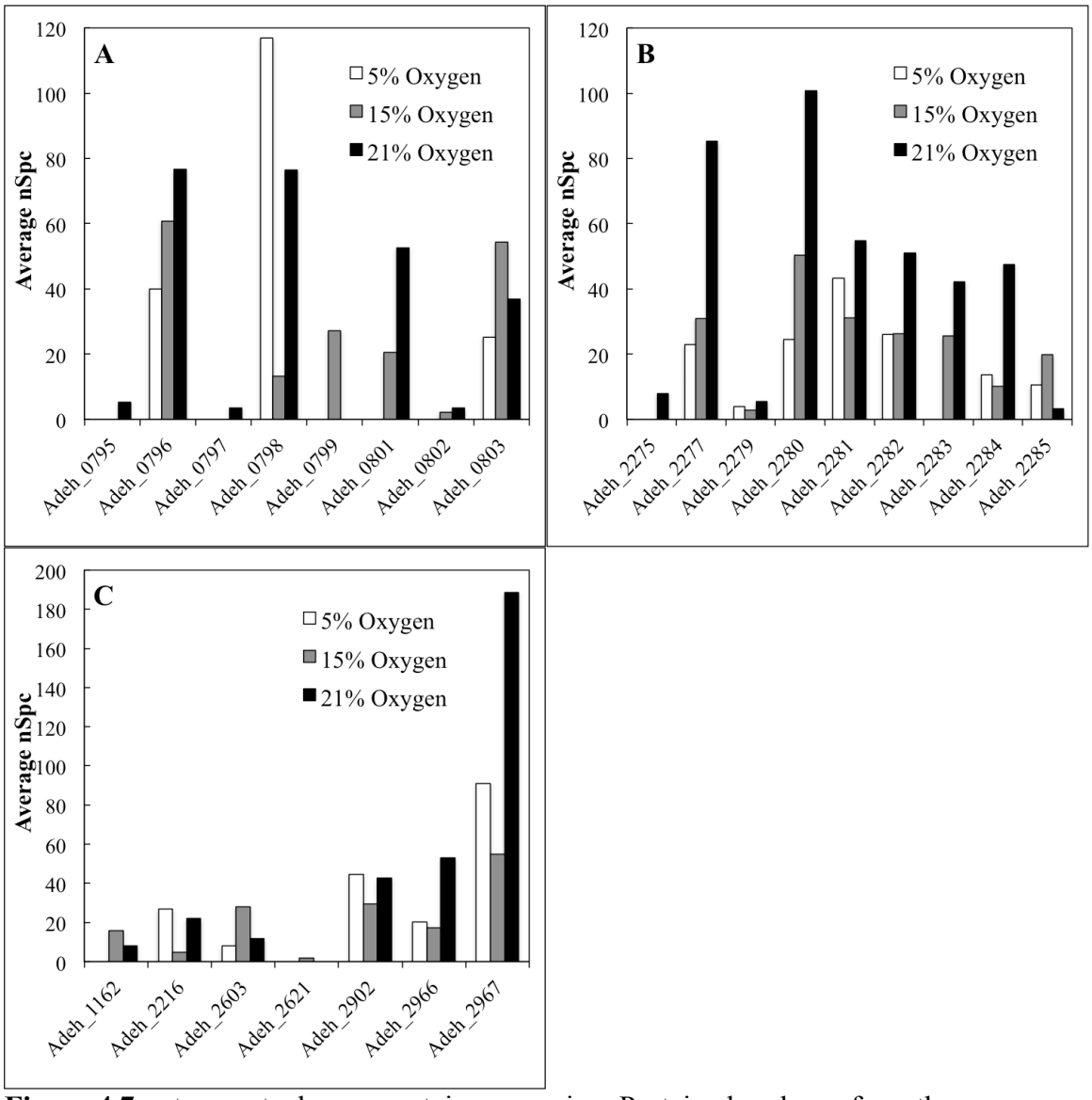

Figure 4.7. *c*-type cytochrome protein expression. Protein abundance from the cytochrome aa_3 gene clusters of *A. dehalogenans* strain 2CP-C (A and B) and other *c*-type cytochromes (C). Average normalized spectral counts (nSpc) are from two independent runs of individual samples. Note the scale difference for C.

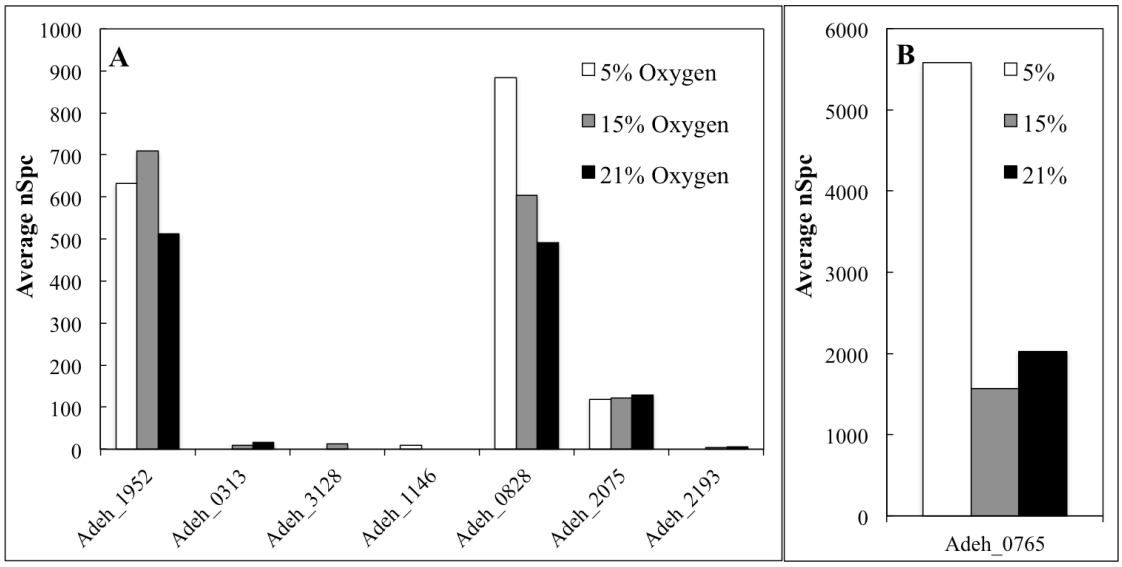

Figure 4.8. Protein abundance of ROS-detoxification proteins. (A) Adeh_1952 (superoxide dismutase), Adeh_0313 and Adeh_3128 (alkyl hydroperoxidases), Adeh_1146 and Adeh_0828 (thiol peroxidases), Adeh_2075 (rubrerythrin), and Adeh_2193 (rubrerythrin-rubredoxin fused protein). (B) Adeh_0765 (rubrerythrin). Note the scale difference for B.

Chapter 5: Conclusions, Perspectives, and Future Directions

N affects human health and the health of the environment more dramatically than almost any other element, and has been studied extensively. Remarkably, the knowledge of the N cycle continues to expand, and with it, a growing list of N_2O sources and sinks. Although the mechanism of chemodenitrification has been known for over 50 years, it has long been regarded as an insignificant process in soils. However, recent interest has emerged regarding chemodenitrification, and evidence of the significance of this process is building (e.g., Zhu *et al.*, 2013; Zhu-Barker *et al.*, 2015; Ostrom *et al.*, 2016). The work presented in this dissertation demonstrates that *Anaeromyxobacter dehalogenans* strain 2CP-C facilitates chemodenitrification, combining abiotic and biotic processes to completely reduce NO_3^- to N_2. This reveals a novel ecophysiology for *A. dehalogenans*, in which *A. dehalogenans* transforms NO_3^- to N_2 by reducing Fe(III) and NO_3^- and by employing a clade II N_2O reductase to utilize N_2O produced by chemodenitrification. Additionally, this work demonstrates abiotic factors that alter the outcome of chemodenitrification, namely sulfide and molybdenum concentrations. Although NO_3^- is reduced to NH_4^+ by *A. dehalogenans* in pure culture, synergistic effects occur when Fe(II) and/or sulfide is present, resulting in NO_3^- reduction to NH_4^+, N_2O, or N_2 (Table 3.2). Combined biotic-abiotic reactions have been observed with other microorganisms, and the effects of chemodenitrification, sulfide, and molybdenum are expected to be observed in the future with other members of the soil microbial community. Thus the prediction of NO_3^- reduction end products in both pure cultures and by a microbial community must take into account not only the genetic content of the organisms (i.e., their N-cycle genes), but also the iron, sulfide, and molybdenum concentrations and speciation. The present work suggests that current techniques inaccurately describe and predict the fate of N fertilizers in soils. Furthermore, the work presented here demonstrates that *A. dehalogenans* can couple growth to O_2 respiration at ambient concentrations (i.e., 21%), and provides evidence that a low-affinity oxidase, cytochrome aa_3, is expressed during O_2 respiration. The ability to grow robustly under fully oxic conditions is one of the many ways *A. dehalogenans* is metabolically versatile and well-equipped to flourish at oxic-anoxic interfaces, where Fe(III)/Fe(II) and a variety of contaminants undergo redox cycling. Additionally, the inconsistency of the present study

with past studies (which demonstrated a lack of aerobic growth with *A. dehalogenans*) suggests that other facultative anaerobes may be mischaracterized as microaerobes.

The new term "chemodenitrifiers" is proposed to describe microorganisms that combine biotic and abiotic reactions to fully reduce NO_3^- to N_2. Potential chemodenitrifiers were identified by analyzing sequenced genomes for the presence of NO_3^- reductase genes (*napA* and *narG*), N_2O reductase genes *(nosZ*), and *c*-type cytochromes and by searching the literature for the ability of organisms to reduce iron. Future studies searching for chemodenitrifiers can start with promising organisms identified by this analysis. For example, *Desulfitobacterium hafniense* strain DCB-2, *Rhodoferax ferrireducens* strain T118, and *Aeromonas media* strain WS fit the profile for potential chemodenitrifiers. Future studies should test these organisms for the ability to facilitate chemodenitrification in a similar manner to *A. dehalogenans*. Organisms that have not been identified as iron-reducing bacteria but contain a large number of multi-heme *c*-type cytochromes should be tested for their ability to utilize Fe(III) as an electron acceptor. As the field moves forward, the prevalence of chemodenitrification and the role of chemodenitrifiers will continue to be uncovered.

References

Buchwald C, Grabb K, Hansel CM, Wankel SD. (2016). Constraining the role of iron in environmental nitrogen transformations: Dual stable isotope systematics of abiotic NO_2^- reduction by Fe(II) and its production of N_2O. *Geochim Cosmochim Acta* **186**: 1–12.

Jones LC, Peters B, Lezama Pacheco JS, Casciotti KL, Fendorf S. (2015). Stable isotopes and iron oxide mineral products as markers of chemodenitrification. *Environ Sci Technol* **49**: 3444–3452.

Ostrom NE, Gandhi H, Trubl G, Murray AE. (2016). Chemodenitrification in the cryoecosystem of Lake Vida, Victoria Valley, Antarctica. *Geobiology*. e-pub ahead of print, doi: 10.1111/gbi.12190.

Zhu-Barker X, Cavazos AR, Ostrom NE, Horwath WR, Glass JB. (2015). The importance of abiotic reactions for nitrous oxide production. *Biogeochemistry* **126**: 251–267.

Zhu X, Silva LCR, Doane TA, Horwath WR. (2013). Iron: The forgotten driver of nitrous oxide production in agricultural soil. *PLoS One* **8**: e60146.

Vita

Jenny Onley was born to parents Stuart and Janine Merryfield and raised in the small town of Enumclaw, WA. Growing up, Jenny was very active in band, playing clarinet and bass clarinet throughout middle school, high school, and college. She was born with a curiosity for how the world works, and throughout her education she had several passionate science teachers who inspired her to pursue science. She attended Whitworth University for her undergraduate degree and graduated *Cum Laude* with a B.S. in Biology and a minor in Theology. It was at Whitworth Jenny met her future husband, Jared Onley. During her undergraduate education Jenny was accepted into the NSF Research Experiences for Undergraduates (REU) program at the University of Iowa, where she worked with Dr. David S. Weiss for the summer of 2010. After graduating from Whitworth University in 2011, Jenny entered graduate school in the Department of Microbiology at the University of Tennessee in Knoxville where she joined Dr. Frank Löffler's lab. Jenny was active in the department, serving as a graduate student advisor for the Microbiology Undergraduate Club, the Graduate Student Senate (GSS) representative for Microbiology, and the GSS Equity and Diversity Committee chair. Jenny won an award for excellent student speaker at the International Conference for Nitrification in 2015 and won third place for best poster at the Southeastern Biogeochemistry Symposium in 2016. In addition to her academic pursuits, Jenny's time at UT included biking, hiking, playing nerdy board games, and learning more about the cultural backgrounds of her fellow students and post-docs.